CONSTRUCTION MATERIALS CONSULTANTS, INC.

Assessments of Concrete Composition, Condition, Strength, and Depth of Penetration of Chloride Ions in a Bridge Substructure from Petrographic Examinations, Compressive Strength Tests, & Chloride Analyses of Four Concrete Cores & Forty Concrete Powders

Hurley Avenue Bridge over Watts Branch Tributary
Rockville, Maryland

February 08, 2022
CMC 0122103

TABLE OF CONTENTS*

* Bridge substructure, alkali-silica reactions of strained quartzite gravels, high chloride, air entrainment.

EXECUTIVE SUMMARY

The present report provides an assessment of overall composition, condition, compressive strength, and depth of penetration of chloride ions into the substructure of Hurley Avenue bridge, located at Watts branch tributary in Rockville, Maryland. The bridge is reportedly 53-year-old, currently under rehabilitation, where the superstructure will be removed and replaced. The purpose of this investigation is to assess the overall condition of the substructure, e.g., if is still in satisfactory condition. However, visible concrete deterioration is seen in the field photos of substructure such as cracking, spalling, and reddish-brown stains from corrosion of reinforcing steel in concrete.

A total of four cores marked as EC-1P, EC-2P, WC-1P, and WC-2P, along with forty concrete powders at distances of 1 in., 3 in., 5 in., 10 in. and 15 in. from the exposed ends of Cores EC-1P, EC-2P, EC-3, EC-4, WC-1P, WC-2P, WC-3, and WC-4 were provided. The four cores were tested for concrete compositions and conditions by detailed petrographic examinations according to the procedures of ASTM C 856. Portions of four cores were also tested for compressive strengths according to the procedures of ASTM C 42. The forty concrete powders were tested for water-soluble chloride ion contents according to the procedures of ASTM C 1218.

All four cores were received in moderately to severely fragmented conditions, which is a testament of overall poor condition of the bridge substructure. Field photos of core locations show various concrete deterioration, e.g., from long cracks mostly at the upper levels of substructure to isolated occurrences of spalls to reddish-brown stains from corrosion of reinforcing steel in concrete. Two of the four cores received, i.e., Cores EC-2P and WC-2P show the presence of a near-surface delamination at depths of 5 to 10 mm from their exposed ends.

Based on detailed petrographic examinations, concrete in the four cores examined, i.e., EC-1P, EC-2P, WC-1P, and WC-2P are determined to be compositionally similar and made using similar quartzite gravel coarse aggregates, natural quartz sand fine aggregates, and Portland cement paste.

The quartzite gravel coarse aggregates contain highly strained quartz grains with characteristic undulose extinction, which are known to be potentially alkali-silica reactive in the presence of moisture and high alkalis in the pore solutions. As a result, evidence of alkali-silica reaction is found in the cores as (a) microcracking within the quartzite gravel particles, (b) microcracking extending from the reactive particles to neighboring paste, (c) dark reaction rims, and (d) alkali-silica reaction gels in microcracks and air voids in the vicinity of reactive quartzite gravels. Profuse development of secondary ettringite deposits lining the walls of coarser air voids, filling the smaller air voids, and filling some microcracks are testaments of prolonged presence of moisture in the concrete during service, which is one of the main pre-requisites for alkali-silica reaction to occur, besides having the reactive quartz in aggregates, and high levels of alkali in the pore solutions.

Coarse aggregate particles are ¾ to 1 in. (19 to 25 mm) in nominal size, dense, hard, light to medium gray, massive crystalline granular textured, subrounded to well-rounded, mostly equidimensional to a few elongated, well-graded in Cores EC-1P and WC-2P to poorly graded (due to the deficiency of some finer and intermediate size particles) in Cores EC-2P and WC-1P, and well-distributed in all four cores.

Fine aggregates are compositionally similar natural siliceous sands of nominal maximum sizes ⅜ in. (9.5 mm) consisting of dominant quartz, and subordinate quartzite, feldspar, and minor amounts of quartz siltstone particles. Fine aggregate particles are variably colored, subangular to subrounded, variably dense and hard, equidimensional to elongated, unaltered, uncoated, and uncracked. There is no evidence of alkali-aggregate reactions, or any other potentially deleterious reactions found in the fine aggregates.

Paste is compositionally similar dense, and hard in the interior bodies except some patchy discoloration at the expose surface ends in Cores EC-2P and WC-2P, which are due to atmospheric carbonation during service. Freshly fractured surfaces have subtranslucent vitreous lusters and subconchoidal fractures. Residual and relict Portland cement particles are present and estimated to constitute 6 to 8 percent of the paste volumes. Besides residual Portland cement, no other pozzolanic or cementitious materials are found. The textural and compositional features of pastes are indicative of Portland cement contents similar in the four cores examined and estimated to be 6 to 6½ bags per cubic yard, and water-cement ratios in the bodies similar in all cores and estimated to be from 0.45 to 0.50.

Concretes in all four cores are found to be variably air entrained where air occur as (a) numerous fine, discrete, spherical and near-spherical voids of sizes 1 mm or less, which are characteristic of entrained air; and (b) a few coarse, near-spherical and irregularly-shaped voids greater than 1 mm in size, which are characteristic of entrapped air. Concrete in EC-1P is marginally air-entrained having an estimated air content of 3 to 4 percent. Concrete in Core EC-2P is air-entrained having an estimated air content of 4.5 to 5.5 percent. Concrete in both cores WC-1P and WC-2P are air-entrained having similar estimated air contents of 3.5 to 4.5 percent.

Despite the presence of air entrainment, the total estimated air contents of 3.5 to 5.5 percent are lower than that needed (at least 4½ percent) for the protection of a moist outdoor concrete substructure against distress due to cyclic freezing and thawing at critically saturated conditions. Therefore, due to the low estimated air contents, potential for freezing-related distress of the substructure, such as cracking and spalling are present, especially at locations where air contents are less than 4½ percent and exposed to moisture during freezing.

Results of water-soluble chloride analyses from 1 in. to 15 in. distances from the exposed ends in all four cores show higher than the industry-recommended threshold maximum chloride content of 0.2 percent, by mass of cement at various depths above which chloride-induced corrosion of reinforcing steel in concrete is possible in the presence of oxygen and moisture. A total of 23 samples out of forth show higher than threshold chloride contents. Therefore, the observed reddish-brown corrosion stains seen in the field photos are judged to be due to chloride-induced corrosion of steel in concrete in the presence of oxygen and moisture during service.

Compressive strengths of cores varied from 3450 psi (in EC-2P) to 5890 psi (in WC-1P). Unit weights are from 139.7 to 144.6 pounds per cubic foot. Three out of four cores have compressive strengths from 3450 psi to 4330 psi, which are less than the common industry-recommended minimum strength of 4500 psi for a moist outdoor concrete exposed to cyclic freezing and thawing. Microcracking developed from alkali-silica reaction of many reactive strained quartzite gravel coarse aggregate particles have deleteriously affected the compressive strength.

Due to the presence of high levels of chloride and lack of adequate air entrainment, a protective membrane is beneficial for protection of concrete from penetration of moisture and potentially deleterious chemicals into the concrete. A thin (nominal 1 mm thickness) protective membrane is indeed found at the exposed ends of Cores EC-2P and WC-2P, which is beneficial for preventing penetration of external agents during service.

Due to the evidence of (a) alkali-silica rection of many reactive quartzite gravel coarse aggregate particles, (b) lack of adequate air entrainment to generate around 6 percent air, and (c) high levels of chlorides in 23 out of 40 concrete powders from various depths, long-term serviceability of the bridge substructure is questionable unless the existing concrete can be adequately protected with the new superstructure and perhaps some additional protection with protective membrane to prevent penetration of moisture and potentially deleterious chemicals into the concrete.

INTRODUCTION

The present report provides an assessment of overall composition, condition, compressive strength, and depth of penetration of chloride ions into the substructure of Hurley Avenue bridge, located at Watts branch tributary in Rockville, Maryland.

BACKGROUND INFORMATION AND FIELD PHOTOGRAPHS

It is reported that the bridge will be rehabilitated. Superstructure will be removed and replaced. City wants to know if substructure is still in satisfactory condition. Visible concrete deterioration is seen in the substructure as cracking, spalling, and reddish-brown stains from corrosion of reinforcing steel in concrete, which are all shown at the locations of all cores collected in the field photos in Figures 1 through 4. The bridge was reportedly constructed in 1969.

Field photos in Figures 1 through 4 show sporadic occurrences of spalling and delamination of concrete as well as long cracks mostly concentrated at the upper levels of substructure. Reddish brown corrosion stains indicate the potential corrosion of reinforcing steel in concrete in the presence of oxygen and moisture, the mechanism which can introduce cracking and spalling of concrete.

PURPOSES

Based on the background information provided, and field photos of concrete deterioration in the substructure of bridge, the purposes of present laboratory investigations are to determine:

a. The overall composition and condition of concrete at the locations of four cores EC-1P, EC-2P, WC-1P, and WC-2P from detailed petrographic examinations;
b. Compressive strengths of concretes at the locations of four cores EC-1P, EC-2P, WC-1P, and WC-2P;
c. Depth of penetration of chloride ions into the substructure at the locations of eight cores EC-1P, EC-2P, EC-3, EC-4, WC-1P, WC-2P, WC-3, and WC-4. For each location, fifteen chloride powder samples were collected at 1 in., 3 in., 5 in., 10 in., and 15 in. depths, i.e., a total of forty concrete powders for determination of water-soluble chloride ions in concrete;
d. Diagnosis of evidence of any potentially deleterious chemical or physical reactions in the concrete from petrographic examinations of four cores to assess their effect on long-term serviceability of the substructure; and,
e. Determination of atmospheric carbonation-induced versus chloride-induced corrosion of steel in concrete in the presence of oxygen and moisture from detailed petrographic examinations, and, water-soluble chloride analyses, respectively to explain formation of reddish-brown corrosion stains and associated cracking and spalling seen in the field photos of substructure.

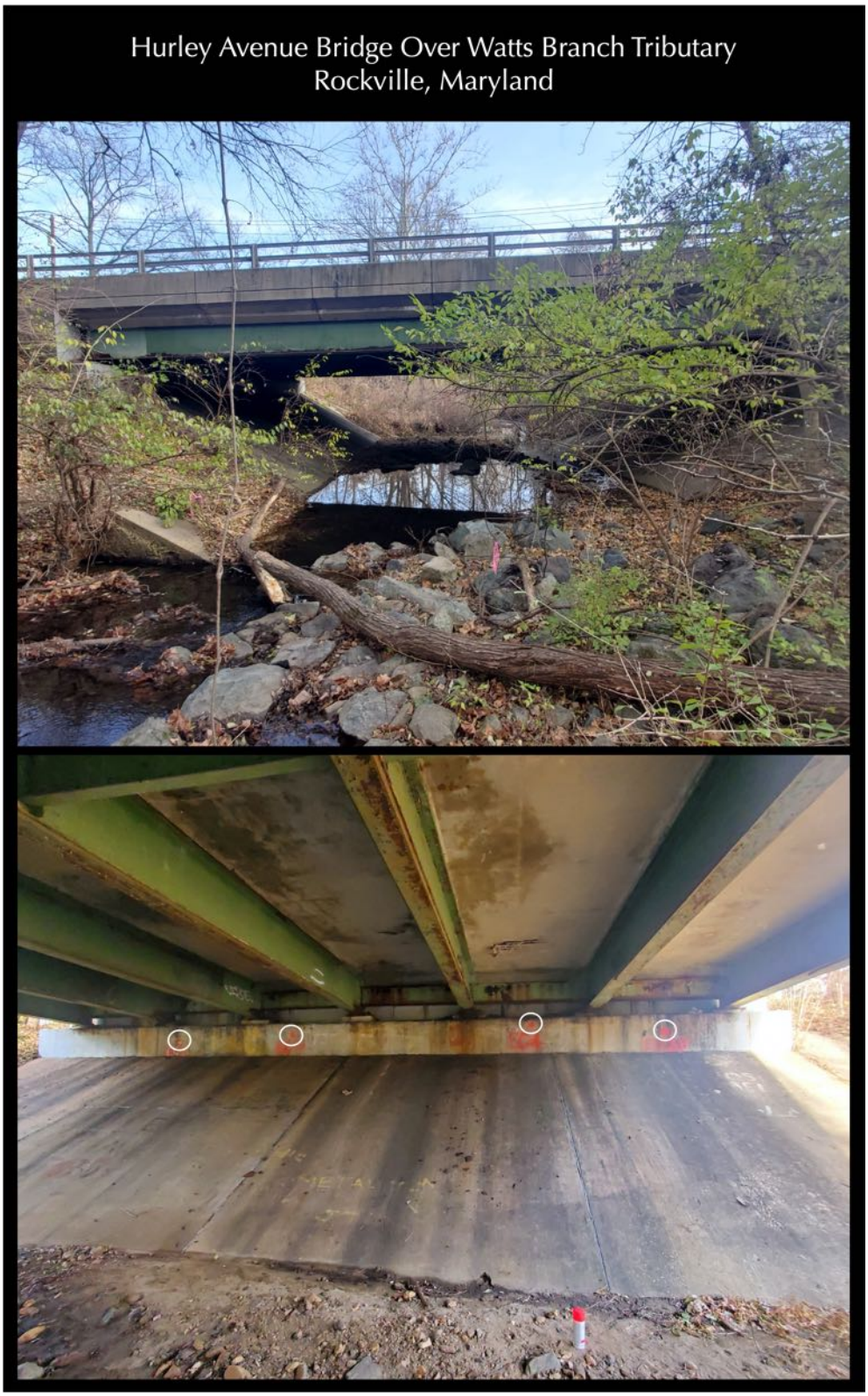

Figure 1: Field photos of Hurley Avenue bridge over Watts branch tributary in Rockville, Maryland from where concrete cores and powers were collected for laboratoty studies. The bottom photo shows the bridge substructure and some of the locations of concrete cores collected (circled).

Figure 2: Field photos of bridge substructure and locations of cores of the EC-series (top) and WC-series (bottom) collected (exact core locations of both series are circled). Also shown are concrete spalls, cracks, and reddish brown stains from corrosion of reinforcing steel in concrete.

Figure 3: Field photos of bridge substructure showing locations of EC-series cores - EC-1P and EC-2P (circled) and associated concrete spalls, cracks, and reddish brown stains from corrosion of reinforcing steel in concrete.

Figure 4: Field photos of bridge substructure showing locations of WC-series cores - WC-1P and WC-2P (circled) and associated concrete spalls, cracks, and reddish brown stains from corrosion of reinforcing steel in concrete.

METHODOLOGIES

PETROGRAPHIC EXAMINATIONS

Four cores EC-1P, EC-2P, WC-1P, and WC-2P were examined using the methods and procedures of ASTM C 856 "Standard Practice for Petrographic Examination of Hardened Concrete." Details of concrete petrography, and sample preparation techniques for petrographic examinations of concrete are provided in Jana (2006).

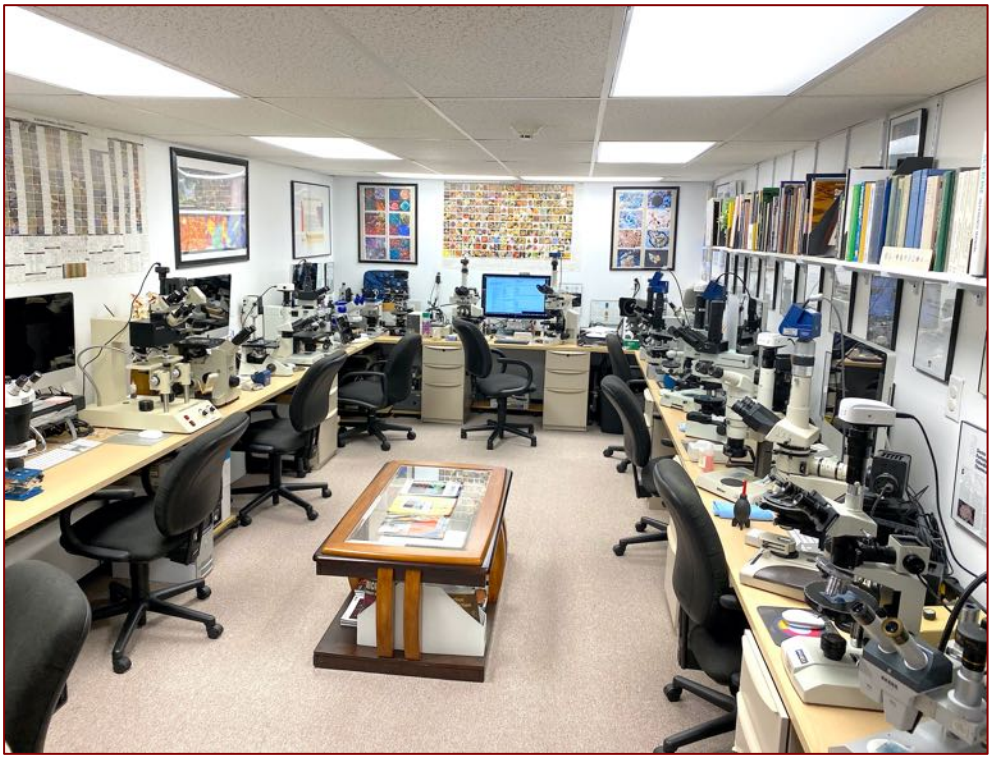

Figure 5: Some of the optical microscopes in the optical microscopy laboratory that were used for this investigation, e.g., from low-power stereo microscope, to high-power transmitted-light stereo-zoom microscope with plane and crossed-polarized light, to epi-fluorescent microscope for observations of florescent dye-mixed epoxy impregnated thin sections, and petrographic microscopes for further observation of thin section of concrete.

Briefly, the steps followed during petrographic examination of sample include:

i. Visual examinations of the cores, as received, including adequate documentation of dimensions, measurements, condition, physical properties, integrity, etc.;
ii. Low-power stereo microscopical examinations of as-received, saw-cut and freshly fractured sections, and lapped cross sections of samples for evaluation of texture, air-void systems, and compositions;
iii. Examinations of oil immersion mounts in a petrographic microscope for mineralogical compositions of specific areas of interests;
iv. Examinations of blue dye-mixed (to highlight open spaces, cracks, air voids, etc.) low-viscosity epoxy-impregnated large area (50 mm × 75 mm) thin sections of concrete in a petrographic microscope for detailed compositional and microstructural analyses;
v. Photographing the samples, as received, and at various stages of preparation with a digital camera and a flatbed scanner; and,
vi. Photomicrographs of lapped sections and thin sections of concrete taken with stereomicroscope and petrographic microscope, respectively to provide detailed compositional and mineralogical information of concrete.

ANALYSES OF CHLORIDE CONTENTS

Water-soluble chloride contents at 1 in., 3 in., 5 in., 1 in., and 15 in. depths at the locations of eight cores were determined by potentiometric titration according to the procedures of ASTM C 1218.

Steps followed in determination of chloride contents are as follows:

- Sample Selection and Sectioning – Approximately 10 grams of concrete powder was collected from each sample bag of concrete powder for chloride analysis.
- Concrete powders were passed through US No. 20 sieve to assure their proper grain size for chloride analyses.
- Water Digestion – About 10±0.01 gm. of powdered sample was measured and dispersed with deionized water in a 250-mL beaker, stirring and breaking up any lumps with a glass rod.
- Further Digestion – Covered the beaker from previous step with a watch glass, and heated rapidly to boiling, but not more than 10 minutes. Removed from hot plate and cooled the filtrate to room temperature.
- Filtration – Filtered the sample solution, under vacuum suction, through two 2.5-micron filter papers fitted to a 90 mm diameter Buchner funnel in a 500-mL filtration flask. Transferred the filtrate from the flask to the original beaker, which was already rinsed twice with water, along with the flask. The final volume was 200-mL.

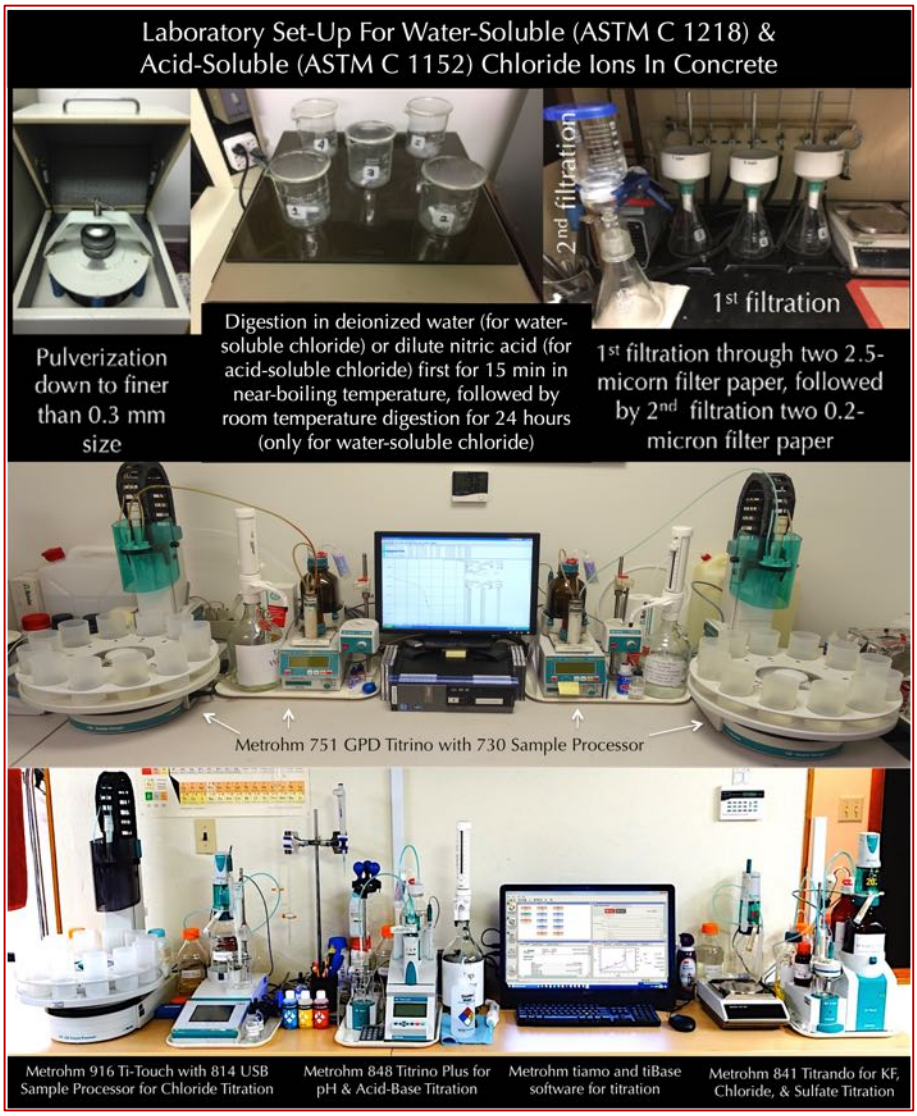

Figure 6: Set-ups for sample preparation and analyses of acid and water-soluble chloride ions of by potentiometric titration.

- Filtrates of water-digested samples were used for determination of chloride ions by potentiometric titration by following the methods of ASTM C 1218 in a Metrohm 751 DMS Titrino titrator with attached 730 automated sample processor.
- Water-soluble chloride contents were determined from sample weights and equivalent points of titration by using the formula percent chloride by weight of concrete = 0.177 times [equivalent point of titration divided by sample weight in grams].

COMPRESSIVE STRENGTHS

Portions of all four concrete cores received were trimmed for compressive strength tests according to the procedures of ASTM C 42. Figures 7 to 10 show the portions that are selected for compressive strengths, and, the remaining portions selected for petrographic examinations.

SAMPLES

Figures 7 through 10 show the four cores as received. The following Table provides preliminary descriptions of cores.

Core ID	Diameter	Lengths	Exposed Surface	Bottom Surface	Cracking	Reinforcing Steel	Core Condition
EC-1P (Fig. 7)	1¾ in. (45 mm)	2¾ in. (70 mm) + 4½ in. (120 mm)	Severely fragmented	Fresh fractured	None	None	Fragmented into two intact pieces and many rubbles, Dry, Ring-sounded
EC-2P (Fig. 8)	1¾ in. (45 mm)	6¼ in. (160 mm)	Severely fragmented; top 5 mm of exposed surface is spalled off from main body	Fresh fractured	Crack at 5 mm depth spalled top portion from main body	None	Intact except top spalling, Dry, Ring-sounded
WC-1P (Fig. 9)	1¾ in. (45 mm)	5¼ in. (130 mm)	Fresh fractured	Fresh fractured with impression of No. 4 reinforcing steel	None	A loose corroded reinforcing steel	Intact except a few rubbles and a loose, corroded reinforcing steel, Dry, Ring-sounded
WC-2P (Fig. 10)	1¾ in. (45 mm)	1¾ in. (45 mm) + 4 in. (100 mm)	Smooth, dense, hard, dark gray, trowel-finished	Fresh fractured	Cracked into two pieces	None	Cracked into two pieces, Dry, Ring-sounded

Table 1: Detailed preliminary descriptions and dimensions of four cores, as received.

- Figures 7 through 10 show the overall conditions of four cores received and the portions selected for petrographic examinations and compressive strength tests.
- Evidence of spalling of concrete and corroded steel are found in the cores.
- Overall fragmented natures of cores are indicative of pre-existing cracks in the substructure at the locations of cores.

- Concrete in all four cores show similar siliceous (quartzite) gravel aggregates that are well-graded and well-distributed through the depths of the cores.
- All cores show some discoloration of paste due to atmospheric carbonation during service.

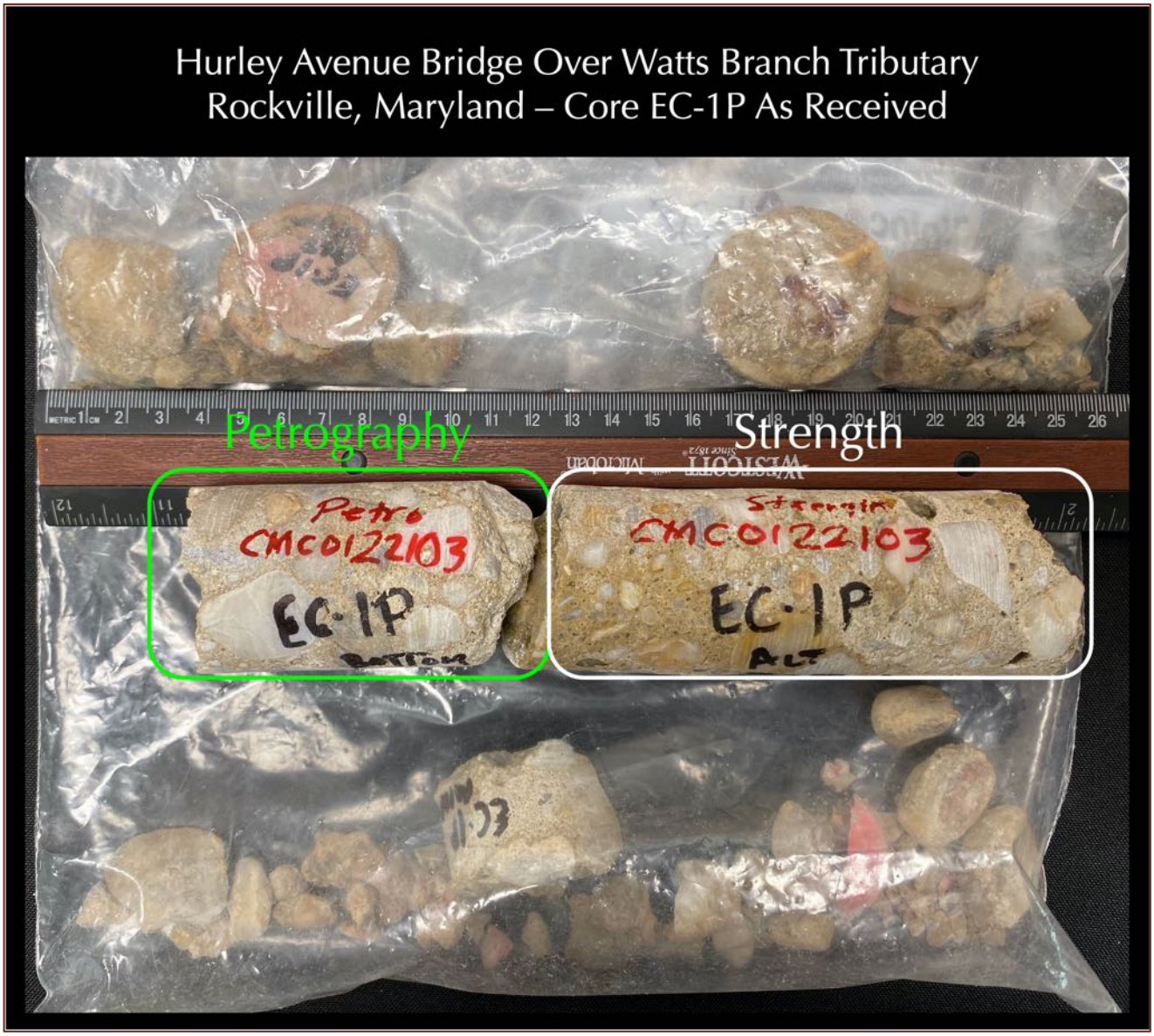

Figure 7: Portions of Core EC-1P, as received as well as the portions selected for compressive strength test and detailed petrographic examinations.

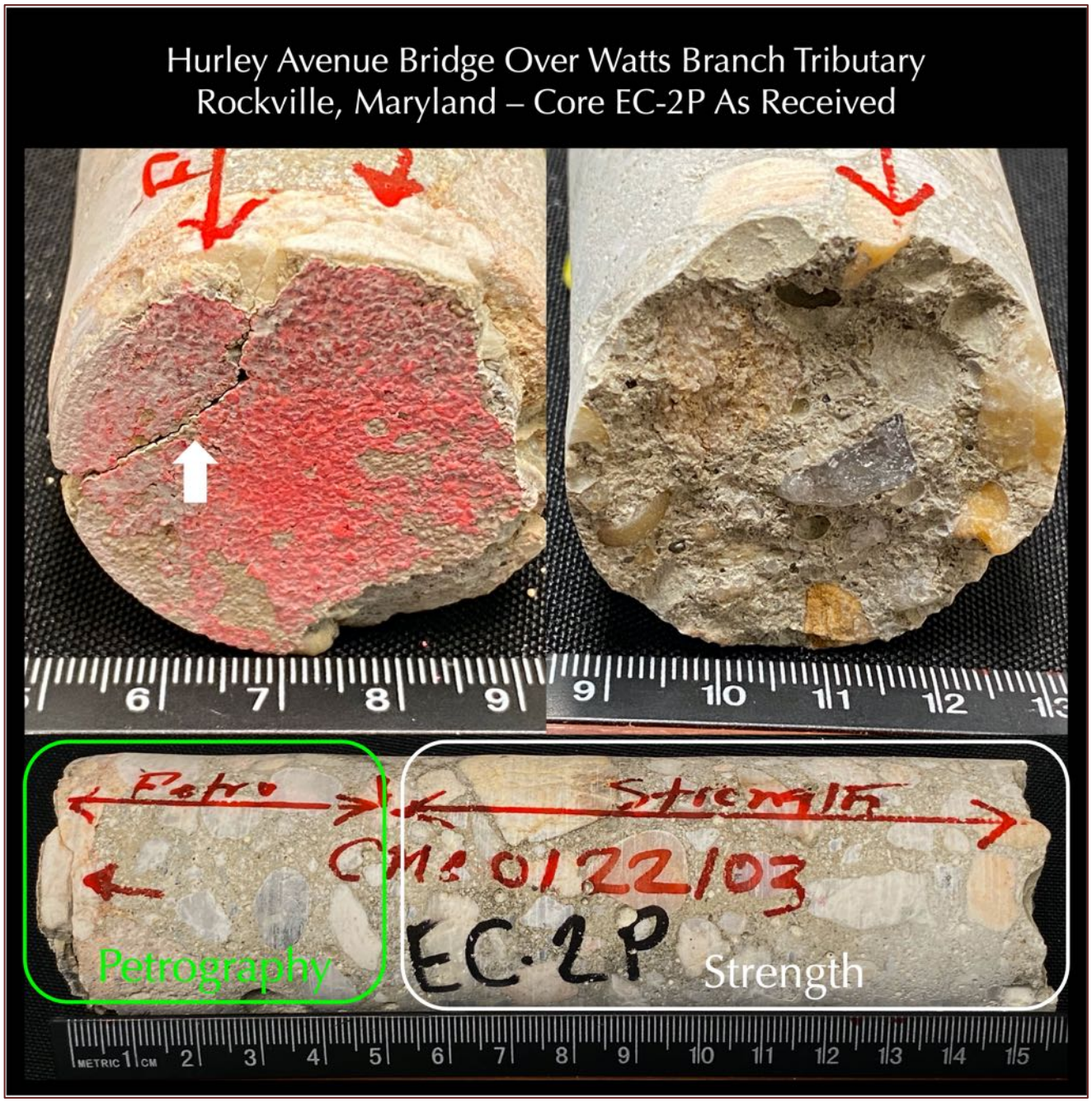

Figure 8: Portions of Core EC-2P, as received as well as the portions selected for compressive strength test and detailed petrographic examinations. Notice the partial spall at a depth of 5 mm from the exposed end and resultant crack on the exposed surface at top left photo and fresh fractured bottom end in the top right photo.

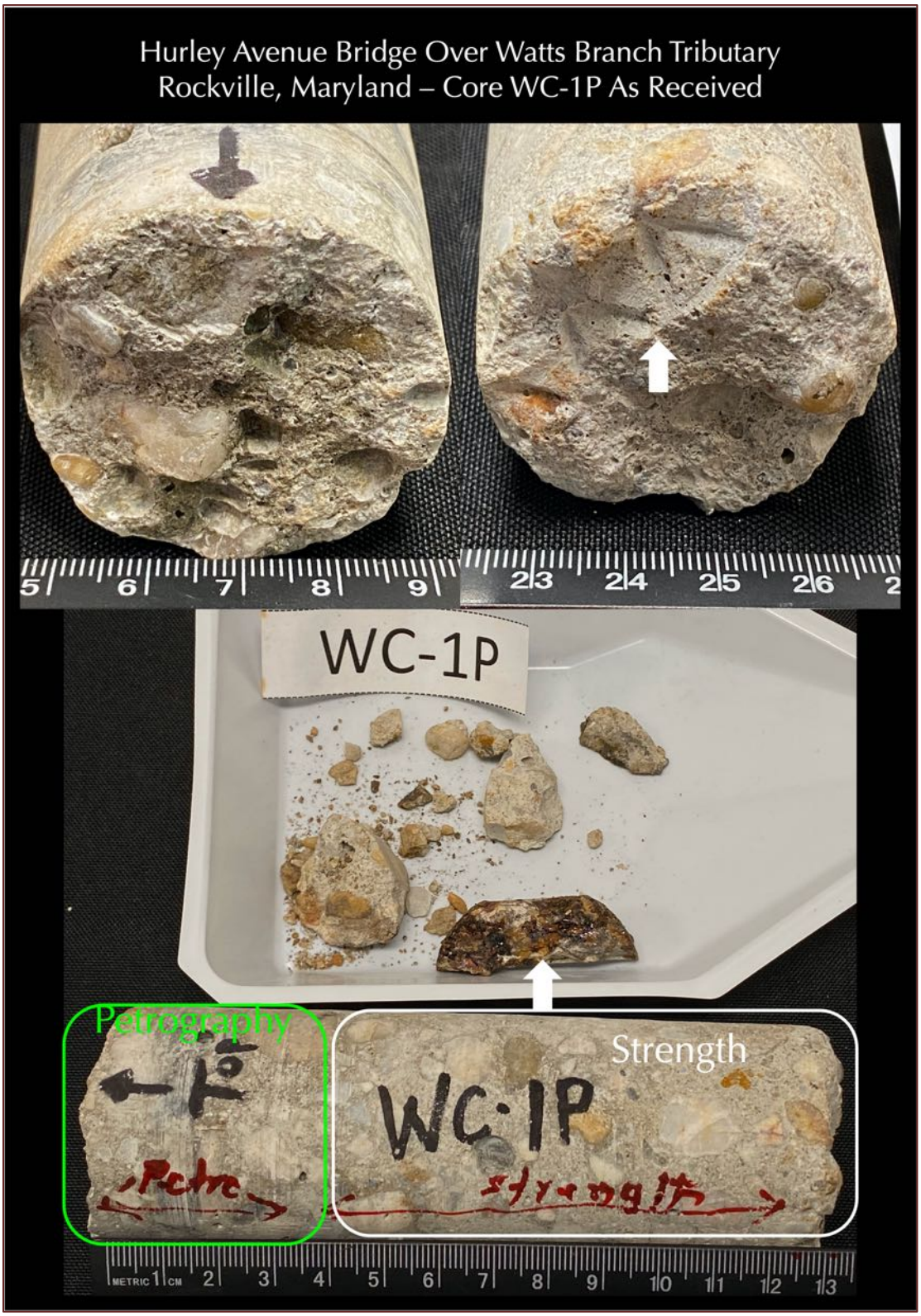

Figure 9: Portions of Core WC-1P, as received as well as the portions selected for compressive strength test and detailed petrographic examinations. Notice the fresh fractured ends of core in the top photo. A corroded steel (arrow) was present in the sample bag along with some rubbles.

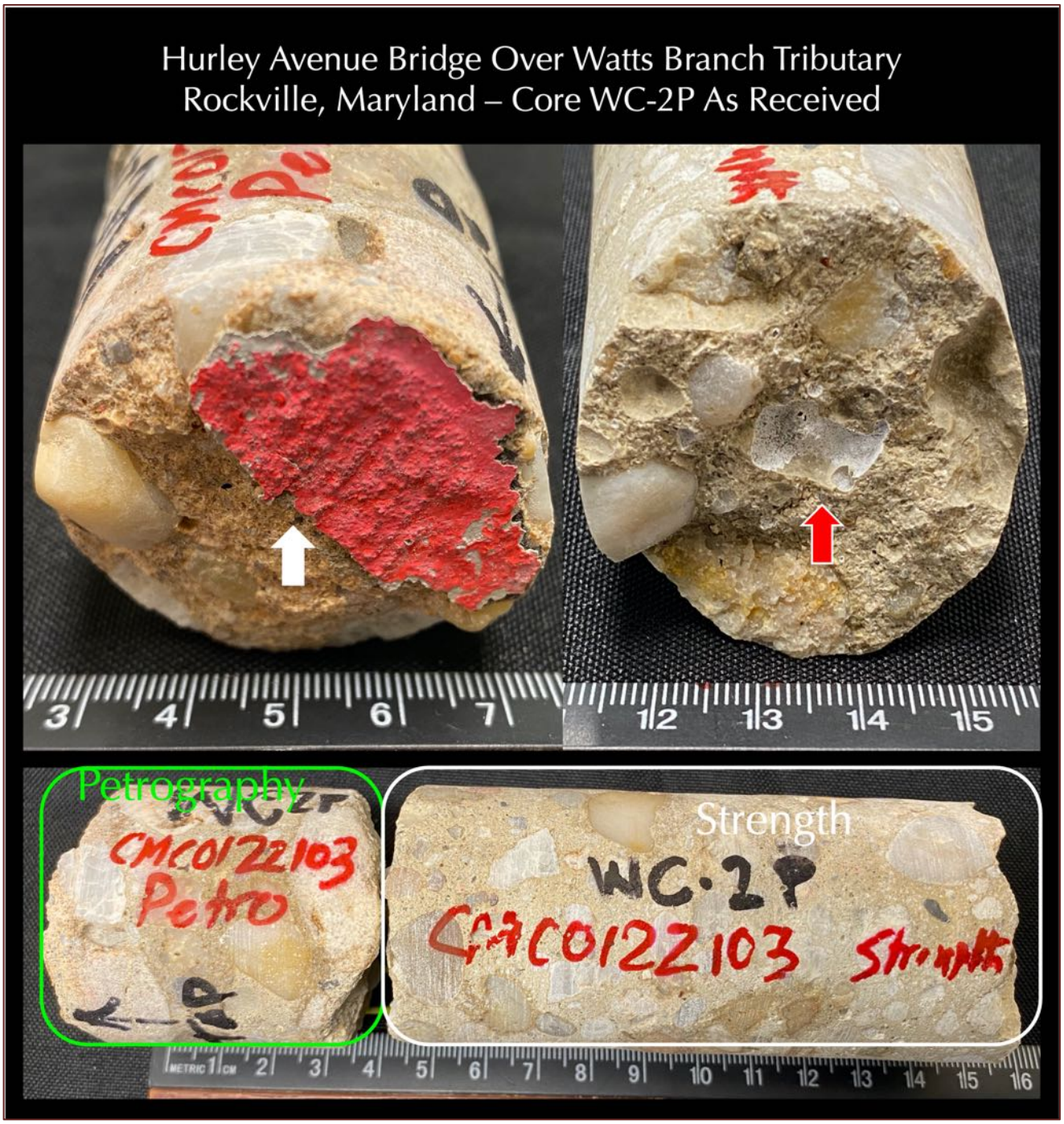

Figure 10: Portions of Core WC-2P, as received as well as the portions selected for compressive strength test and detailed petrographic examinations. Notice the partial spall from the exposed end at top left photo, and, fresh fractured bottom end in the top right photo. The red arrow in the fresh fractured surface shows a large entrapped void, which is lined with white secondary deposits that are determined to be alkali-silica reaction gel.

PETROGRAPHIC EXAMINATIONS

LAPPED CROSS SECTIONS

Figure 11: Lapped cross section of Core EC-1P showing siliceous (quartzite) gravel coarse aggregate having a nominal maximum size of ¾ in. (19 mm); natural siliceous (quartz, feldspar) sand fine aggregate, and interstitial paste. Coarse aggregate particles are well-graded, and well-distributed, some gravel particles show dark weathering and reaction rims.

Figure 12: Lapped cross section of Core EC-2P showing siliceous (quartzite) gravel coarse aggregate having a nominal maximum size of ¾ in. (19 mm); natural siliceous (quartz, feldspar) sand fine aggregate, and interstitial paste. The very top ash-colored thin, discontinuous protective membrane is marked by thin yellow arrows whereas the thick white arrows show the near-surface crack at a depth of 5 mm that has delaminated the top portion from the main body. Coarse aggregate particles are poorly graded, and well-distributed. Some gravel particles show dark weathering and reaction rims.

Figure 13: Lapped cross section of Core WC-1P showing siliceous (quartzite) gravel coarse aggregate having a nominal maximum size of 1 in. (25 mm); natural siliceous (quartz, feldspar) sand fine aggregate, and interstitial paste. Coarse aggregate particles are poorly graded, and well-distributed. Some gravel particles show dark weathering and reaction rims.

Figure 14: Lapped cross section of Core WC-2P showing lightly crushed siliceous (quartzite) gravel coarse aggregate having a nominal maximum size of ¾ in. (19 mm); natural siliceous (quartz, feldspar) sand fine aggregate, and interstitial paste. Coarse aggregate particles are well-graded, and well-distributed. Some gravel particles show dark weathering and reaction rims.

SAW-CUT CROSS SECTIONS AND CARBONATION

Figure 15: Saw-cut cross section of Core EC-1P (portion left after preparation of thin section, hence showing remains of some blue epoxy mostly in the cracks and voids, which was used for impregnation of the section for thin sectioning). The cross section was treated with phenolphthalein alcoholic solution to determine the depth of carbonation, where the non-carbonated concrete turns pink from treatment, whereas carbonated concrete maintains the original color tone. The section shows non-carbonated concrete throughout the examined area.

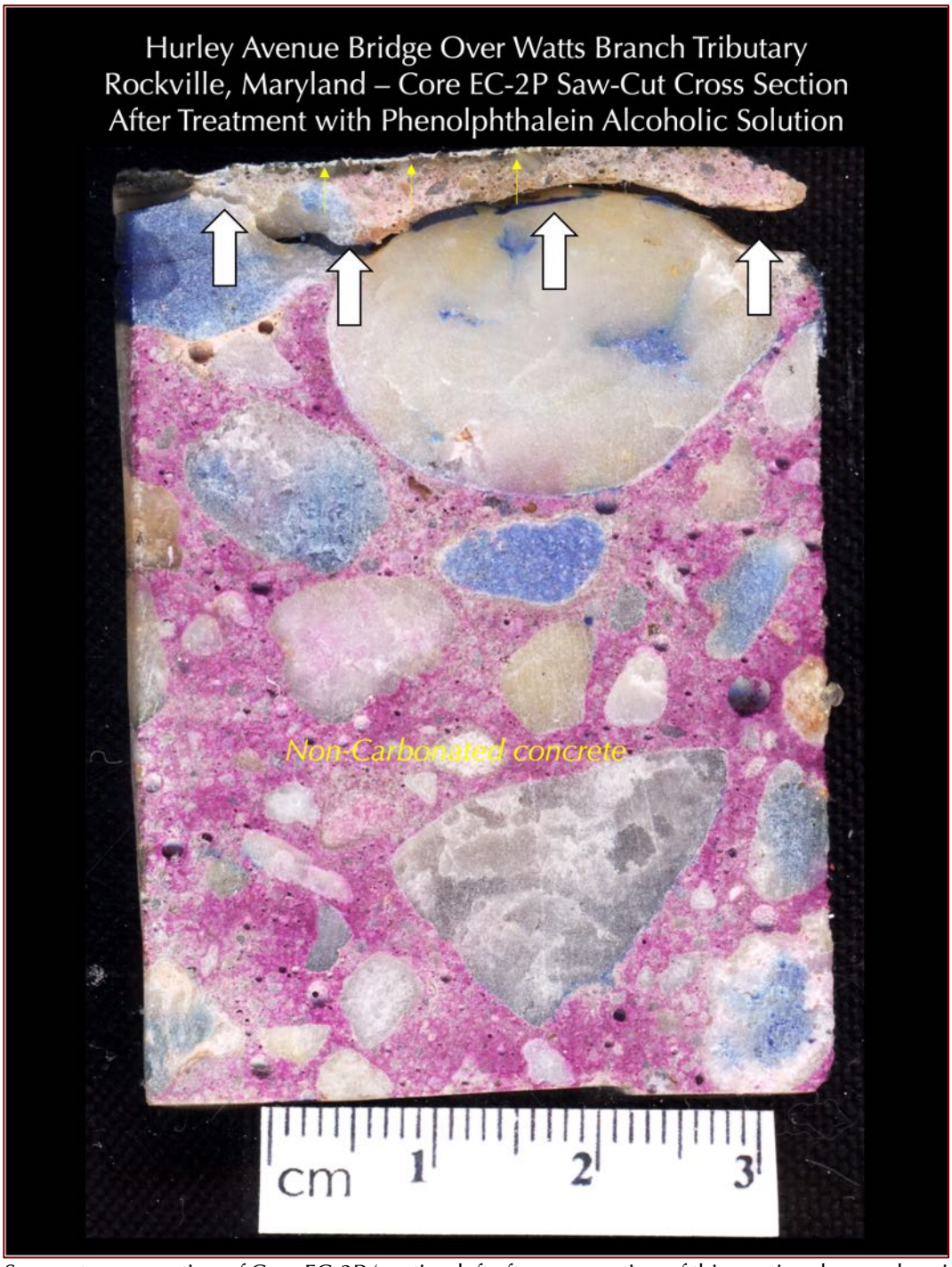

Figure 16: Saw-cut cross section of Core EC-2P (portion left after preparation of thin section, hence showing remains of some blue epoxy mostly in the cracks and voids, which was used for impregnation of the section for thin sectioning). The cross section was treated with phenolphthalein alcoholic solution to determine the depth of carbonation, where the non-carbonated concrete turns pink from treatment, whereas carbonated concrete maintains the original color tone. The section shows non-carbonated concrete throughout the examined area except the top 5 mm that shows atmospheric carbonation during service. Thin yellow arrows show discontinuous protective membrane, whereas thick white arrows show the near-surface crack.

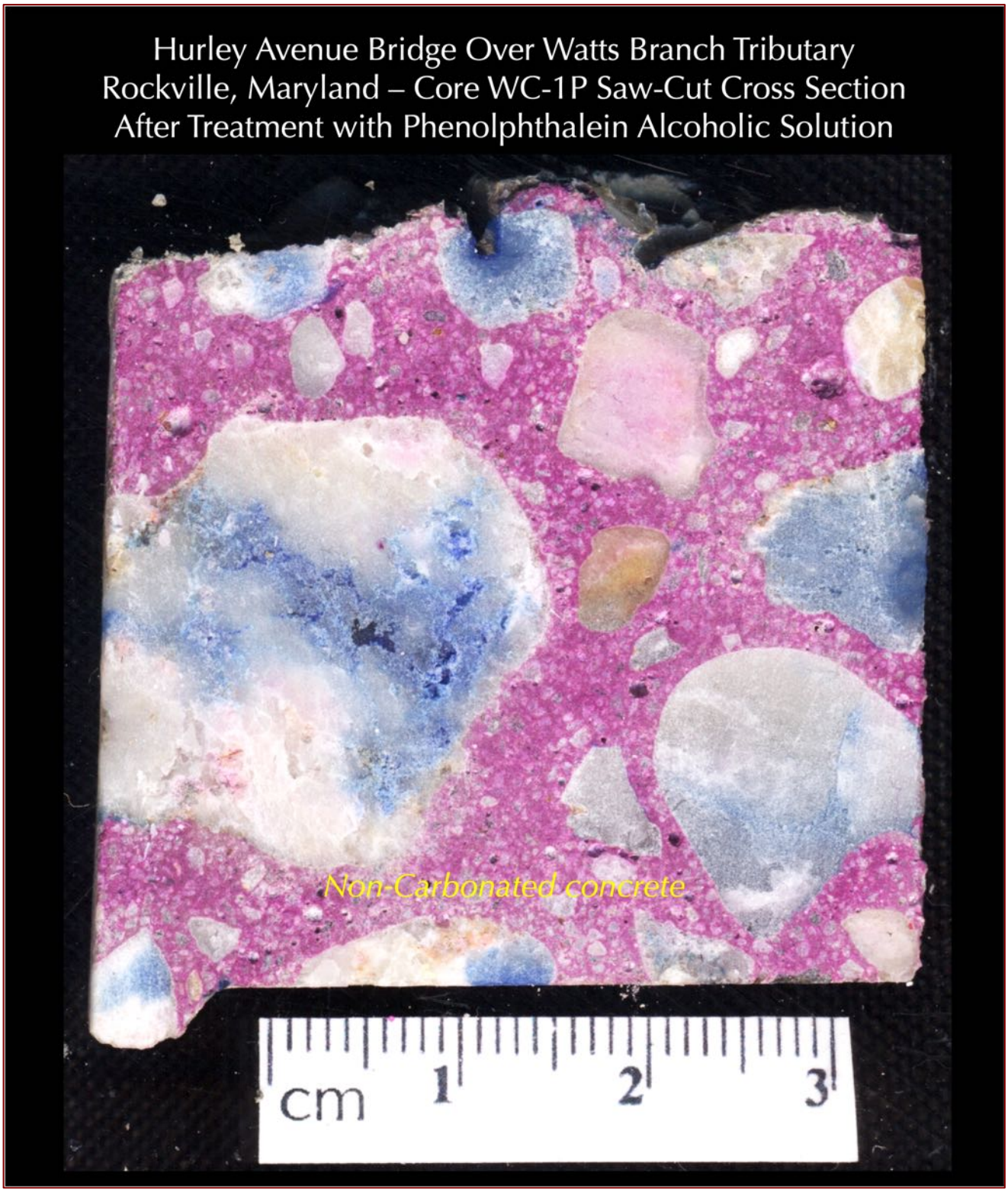

Figure 17: Saw-cut cross section of Core WC-1P (portion left after preparation of thin section, hence showing remains of some blue epoxy mostly in the cracks and voids, which was used for impregnation of the section for thin sectioning). The cross section was treated with phenolphthalein alcoholic solution to determine the depth of carbonation, where the non-carbonated concrete turns pink from treatment, whereas carbonated concrete maintains the original color tone. The section shows non-carbonated concrete throughout the examined area.

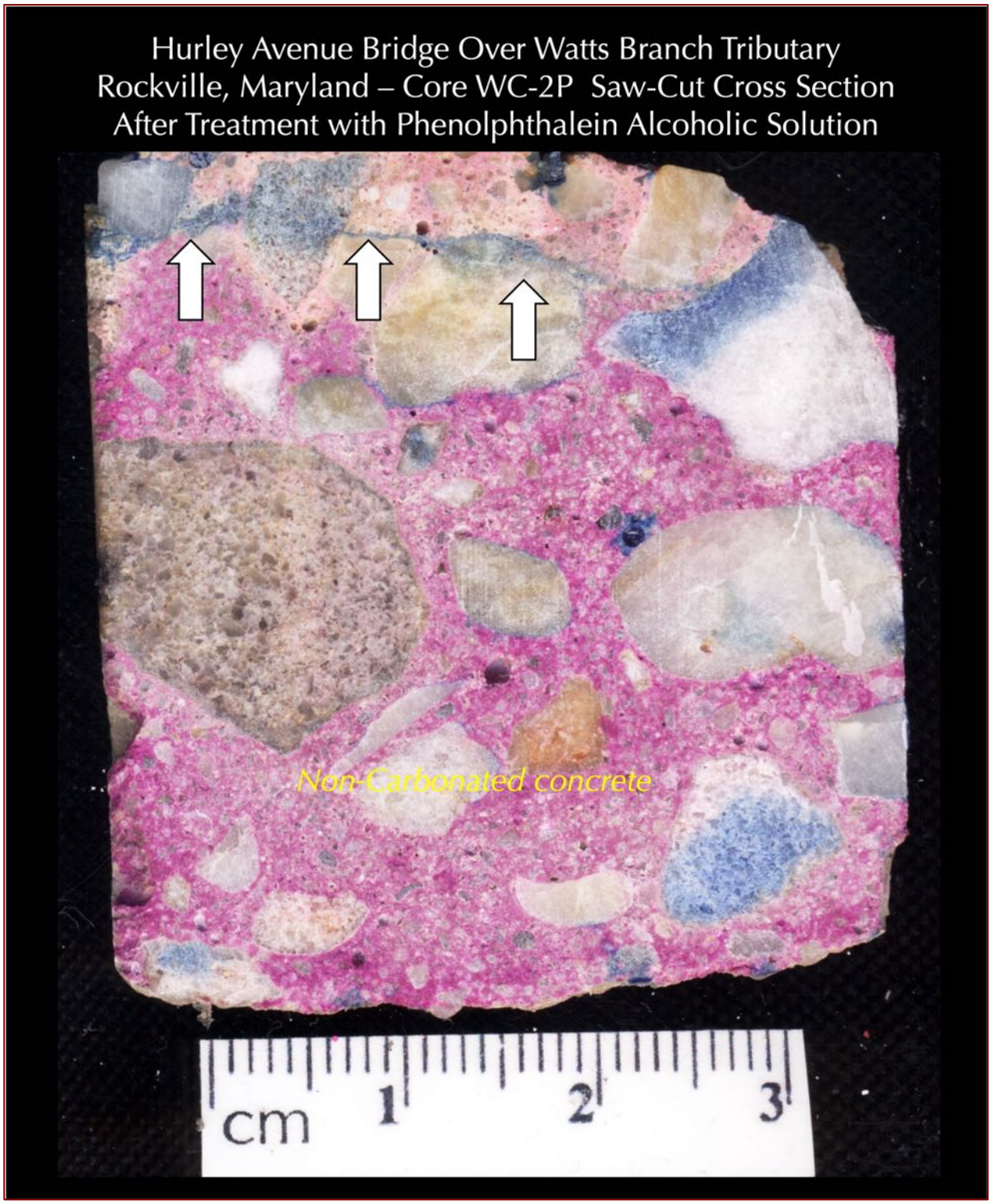

Figure 18: Saw-cut cross section of Core WC-2P (portion left after preparation of thin section, hence showing remains of some blue epoxy mostly in the cracks and voids, which was used for impregnation of the section for thin sectioning). The cross section was treated with phenolphthalein alcoholic solution to determine the depth of carbonation, where the non-carbonated concrete turns pink from treatment, whereas carbonated concrete maintains the original color tone. The section shows non-carbonated concrete throughout the examined area except the top 5 mm that shows atmospheric carbonation during service.

MICROGRAPHS OF LAPPED CROSS SECTIONS

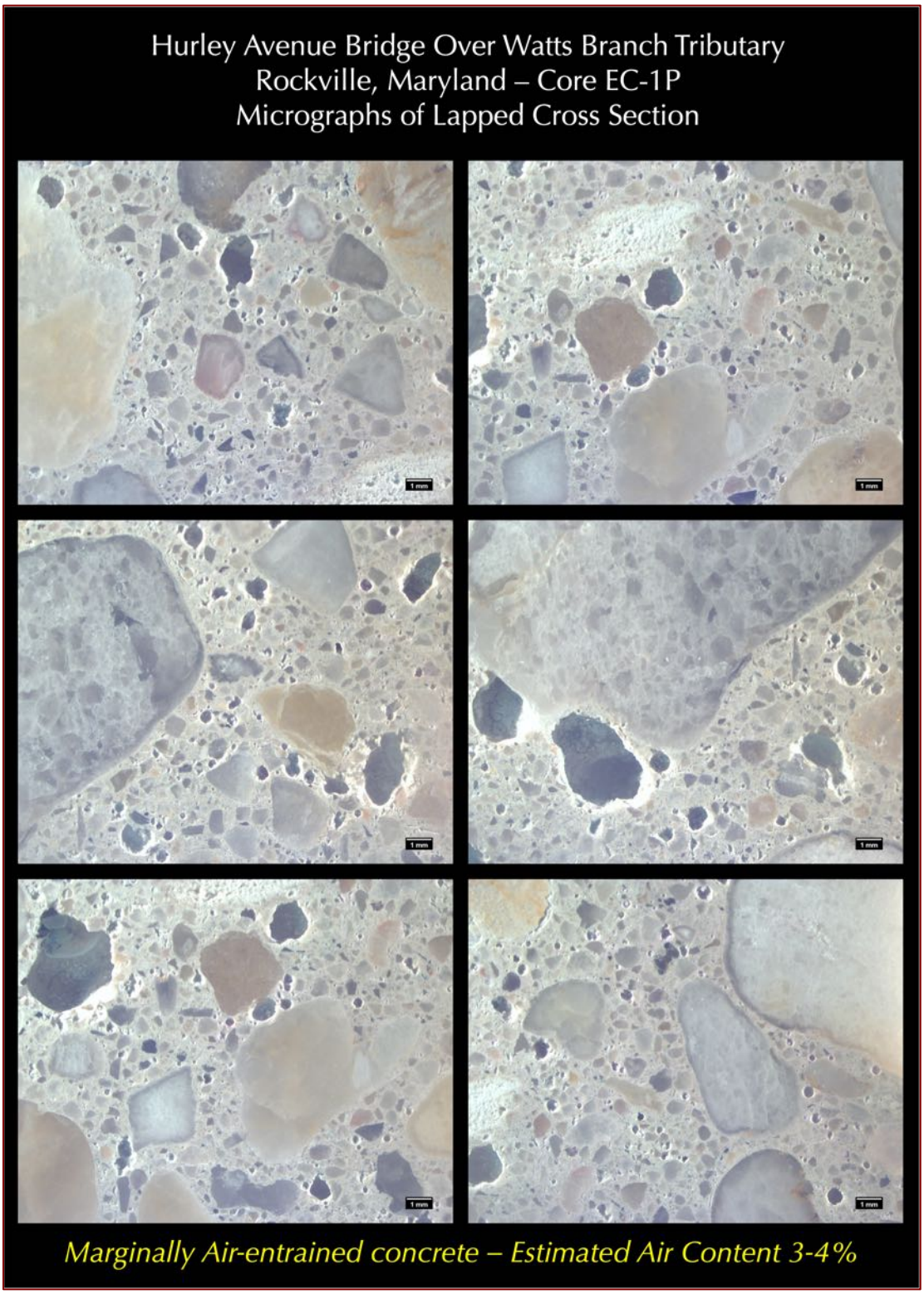

Figure 19: Micrographs of lapped cross section of Core EC-1P showing the overall marginally air-entrained nature of concrete consisting of: (a) numerous fine, discrete, spherical and near-spherical entrained air voids of sizes 1 mm or less, and (b) a few coarse, near-spherical, and irregularly-shaped entrapped air voids of sizes greater than 1 mm. Total air content is estimated to be 3 to 4 percent.

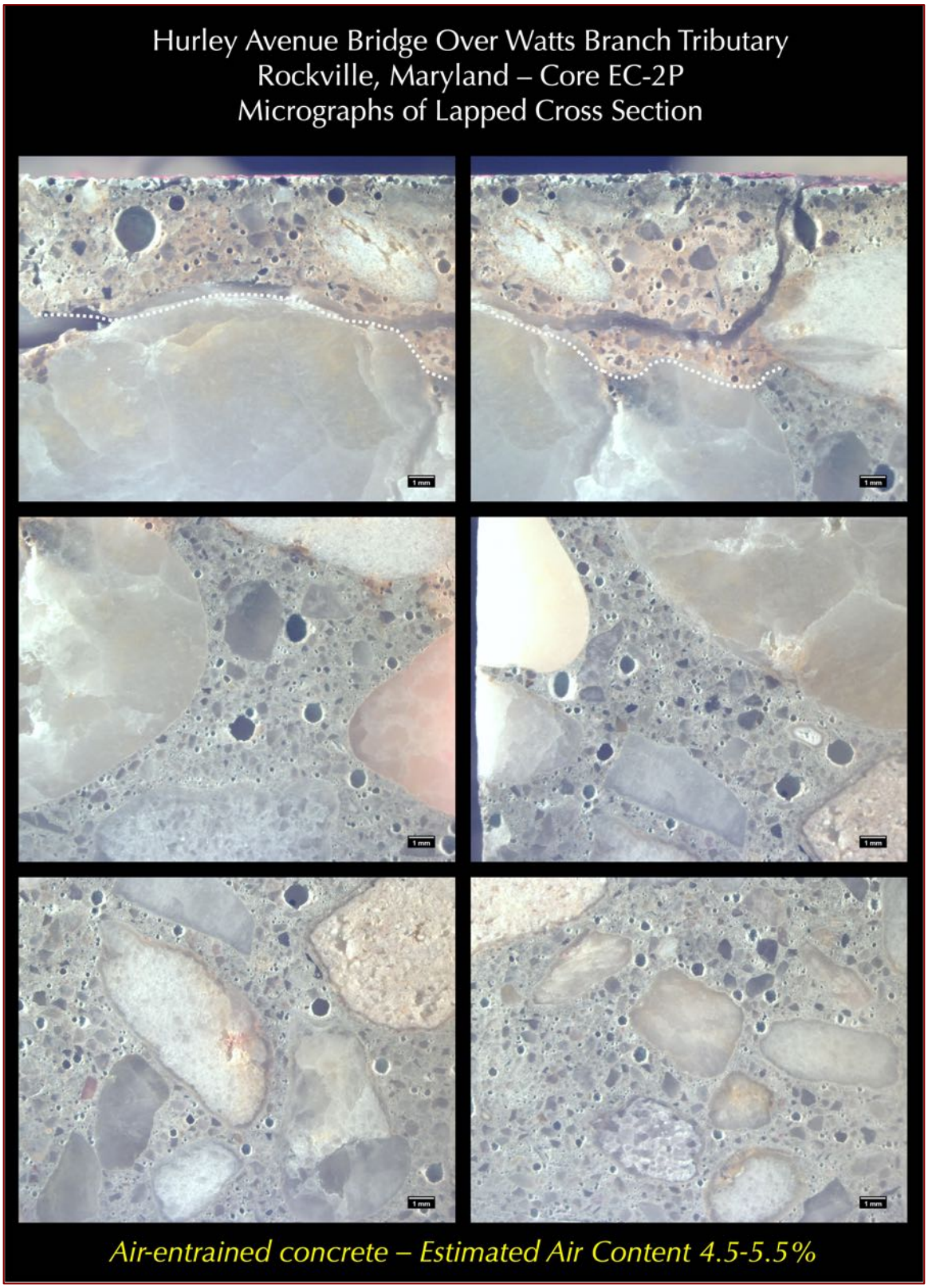

Figure 20: Micrographs of lapped cross section of Core EC-2P showing the overall air-entrained nature of concrete consisting of: (a) numerous fine, discrete, spherical and near-spherical entrained air voids of sizes 1 mm or less, and (b) a few coarse, near-spherical, and irregularly-shaped entrapped air voids of sizes greater than 1 mm. Total air content is estimated to be 4.5 to 5.5 percent.

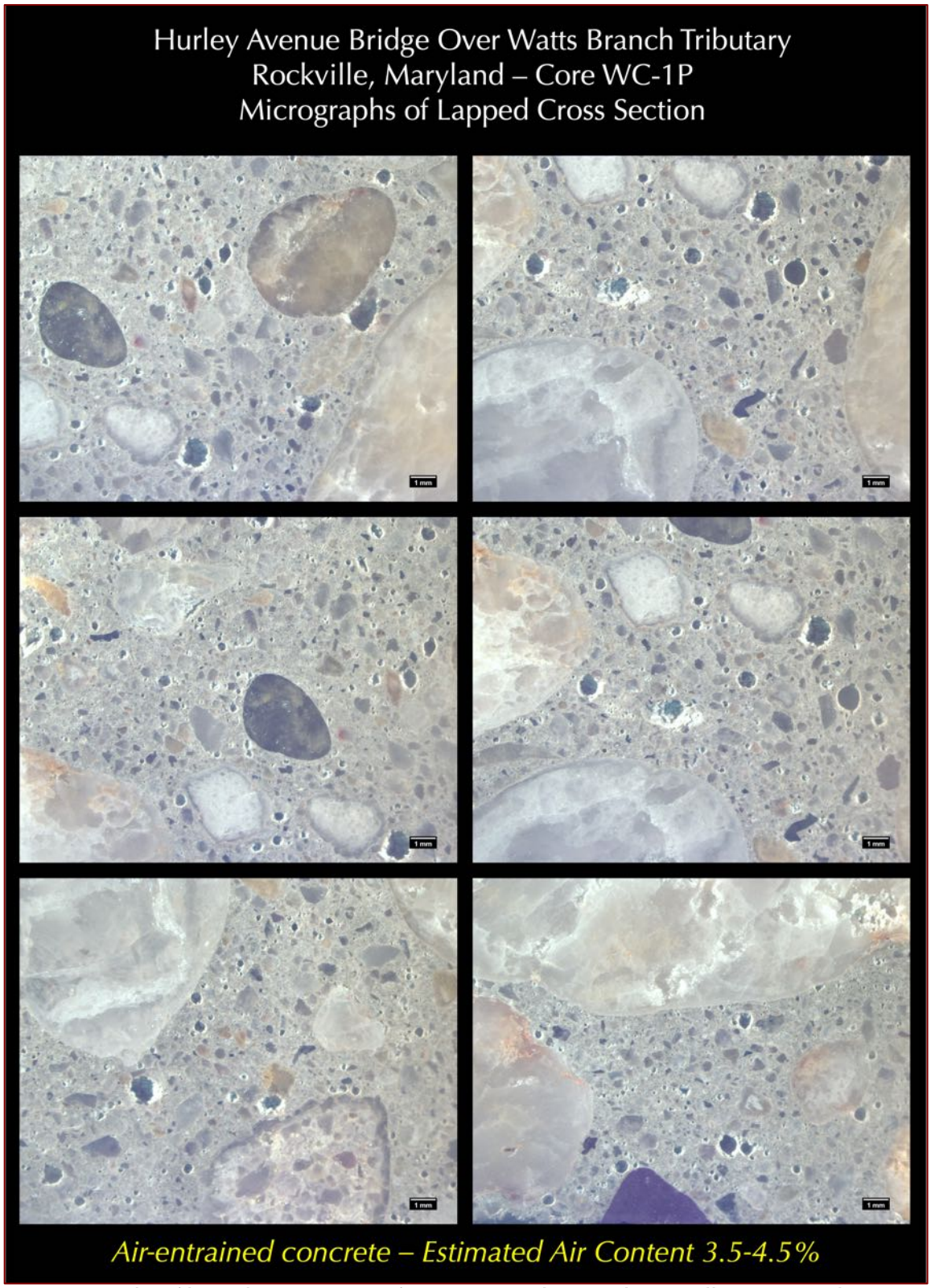

Figure 21: Micrographs of lapped cross section of Core WC-1P showing the overall air-entrained nature of concrete consisting of: (a) numerous fine, discrete, spherical and near-spherical entrained air voids of sizes 1 mm or less, and (b) a few coarse, near-spherical, and irregularly-shaped entrapped air voids of sizes greater than 1 mm. Total air content is estimated to be 3.5 to 4.5 percent.

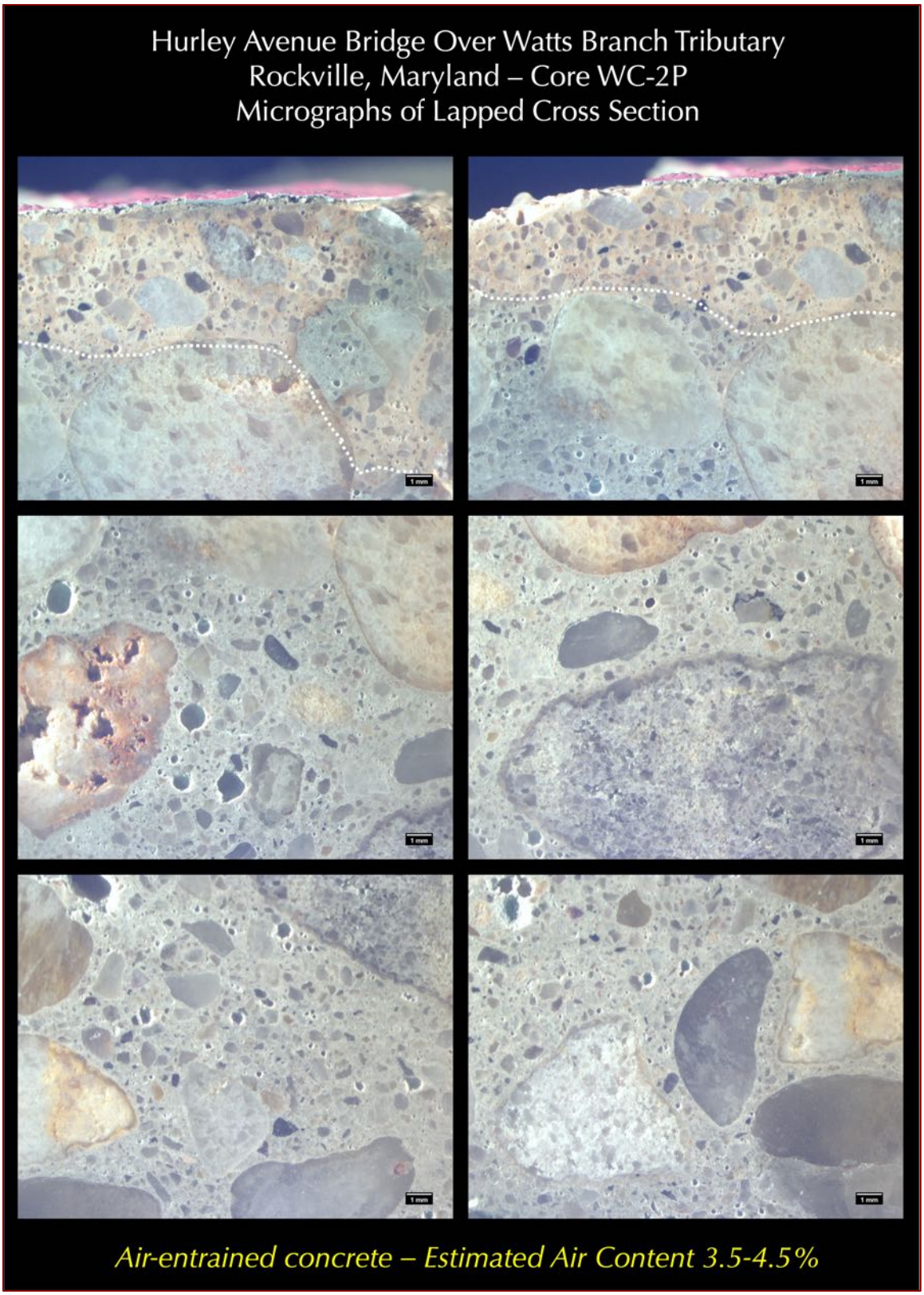

Figure 22: Micrographs of lapped cross section of Core WC-2P showing the overall air-entrained nature of concrete consisting of: (a) numerous fine, discrete, spherical and near-spherical entrained air voids of sizes 1 mm or less, and (b) a few coarse, near-spherical, and irregularly-shaped entrapped air voids of sizes greater than 1 mm. Total air content is estimated to be 3.5 to 4.5 percent.

THIN SECTIONS

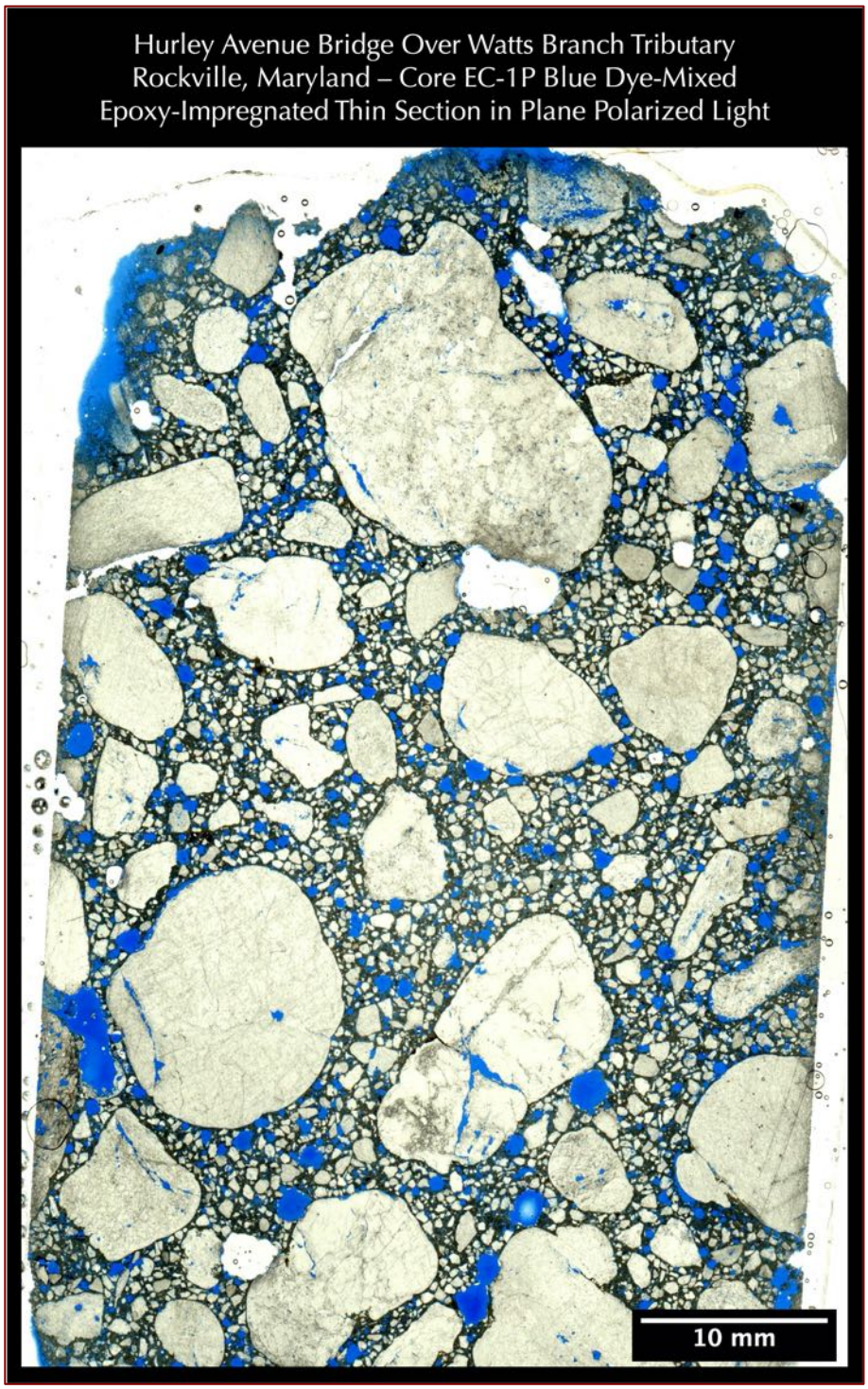

Figure 23: Blue dye-mixed epoxy-impregnated thin section of Core EC-1P in plane polarized light (PPL) showing: (a) siliceous (quartzite) gravel coarse aggregate particles that are ¾ in. (19 mm) in nominal size, well-graded, well-distributed; (b) well-graded, well-distributed natural siliceous sand fine aggregate; and (c) interstitial paste fraction of air-entrained concrete where many entrained and entrappd air voids are highlighted by blue epoxy. The image was formed after scanning the thin section on a film scanner with a polarizing filter.

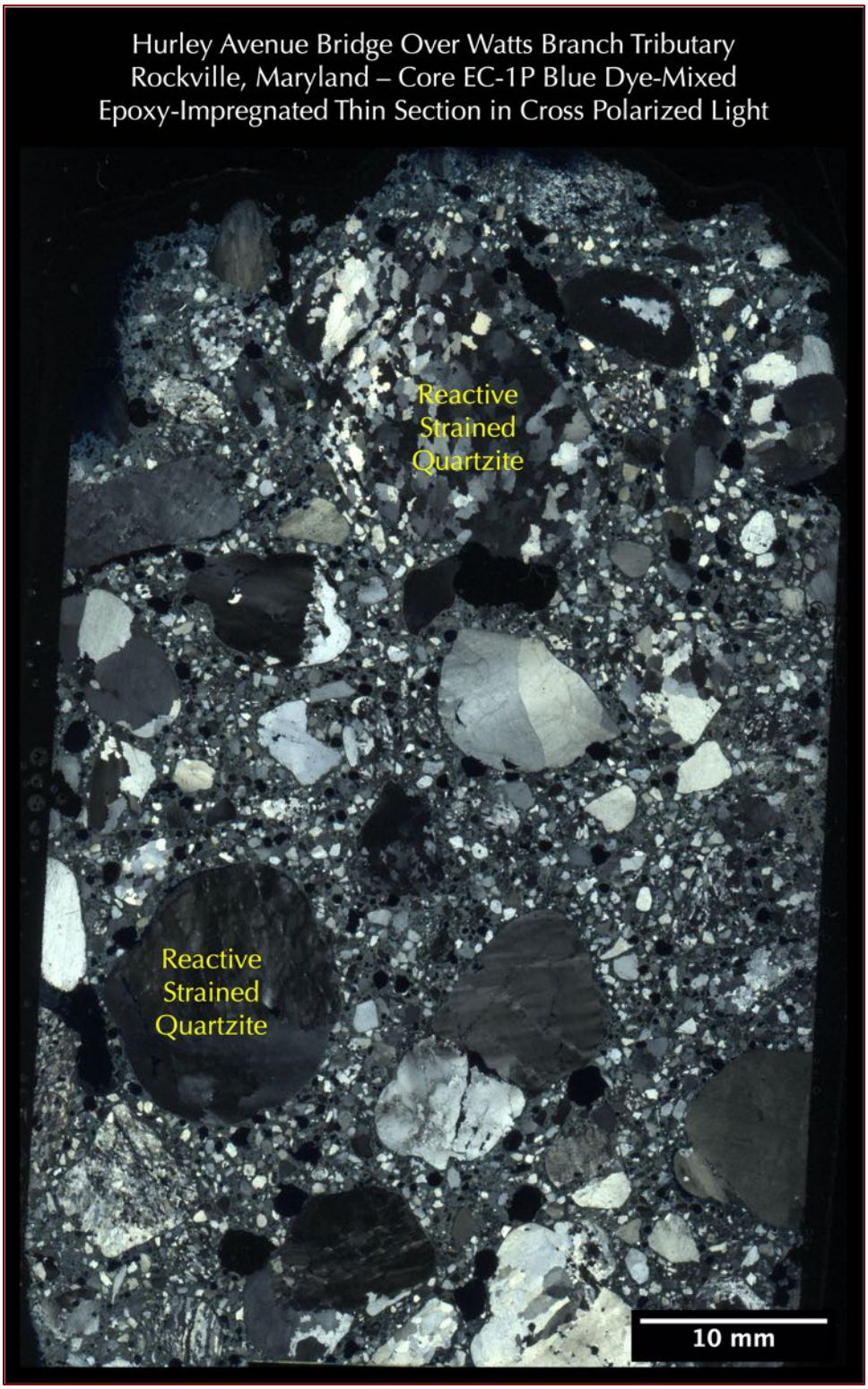

Figure 24: : Blue dye-mixed epoxy-impregnated thin section of Core EC-1P in cross polarized light (XPL) showing: (a) siliceous (quartzite) gravel coarse aggregate particles that are ¾ in. (19 mm) in nominal size; (b) natural siliceous sand fine aggregate; and (c) interstitial paste fraction. Notice the highly strained (deformed) nature of quartzite gravel particles showing undulose (wavy) extinction of strained quartz grains, which are potentially alkali-silica reactive in the presence of moisture and high alkalis in the pore solution of concrete. The image was formed after scanning the thin section on a film scanner with two polarizing filters at perpendicular orientation.

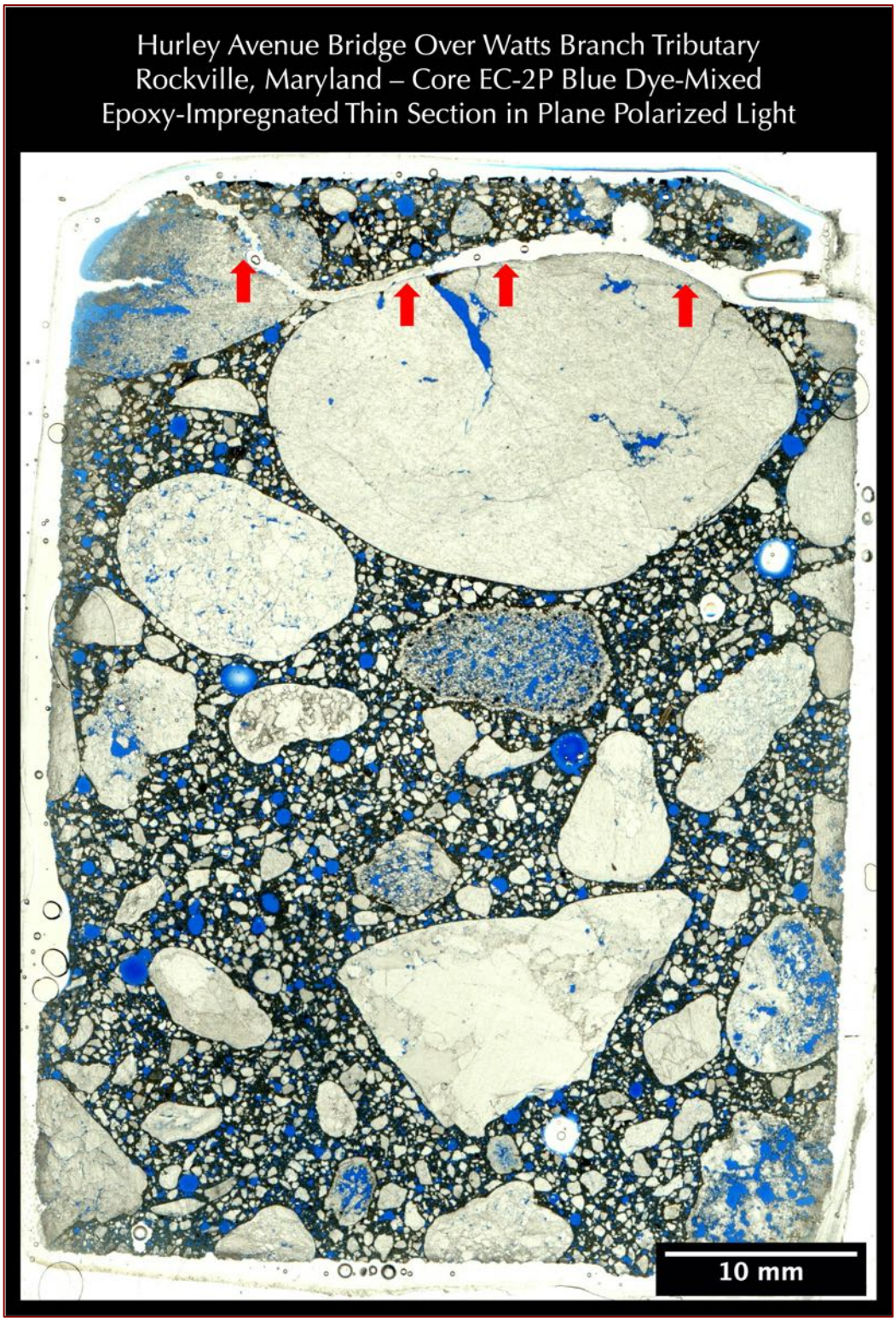

Figure 25: Blue dye-mixed epoxy-impregnated thin section of Core EC-2P in plane polarized light (PPL) showing: (a) siliceous (quartzite) gravel coarse aggregate particles that are ¾ in. (19 mm) in nominal size, poorly graded, well-distributed; (b) well-graded, well-distributed natural siliceous sand fine aggregate; and (c) interstitial paste fraction of air-entrained concrete where many entrained and entrappd air voids are highlighted by blue epoxy. The image was formed after scanning the thin section on a film scanner with a polarizing filter. Some porous gravel particles are highlighted by blue epoxy. The surface crack is shown by red arrows.

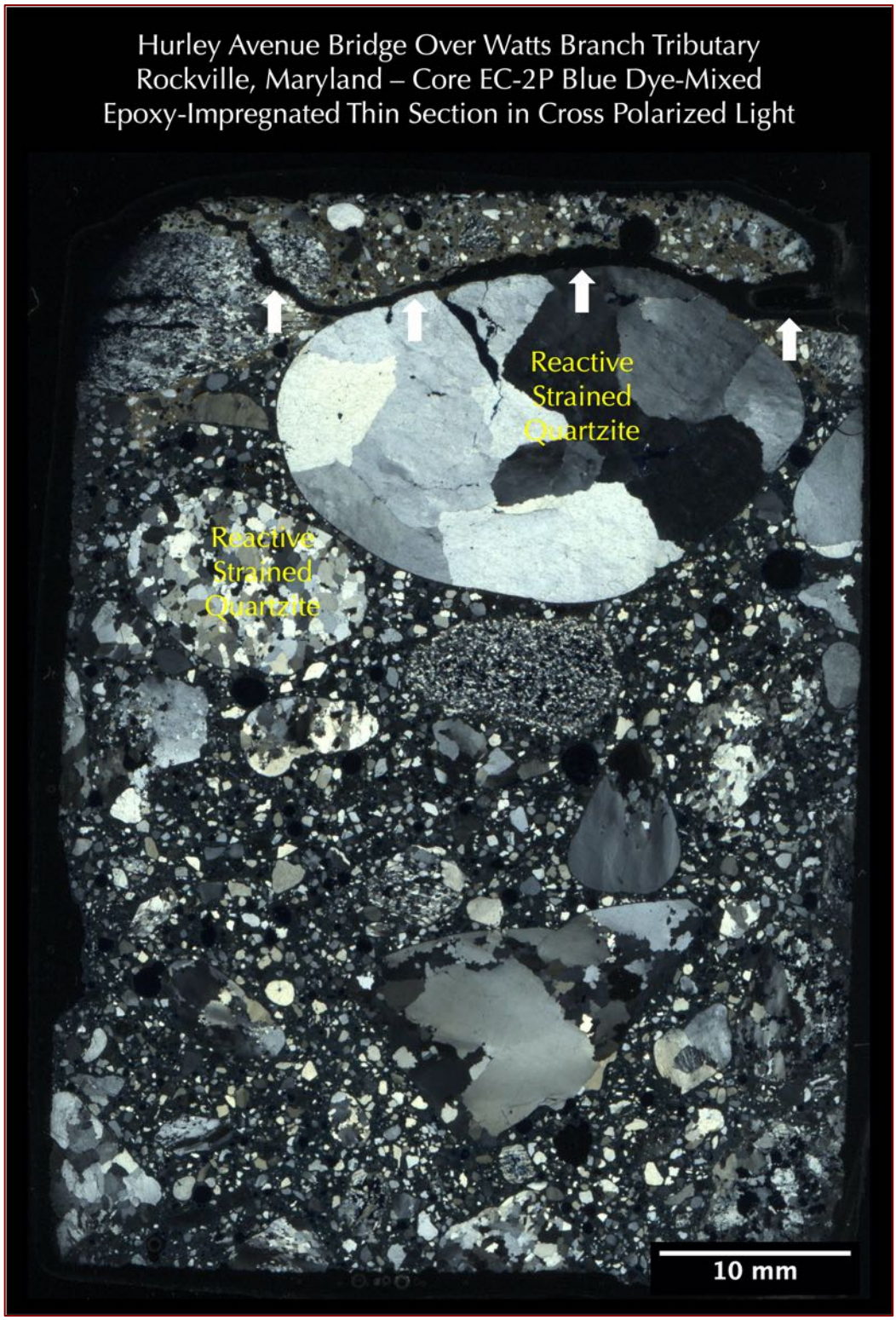

Figure 26: : Blue dye-mixed epoxy-impregnated thin section of Core EC-2P in cross polarized light (XPL) showing: (a) siliceous (quartzite) gravel coarse aggregate particles that are ¾ in. (19 mm) in nominal size; (b) natural siliceous sand fine aggregate; and (c) interstitial paste fraction. Notice the highly strained (deformed) nature of quartzite gravel particles showing undulose (wavy) extinction of strained quartz grains, which are potentially alkali-silica reactive in the presence of moisture and high alkalis in the pore solution of concrete. The image was formed after scanning the thin section on a film scanner with two polarizing filters at perpendicular orientation.

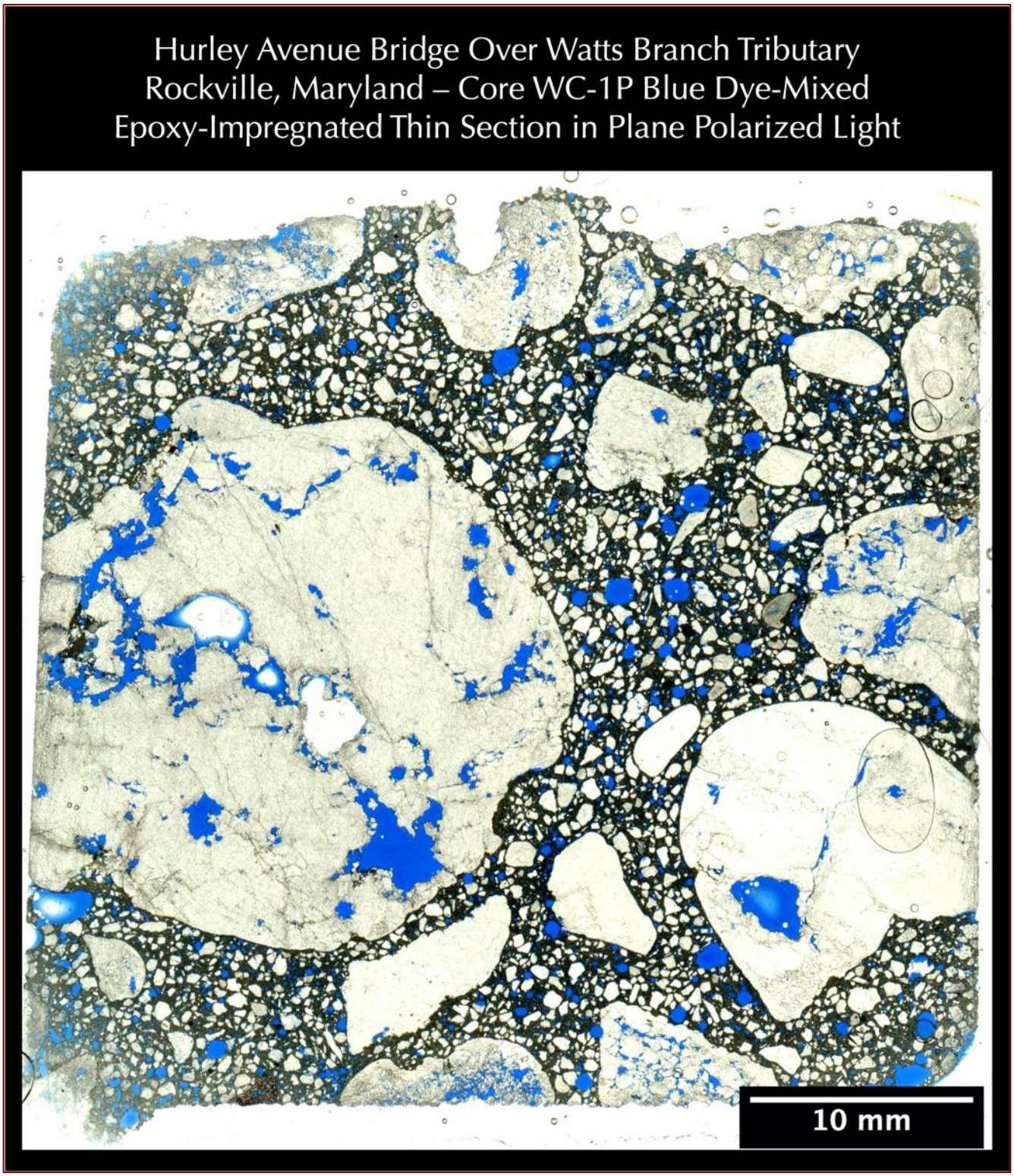

Figure 27: Blue dye-mixed epoxy-impregnated thin section of Core WC-1P in plane polarized light (PPL) showing: (a) siliceous (quartzite) gravel coarse aggregate particles that are ¾ in. (19 mm) in nominal size, poorly graded, well-distributed; (b) well-graded, well-distributed natural siliceous sand fine aggregate; and (c) interstitial paste fraction of air-entrained concrete where many entrained and entrappd air voids are highlighted by blue epoxy. The image was formed after scanning the thin section on a film scanner with a polarizing filter. Some porous gravel particles are highlighted by blue epoxy.

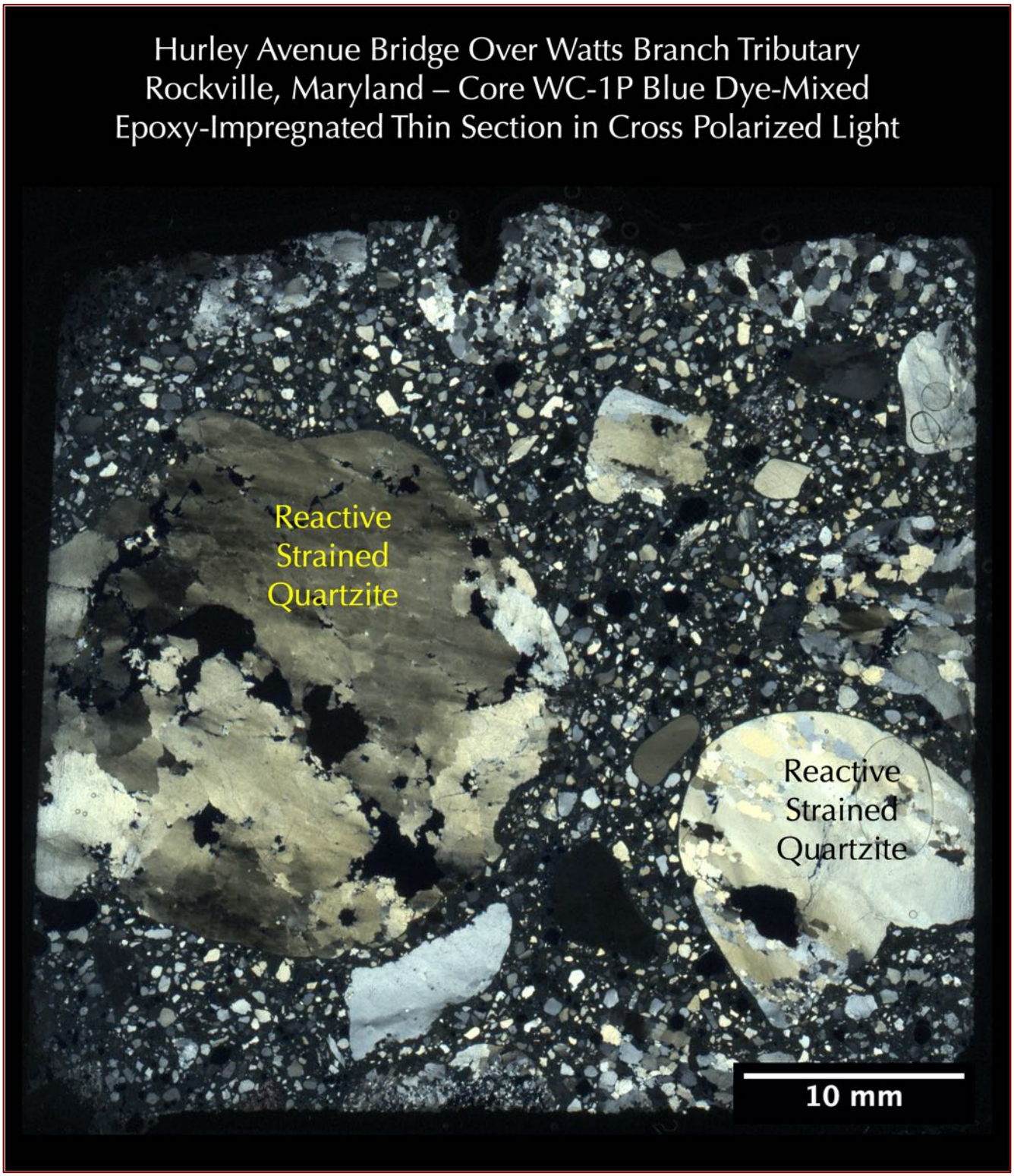

Figure 28: : Blue dye-mixed epoxy-impregnated thin section of Core WC-1P in cross polarized light (XPL) showing: (a) siliceous (quartzite) gravel coarse aggregate particles that are ¾ in. (19 mm) in nominal size; (b) natural siliceous sand fine aggregate; and (c) interstitial paste fraction. Notice the highly strained (deformed) nature of quartzite gravel particles showing undulose (wavy) extinction of strained quartz grains, which are potentially alkali-silica reactive in the presence of moisture and high alkalis in the pore solution of concrete. The image was formed after scanning the thin section on a film scanner with two polarizing filters at perpendicular orientation.

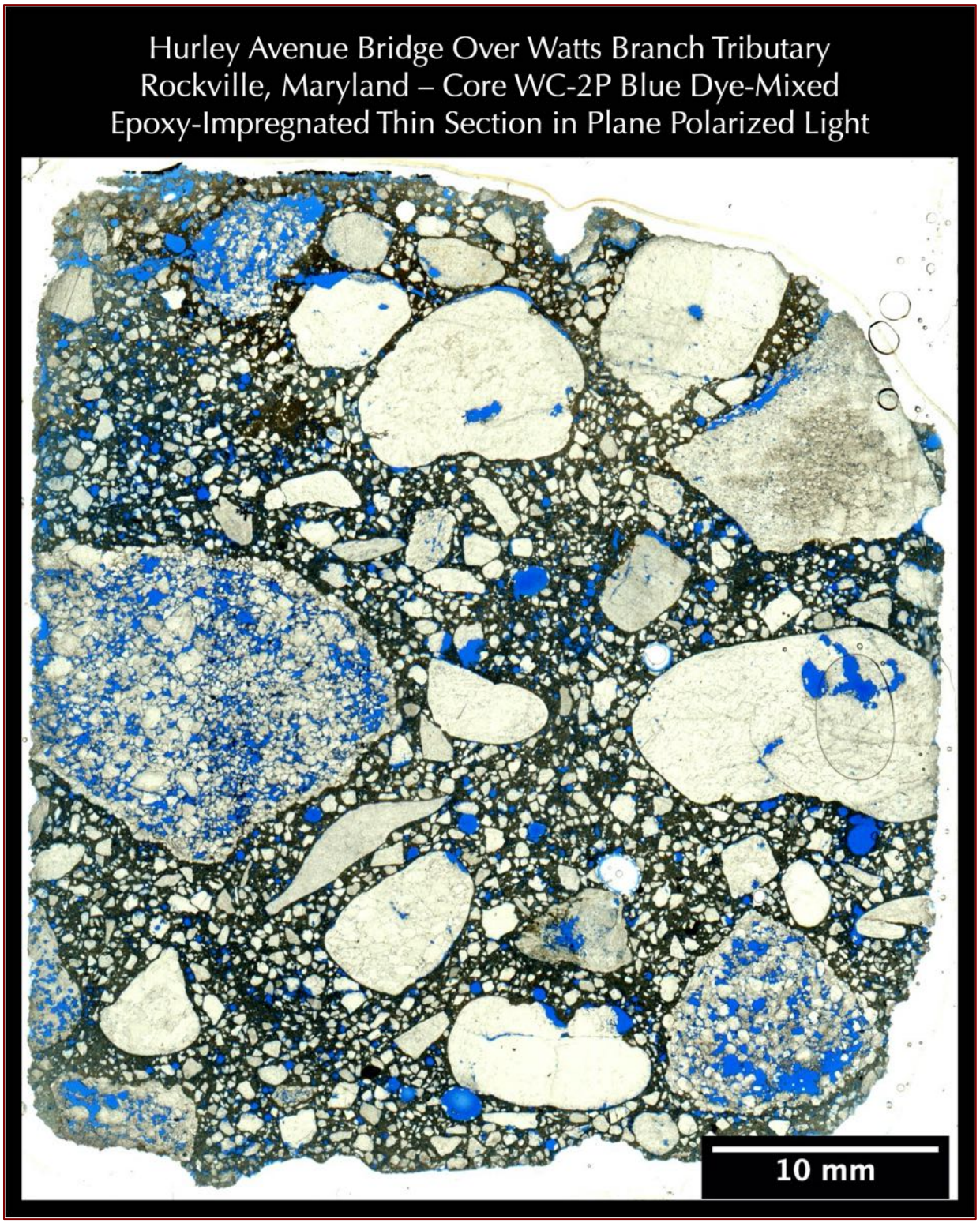

Figure 29: Blue dye-mixed epoxy-impregnated thin section of Core WC-2P in plane polarized light (PPL) showing: (a) siliceous (quartzite) gravel coarse aggregate particles that are ¾ in. (19 mm) in nominal size, well-graded, well-distributed; (b) well-graded, well-distributed natural siliceous sand fine aggregate; and (c) interstitial paste fraction of air-entrained concrete where many entrained and entrappd air voids are highlighted by blue epoxy. The image was formed after scanning the thin section on a film scanner with a polarizing filter. Some porous gravel particles are highlighted by blue epoxy.

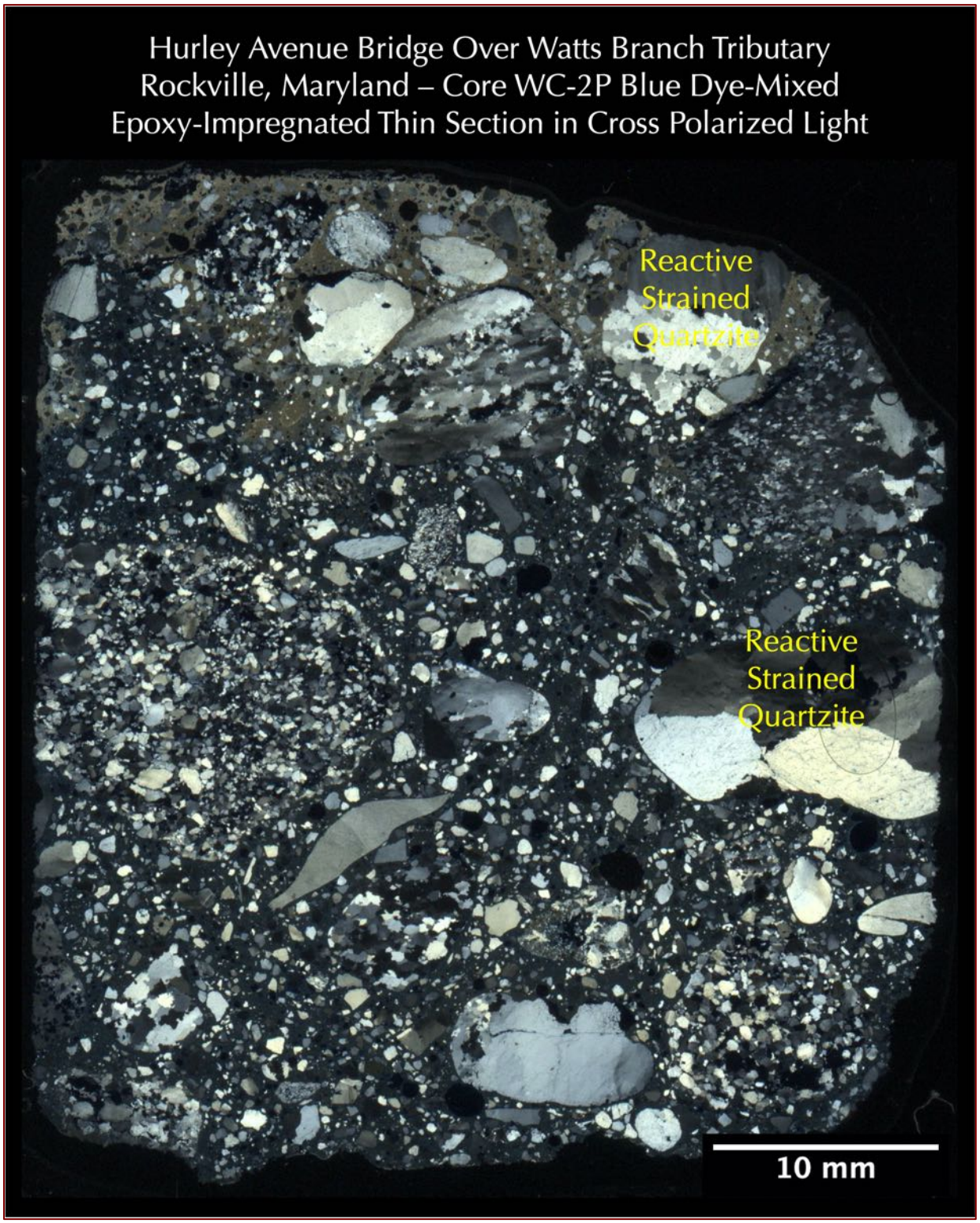

Figure 30: : Blue dye-mixed epoxy-impregnated thin section of Core WC-2P in cross polarized light (XPL) showing: (a) siliceous (quartzite) gravel coarse aggregate particles that are ¾ in. (19 mm) in nominal size; (b) natural siliceous sand fine aggregate; and (c) interstitial paste fraction. Notice the highly strained (deformed) nature of quartzite gravel particles showing undulose (wavy) extinction of strained quartz grains, which are potentially alkali-silica reactive in the presence of moisture and high alkalis in the pore solution of concrete. The image was formed after scanning the thin section on a film scanner with two polarizing filters at perpendicular orientation.

MICROGRAPHS OF THIN SECTIONS

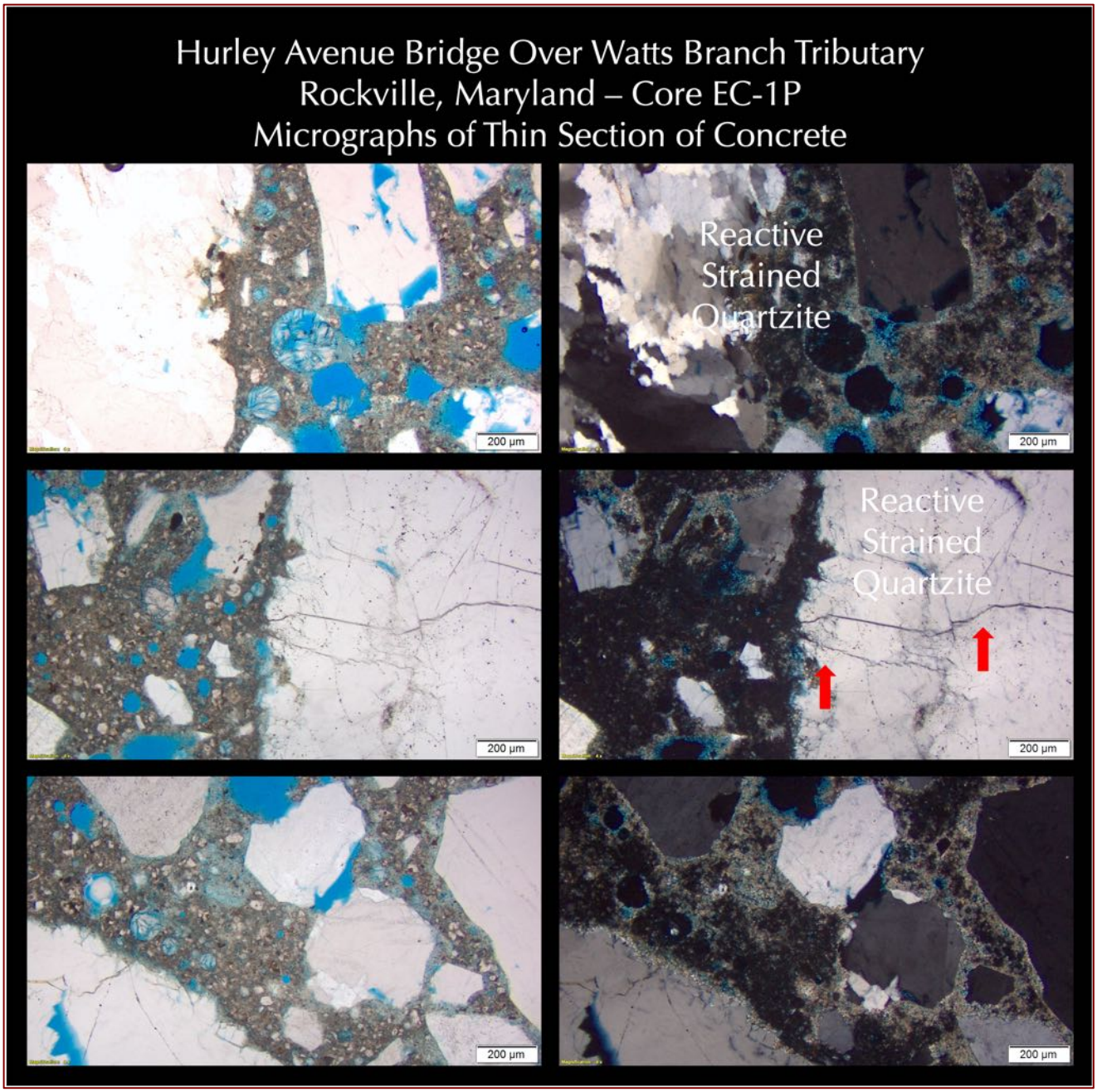

Figure 31: Micrographs of thin section of concrete from Core EC-1P showing: (a) air voids filled or lined with abundant secondary ettringite deposits that are indicative of prolonged presence of moisture in the concrete during service; (b) variably carbonated nature of paste, which is evident from golden yellow interference color of carbonated paste in cross polarized light mode; (c) strained quartz grains in alkali-silica reactive quartzite gravel coarse aggregate; (d) microcracks in alkali-silica reactive strained quartzite gravel coarse aggregate particle (marked by red arrows). The micrographs were taken from a petrographic microscope.

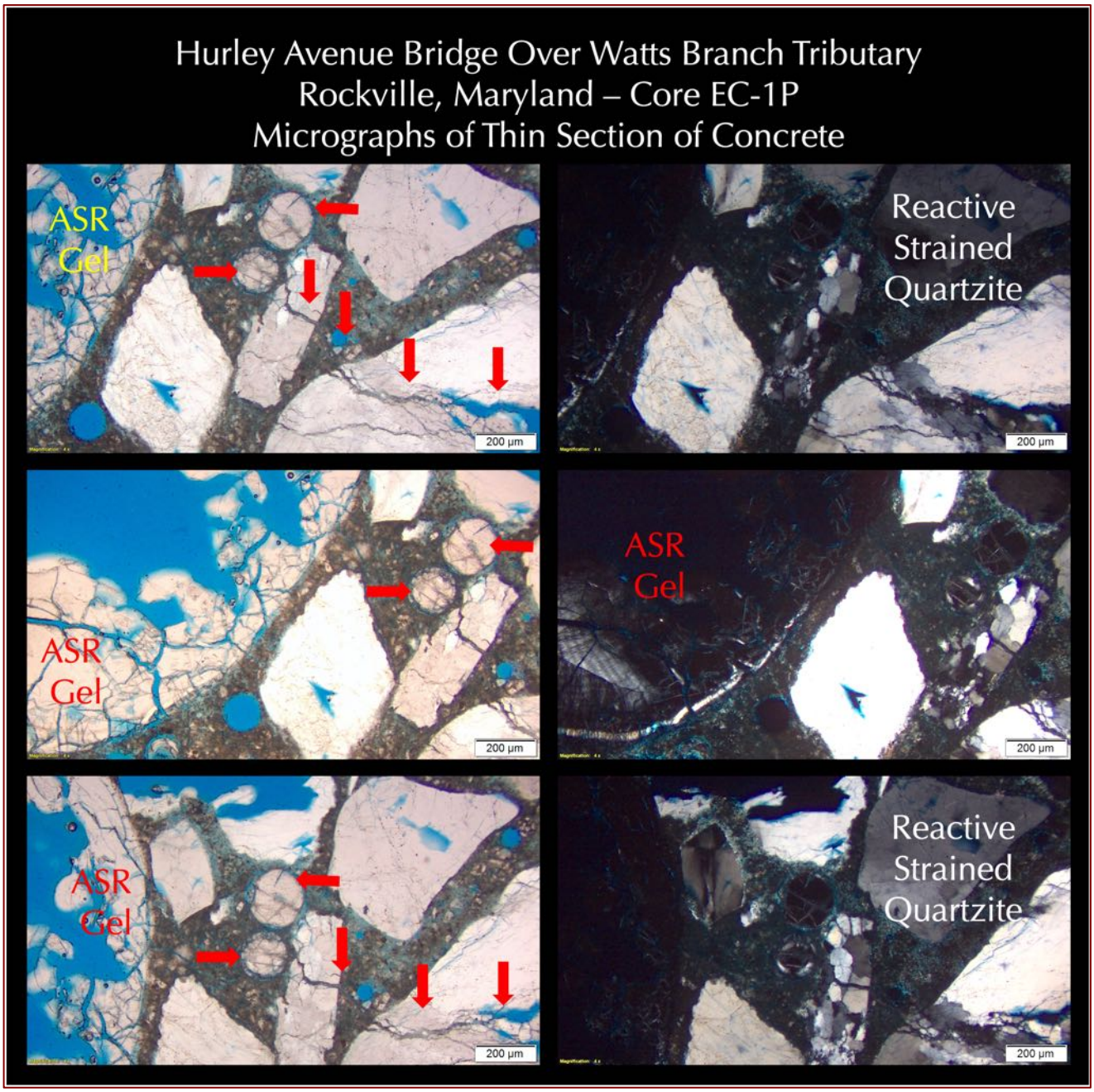

Figure 32: Micrographs of thin section of concrete from Core EC-1P showing: (a) specticular development of alkali-silica reaction gel lining the large air void at left and filling smaller air voids in the center and right side of photos; (b) variably carbonated nature of paste, which is evident from golden yellow interference color of carbonated paste in cross polarized light mode; (c) strained quartz grains in alkali-silica reactive quartzite gravel coarse aggregate; (d) microcracks in alkali-silica reactive strained quartzite gravel coarse aggregate particle extending into paste and occasionally filled with alkali-silica reaction gel (marked by red arrows). The micrographs were taken from a petrographic microscope.

Figure 33: Micrographs of thin section of concrete from Core EC-2P showing: (a) remains of a discontinuous protective coat that has vertical shrinkage microcracks (boxed at left photos); (b) carbonated nature of paste immediately beneath the protective coat from atmospheric carbonation of concrete at the exposed surface region, which is evident from golden yellow interference color of carbonated paste in cross polarized light mode; (c) a vertical microcrack at the surface region (marked by red arrows) that is filled with alkali-silica reaction gel. Micrographs were taken from a petrographic microscope.

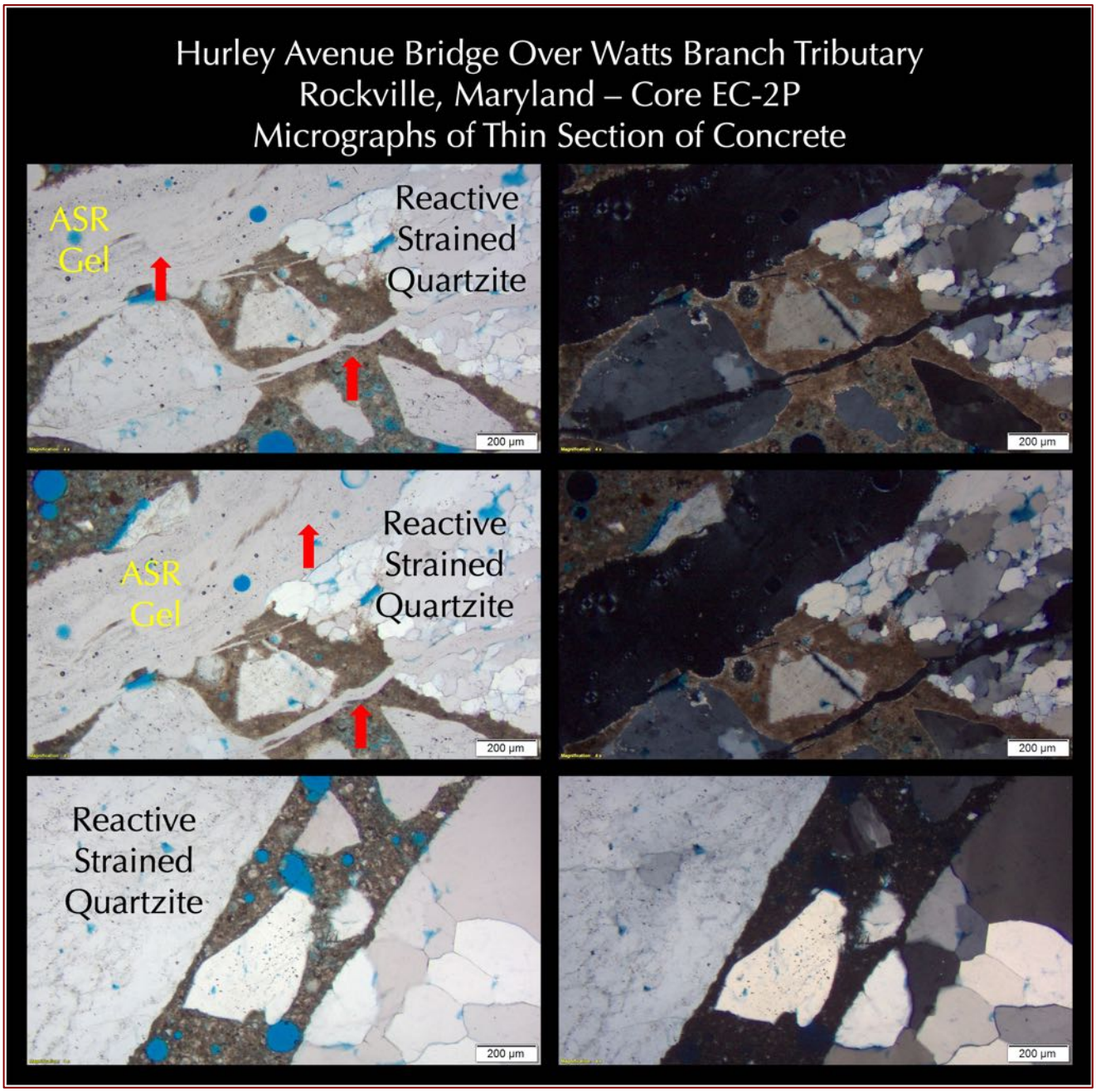

Figure 34: Micrographs of thin section of concrete from Core EC-2P showing: (a) variably carbonated nature of paste, which is evident from golden yellow interference color of carbonated paste in cross polarized light mode; (b) strained quartz grains in alkali-silica reactive quartzite gravel coarse aggregate; (c) microcracks in alkali-silica reactive strained quartzite gravel coarse aggregate particle; and (d) alkali-silica reaction gel in the crack (marked by red arrows). The micrographs were taken from a petrographic microscope.

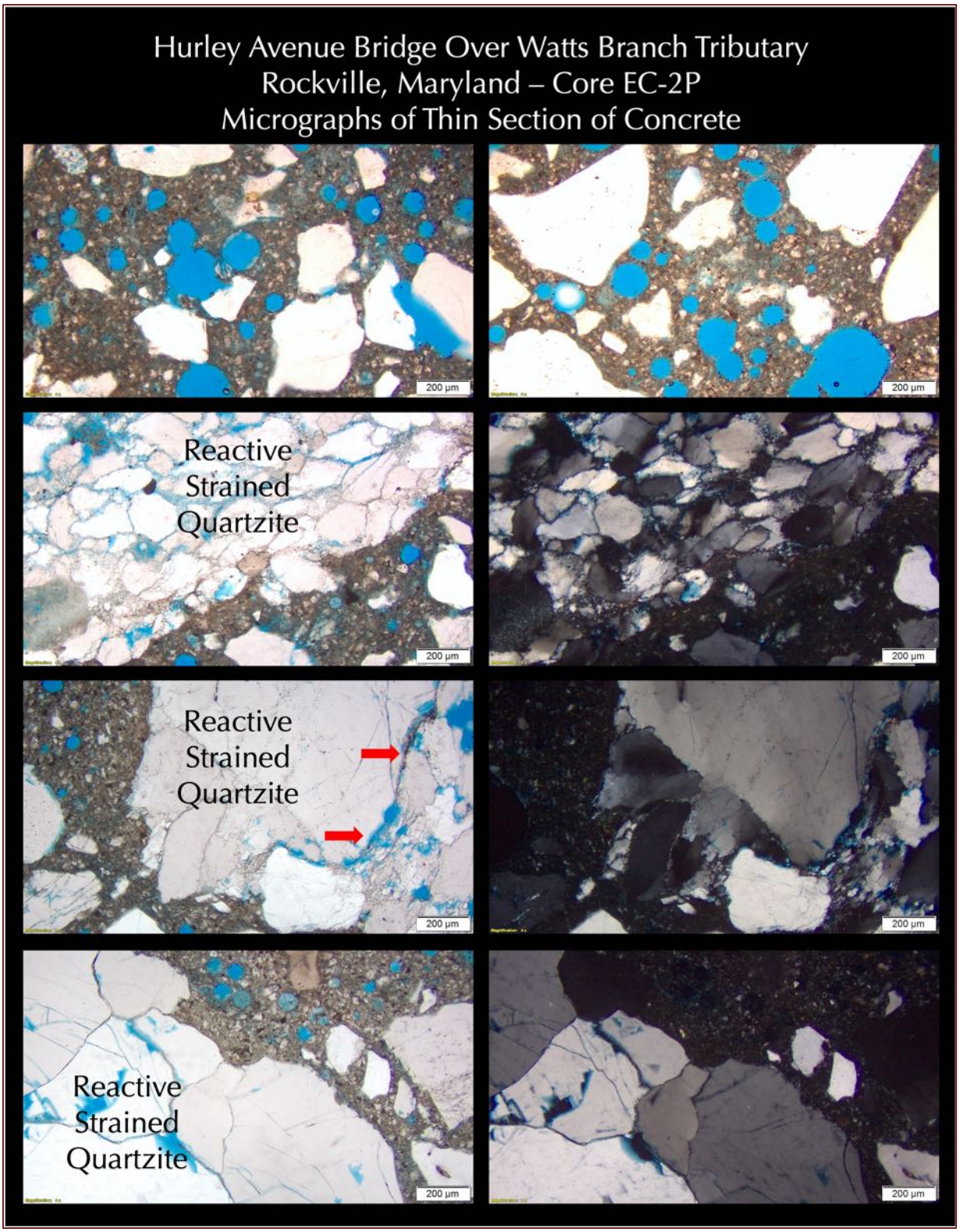

Figure 35: Micrographs of thin section of concrete from Core EC-2P showing: (a) spherical entrained air voids highlighted by blue epoxy in top row; (b) strained quartz grains in alkali-silica reactive quartzite gravel coarse aggregate; (c) microcracks in alkali-silica reactive strained quartzite gravel coarse aggregate particle; and (d) alkali-silica reaction gel in the crack (marked by red arrows). The micrographs were taken from a petrographic microscope.

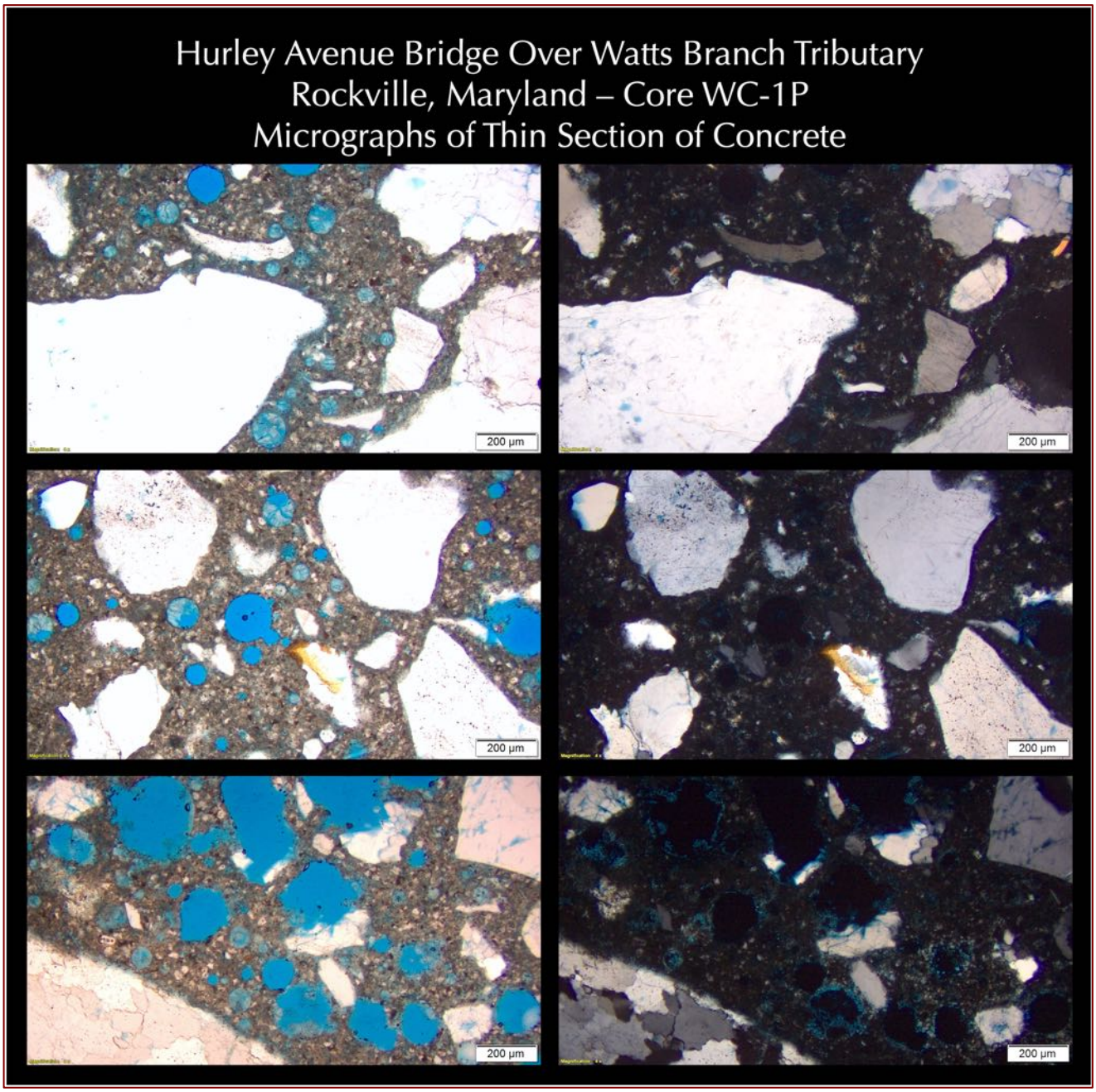

Figure 36: Micrographs of thin section of concrete from Core WC-1P showing: (a) spherical entrained air voids highlighted by blue epoxy in left column photos; (b) siliceous (quartz) sand fine aggregate particles; and (c) interstitial non-carbonated Portland cement paste containing cement hydration products and many residual Portland cement particles. The micrographs were taken from a petrographic microscope.

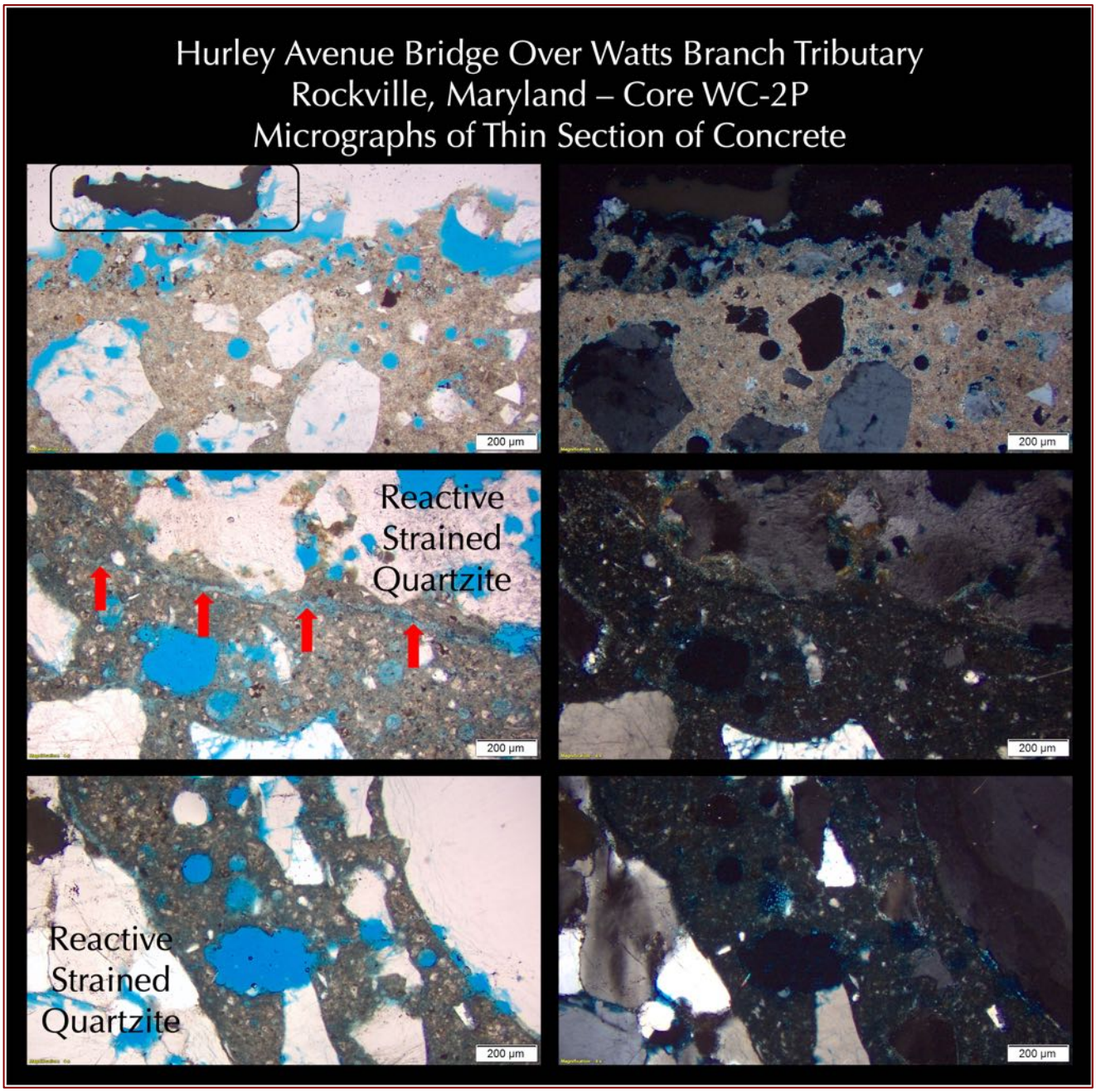

Figure 37: Micrographs of thin section of concrete from Core WC-2P showing: (a) remains of a discontinuous protective coat (boxed at top left photo); (b) carbonated nature of paste immediately beneath the protective coat from atmospheric carbonation of concrete at the exposed surface region, which is evident from golden yellow interference color of carbonated paste in cross polarized light mode; (c) a microcrack filled with secondary deposits (marked by red arrows); (d) spherical entrained air voids highlighted by blue epoxy in left column photos; (e) siliceous (quartz) sand fine aggregate particles; and (d) interstitial non-carbonated Portland cement paste in the middle and bottom row photos containing cement hydration products and many residual Portland cement particles. Micrographs were taken from a petrographic microscope.

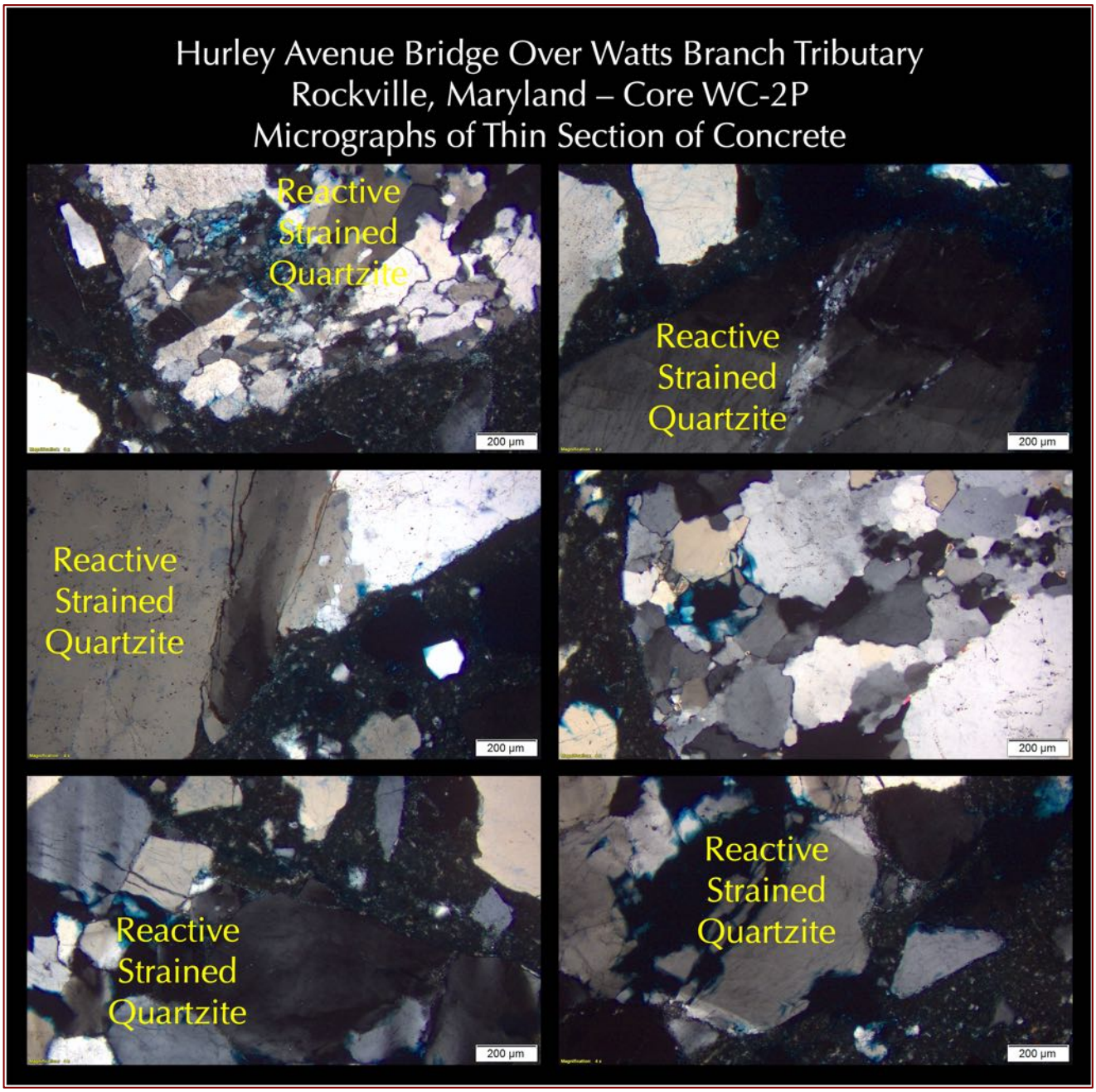

Figure 38: Micrographs of thin section of concrete from Core WC-2P showing strained quartz grains in alkali-silica reactive quartzite gravel coarse aggregate particles. Micrographs were taken from a petrographic microscope.

COARSE AGGREGATES

Coarse aggregates are compositionally similar strained quartzite gravel consisting of interlocking crystals of highly strained quartz with characteristic undulose extinction. These quartzite gravels are known to be potentially alkali-silica reactive in the presence of moisture and high alkalis in the pore solution.

As a result, many of these particles show evidence of alkali-silica reaction as (a) microcracking within the particles, (b) microcracking extending from the reactive particles to neighboring paste, (c) dark reaction rims, and (d) alkali-silica reaction gels in microcracks and air voids in the vicinity of reactive quartzite gravels.

Particles that are ¾ to 1 in. (19 to 25 mm) in nominal size, dense, hard, light to medium gray, massive crystalline granular texture, subrounded to well-rounded, mostly equidimensional to a few elongated, well-graded in EC-1P and WC-2P to poorly graded in EC-2P and WC-1P, and well-distributed.

FINE AGGREGATES

Fine aggregates are compositionally similar natural siliceous sands of nominal maximum sizes 3/8 in. (9.5 mm) consisting of dominant quartz, and subordinate quartzite, feldspar, and minor amounts of quartz siltstone particles. Fine aggregate particles are variably colored, subangular to subrounded, variably dense and hard, equidimensional to elongated, unaltered, uncoated, and uncracked. There is no evidence of alkali-aggregate reactions, or any other potentially deleterious reactions found in the fine aggregate.

The following Table summarizes properties of coarse and fine aggregates in four cores.

Properties and Compositions of Aggregates	Cores EC-1P, EC-2P, WC-1P, and WC-2P
Coarse Aggregates	
Types	Gravels
Nominal maximum size (in.)	¾ to 1 in. (19 to 25 mm)
Rock Types	Strained quartzite
Angularity, Density, Hardness, Color, Texture, Sphericity	Dense, hard, light to medium gray, massive crystalline granular texture, mostly equidimensional to a few elongated
Cracking, Alteration, Coating	Unaltered, Uncoated, and Uncracked
Grading & Distribution	Well-graded in EC-1P and WC-2P to poorly graded in EC-2P and WC-1P, and well-distributed
Soundness	Unsound - Alkali-silica reaction
Alkali-Aggregate Reactivity	Present
Fine Aggregates	
Types	Natural siliceous sands
Nominal maximum size (in.)	3/8 in. (9.5 mm)
Rock Types	Dominant quartz, and subordinate quartzite, feldspar, and minor amounts of quartz siltstone particles

Properties and Compositions of Aggregates	Cores EC-1P, EC-2P, WC-1P, and WC-2P
Cracking, Alteration, Coating	Variably colored, subangular to rounded, dense, hard, equant to elongated
Grading & Distribution	Well-graded and Well-distributed
Soundness	Sound
Alkali-Aggregate Reactivity	None

Table 2: Properties of coarse and fine aggregates of concretes in four cores.

PASTE

Properties and composition of hardened cement pastes are summarized in Table 3. Paste is compositionally similar dense, and hard in the interior bodies except some patchy discoloration at the expose surface ends in Cores EC-2P and WC-2P, which are due to atmospheric carbonation. Freshly fractured surfaces have subtranslucent vitreous lusters and subconchoidal fractures. Residual and relict Portland cement particles are present and estimated to constitute 6 to 8 percent of the paste volumes. Besides residual Portland cement, no other pozzolanic or cementitious materials are found.

The textural and compositional features of pastes are indicative of Portland cement contents similar in the four cores examined and estimated to be 6 to 6$^{1}/_{2}$ bags per cubic yard, and water-cement ratios in the bodies similar in all cores and estimated to be from 0.45 to 0.50.

Properties and Compositions of Paste	Cores EC-1P, EC-2P, WC-1P, and WC-2P
Color, Hardness, Porosity, Luster	Compositionally similar dense, and hard in the interior bodies except some patchy discoloration at the carbonated expose surface ends. Freshly fractured surfaces have subvitreous lusters and subconchoidal textures
Residual Portland Cement Particles	Normal, 6 to 8 percent by paste volume
Calcium hydroxide from cement hydration	Normal, 10 to 14 percent by paste volume
Pozzolans, Slag, etc.	None
Water-cementitious materials ratio (*w/cm*), estimated	0.45 to 0.50 in the interior bodies
Portland cement content (bags per cubic yard)	6 to 6$^{1}/_{2}$ bags
Secondary Deposits	Abundant secondary ettringite in air voids and microcracks that are indicative of the presence of moisture for prolonged periods; alkali-silica reaction gel
Depth of Carbonation, mm	Patchy carbonation extended to depths of 10 mm at the exposed ends of Cores EC-2P and WC-2P
Microcracking	Microcracking due to shrinkage and alkali-silica reaction
Aggregate-paste Bond	Moderately tight
Bleeding, Tempering	None
Chemical deterioration	None

Table 3: Proportions and composition of hardened cement paste in all four cores.

AIR

Concrete in all cores show evidence of addition of an air entraining agent though at amounts lower than that needed for formation of around 6 percent air needed for a moist outdoor exposure of cyclic freezing and thawing. Therefore concrete is marginally air-entrained to air-entrained having: (a) numerous fine, discrete, spherical and near-spherical voids of sizes 1 mm or less, which are characteristic of entrained air and (b) a few coarse, near-spherical and irregularly-shaped voids greater than 1 mm in size, which are characteristic of entrapped air.

The following Table 4 provides estimated air contents in the four cores.

Core	Air Entrainment	Estimated Air Content	Figures
EC-1P	Marginally air-entrained	3 to 4 percent	19
EC-2P	Air-Entrained	4.5 to 5.5 percent	20
WC-1P	Air-Entrained	3.5 to 4.5 percent	21
WC-2P	Air-Entrained	3.5 to 4.5 percent	22

Table 4: Air entrainment and estimated air contents in four cores.

COMPRESSIVE STRENGTHS

Core ID	Capped Length (in.)	Diameter (in.)	Area (sq. in.)	L/D	Load (lbs.)	Corrected Strength (corrected psi)	Type of Fracture	Unit Weight (lbs.)
EC-1P	3.48	1.73	2.35	2.01	9155	**3890**	Column	139.7
EC-2P	3.42	1.73	2.35	1.98	8115	**3450**	Column	139.7
WC-1P	3.42	1.74	2.38	1.97	13995	**5890**	Column	141.7
WC-2P	3.28	1.73	2.35	1.90	10180	**4330**	Column	144.6

Table 5: Compressive strengths of four cores.

Portions of cores selected for strength testing are shown in Figures 7 through 10. Strength results varied from 3450 psi (in EC-2P) to 5890 psi (in WC-1P). Unit weights are from 139.7 to 144.6 pounds per cubic foot.

WATER-SOLUBLE CHLORIDE CONTENTS

Water-soluble chloride contents were determined from potentiometric titration according to the procedures of ASTM C 1218. Results are presented below in Table 4 and in Figures.

Core IDs & Distance From Exposed End From Where Powder Sample Was Collected from Each Core		% Water-Soluble Chloride by mass of concrete	% Water-Soluble Chloride by mass of cement (assuming a Portland cement content of 15 percent by mass of concrete)	Titration Curve Figures
EC-1P	1 in.	0.0693	0.46	40
	3 in.	0.0583	0.39	41
	5 in.	0.0858	0.57	42
	10 in.	0.0632	0.42	43
	15 in.	0.0215	0.14	44
EC-2P	1 in.	0.0622	0.41	45
	3 in.	0.0489	0.33	46
	5 in.	0.0264	0.18	47
	10 in.	0.0200	0.13	48
	15 in.	0.0031	0.02	49
EC-3	1 in.	0.0431	0.29	50
	3 in.	0.0209	0.14	51
	5 in.	0.0506	0.34	52
	10 in.	0.0320	0.21	53
	15 in.	0.0008	0.01	54
EC-4	1 in.	0.0090	0.06	55
	3 in.	0.0147	0.10	56
	5 in.	0.0577	0.38	57
	10 in.	0.0833	0.56	58
	15 in.	0.0440	0.29	59
WC-1P	1 in.	0.0619	0.41	60
	3 in.	0.0800	0.53	61
	5 in.	0.0370	0.25	62
	10 in.	0.0324	0.22	63
	15 in.	0.0182	0.12	64
WC-2P	1 in.	0.0397	0.26	65
	3 in.	0.0249	0.17	66
	5 in.	0.0134	0.09	67
	10 in.	0.0055	0.04	68
	15 in.	0.0055	0.04	69
WC-3	1 in.	0.0246	0.16	70
	3 in.	0.0522	0.35	71
	5 in.	0.0481	0.32	72
	10 in.	0.0303	0.20	73
	15 in.	0.0134	0.09	74
WC-4	1 in.	0.0892	0.59	75
	3 in.	0.1395	0.93	76
	5 in.	0.0557	0.37	77
	10 in.	0.0435	0.29	78
	15 in.	0.0208	0.14	79

Table 6: Results of water-soluble chloride contents in concrete determined by potentiometric titration. Results in red (a total of 23 analyses) have exceeded the common industry-recommended maximum threshold chloride level of 0.2 percent chloride by mass of cement above which chloride-induced corrosion of steel in concrete is possible in the presence of oxygen and moisture.

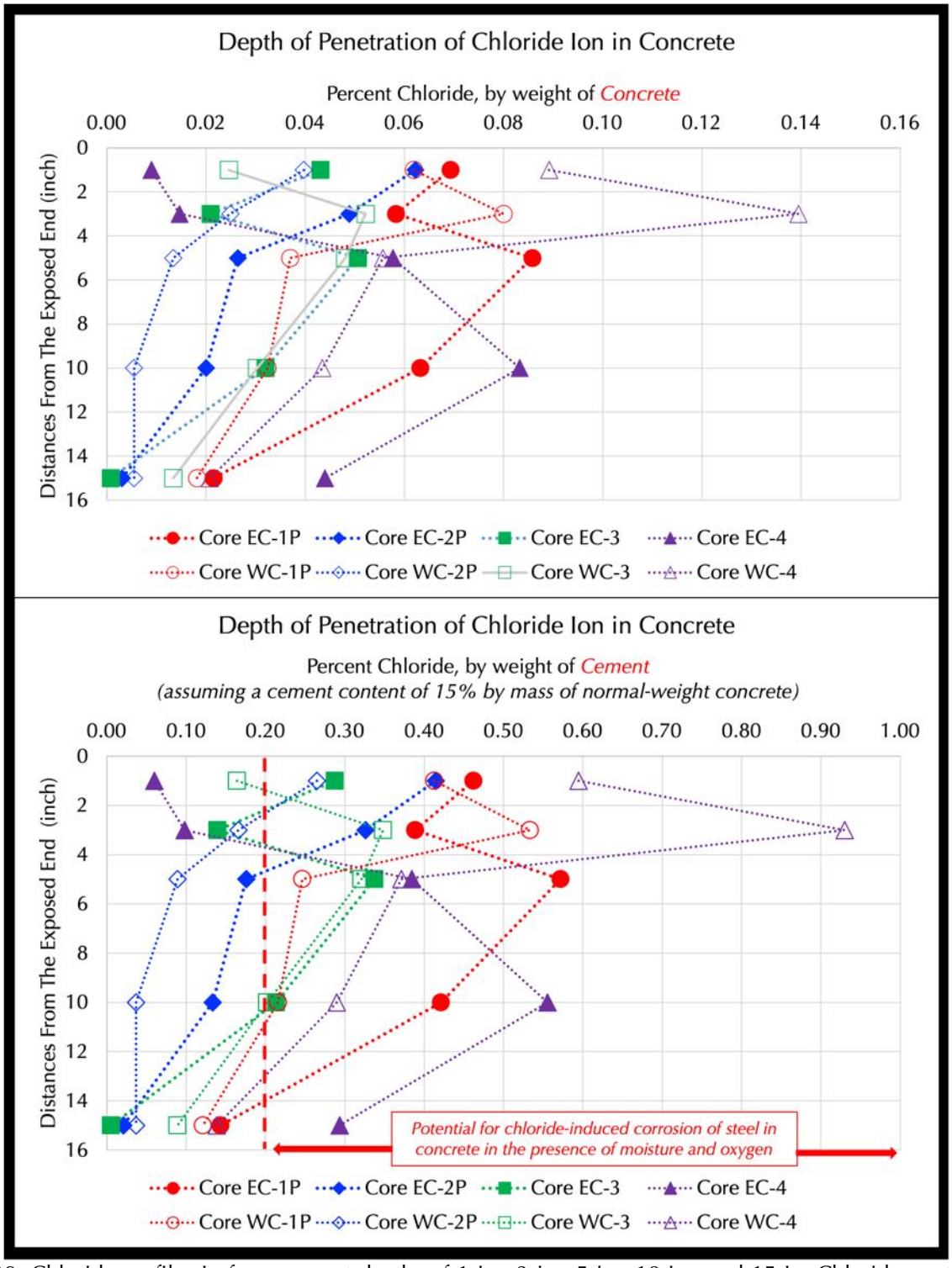

Figure 39: Chloride profiles in four cores at depths of 1 in., 3 in., 5 in., 10 in., and 15 in. Chloride contents are plotted first with the raw data of percent chloride by mass of concrete at the top, and, then re-calculated data of percent chloride by mass of cement in the bottom plot (assuming a Portland cement content of 15 percent by mass of a normal-weight concrete). Common industry-threshold chloride level to cause corrosion of steel in concrete in the presence of oxygen and moisture is 0.2 percent by mass of cement, which is shown in the bottom plot as the vertical red dashed line. Remaining Figures show the actual potentiometric titration curves from which chloride contents are determined.

License ID 4017173 Program version tiamo 2.5 - 116 - 1
Computer name Titration-909
User Metrohm Titration 2022-02-06 10:50:08 AM

Results report

Determination of Acid-Soluble (ASTM C 1152) or Water-Soluble (ASTM C 1218) Chloride Contents

Method . . . . . DET U Chloride Auto 808
Method saving date 2020-12-05 13:32:13 UTC-5

Sample data

ID1 . . . . . CMC 0122103
ID2 . . . . . EC-1P
ID3 . . . . . 1 inch.
Sample size . . . . . 9.669 g

End points

DET U **DET U Chloride Auto 808.1**
EP1 . . . . . 141.7 mV . . . . . 3.7850 mL

Results

% Chloride . . . . . **0.0693 %**

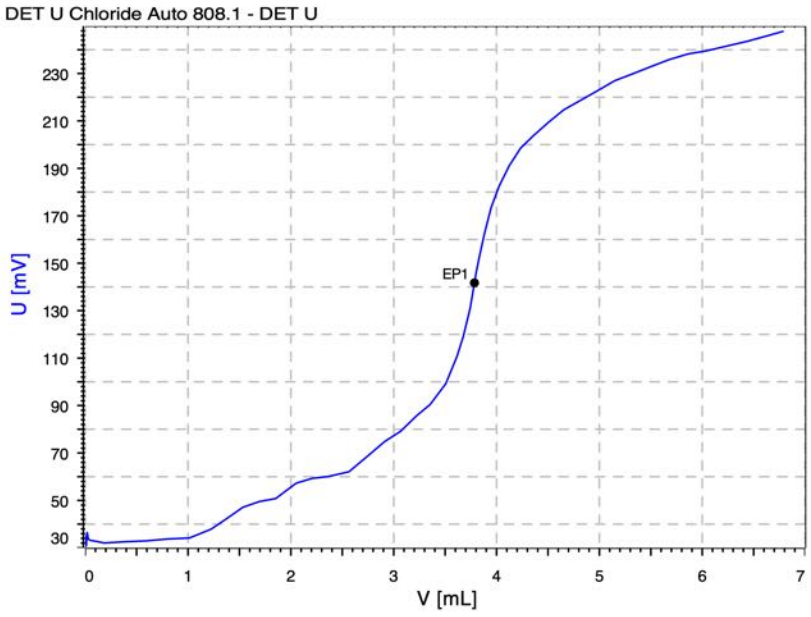

tiamo Page 1 of 1 Metrohm

Figure 40: Water-soluble chloride analysis from potentiometric titration of the filtrate from digestion of concrete powder in deionized water, where chloride content is determined from the equivalent point of titration plotted against milliliters of silver chloride titrant added during titration and corresponding changes in millivolts where the steepest point in the titration curve defines the equivalent point. Chloride content is determined from the milliliters of silver nitrate used to reach the equivalent point, and the sample weight.

License ID 4017173 Program version tiamo 2.5 - 116 - 1
Computer name Titration-909
User Metrohm Titration 2022-02-06 10:50:07 AM

Results report

Determination of Acid-Soluble (ASTM C 1152) or Water-Soluble (ASTM C 1218) Chloride Contents

Method . . . . . DET U Chloride Auto 808
Method saving date 2020-12-05 13:32:13 UTC-5

Sample data

ID1 . . . . . CMC 0122103
ID2 . . . . . EC-1P
ID3 . . . . . 3 inch.
Sample size . . . . . 9.788 g

End points

DET U **DET U Chloride Auto 808.1**

EP1 . . . . . 153.6 mV . . . . . 3.2266 mL

Results

% Chloride . . . . . **0.0583 %**

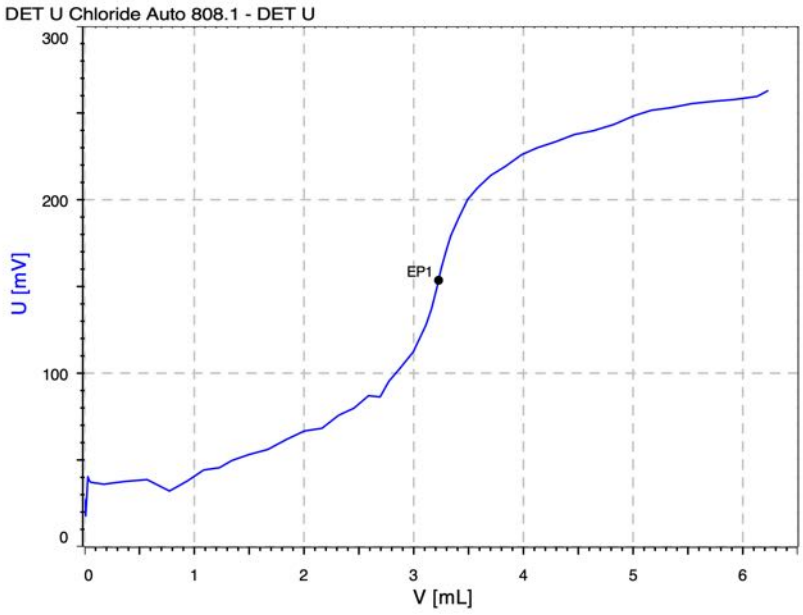

tiamo Page 1 of 1 Metrohm

Figure 41: Water-soluble chloride analysis from potentiometric titration of the filtrate from digestion of concrete powder in deionized water, where chloride content is determined from the equivalent point of titration plotted against milliliters of silver chloride titrant added during titration and corresponding changes in millivolts where the steepest point in the titration curve defines the equivalent point. Chloride content is determined from the milliliters of silver nitrate used to reach the equivalent point, and the sample weight.

License ID 4017173 Program version tiamo 2.5 - 116 - 1
Computer name Titration-909
User Metrohm Titration 2022-02-06 10:50:05 AM

Results report

Determination of Acid-Soluble (ASTM C 1152) or Water-Soluble (ASTM C 1218) Chloride Contents

Method . . . . . DET U Chloride Auto 808
Method saving date 2020-12-05 13:32:13 UTC-5

Sample data

ID1 . . . . . CMC 0122103
ID2 . . . . . EC-1P
ID3 . . . . . 5 inch.
Sample size . . . . . 10.706 g

End points

DET U **DET U Chloride Auto 808.1**

EP1 . . . . . 151.0 mV . . . . . 5.1876 mL

Results

% Chloride . . . . . 0.0858 %

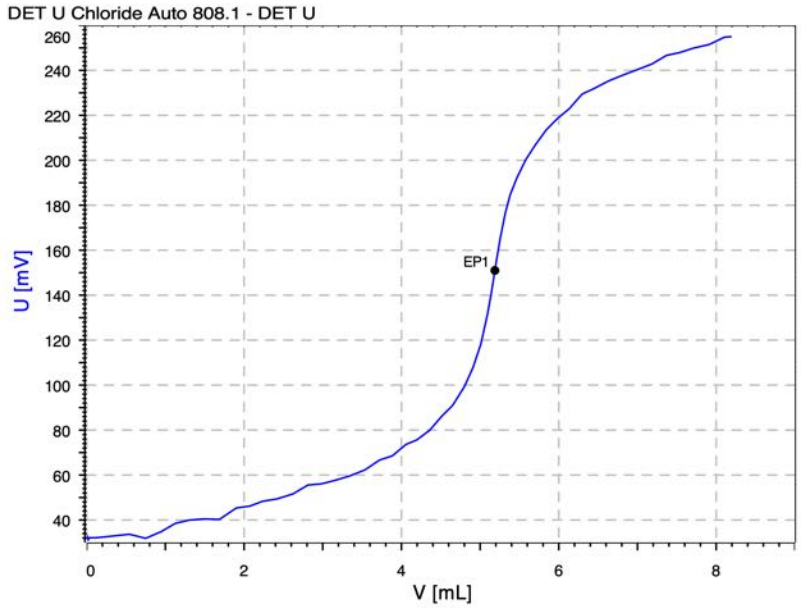

tiamo Page 1 of 1 Metrohm

Figure 42: Water-soluble chloride analysis from potentiometric titration of the filtrate from digestion of concrete powder in deionized water, where chloride content is determined from the equivalent point of titration plotted against milliliters of silver chloride titrant added during titration and corresponding changes in millivolts where the steepest point in the titration curve defines the equivalent point. Chloride content is determined from the milliliters of silver nitrate used to reach the equivalent point, and the sample weight.

License ID 4017173 Program version tiamo 2.5 - 116 - 1
Computer name Titration-909
User Metrohm Titration 2022-02-06 10:50:04 AM

Results report

Determination of Acid-Soluble (ASTM C 1152) or Water-Soluble (ASTM C 1218) Chloride Contents

Method . . . . . DET U Chloride Auto 808
Method saving date 2020-12-05 13:32:13 UTC-5

Sample data

ID1 . . . . . CMC 0122103
ID2 . . . . . EC-1P
ID3 . . . . . 10 inch.
Sample size . . . . . 9.228 g

End points

DET U **DET U Chloride Auto 808.1**

EP1 . . . . . 173.9 mV . . . . . 3.2956 mL
EP2 . . . . . 256.3 mV . . . . . 4.9034 mL

Results

% Chloride . . . . . **0.0632 %**

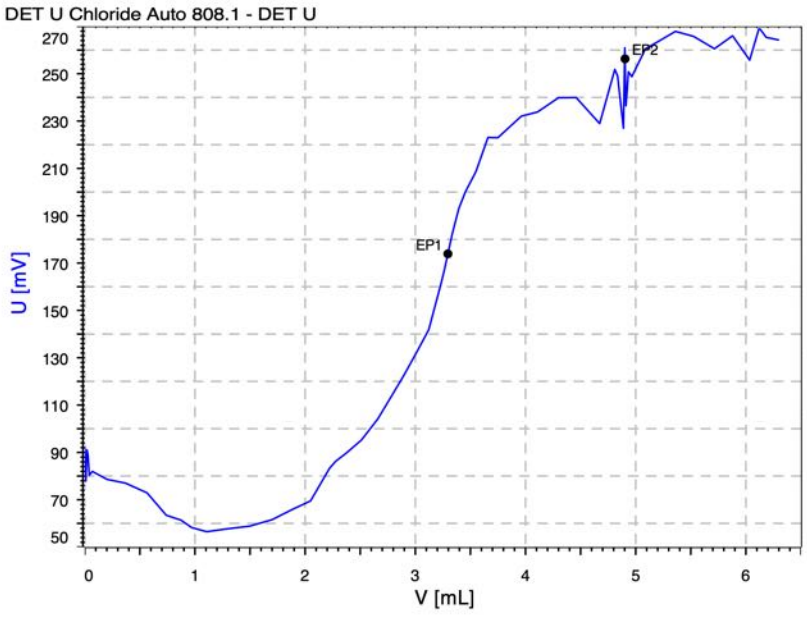

tiamo Page 1 of 1 Metrohm

Figure 43: Water-soluble chloride analysis from potentiometric titration of the filtrate from digestion of concrete powder in deionized water, where chloride content is determined from the equivalent point of titration plotted against milliliters of silver chloride titrant added during titration and corresponding changes in millivolts where the steepest point in the titration curve defines the equivalent point. Chloride content is determined from the milliliters of silver nitrate used to reach the equivalent point, and the sample weight.

License ID 4017173 Program version tiamo 2.5 - 116 - 1
Computer name Titration-909
User Metrohm Titration 2022-02-06 10:50:02 AM

Results report

Determination of Acid-Soluble (ASTM C 1152) or Water-Soluble (ASTM C 1218) Chloride Contents

Method . . . . . DET U Chloride Auto 808
Method saving date 2020-12-05 13:32:13 UTC-5

Sample data

ID1 . . . . . CMC 0122103
ID2 . . . . . EC-1P
ID3 . . . . . 15 inch.
Sample size . . . . . 10.019 g

End points

DET U **DET U Chloride Auto 808.1**

EP1 . . . . . 93.8 mV . . . . . 1.2152 mL
EP2 . . . . . 171.8 mV . . . . . 2.4290 mL

Results

% Chloride . . . . . **0.0215 %**

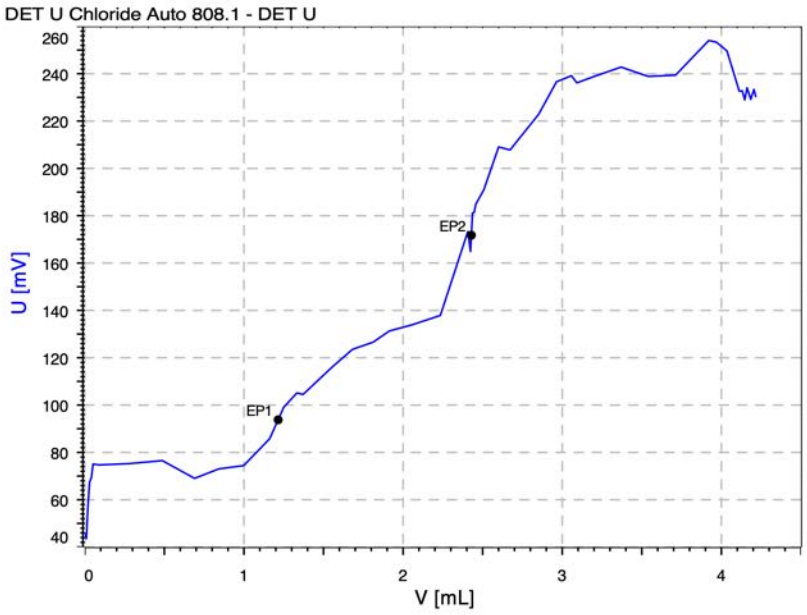

tiamo Page 1 of 1 Metrohm

Figure 44: Water-soluble chloride analysis from potentiometric titration of the filtrate from digestion of concrete powder in deionized water, where chloride content is determined from the equivalent point of titration plotted against milliliters of silver chloride titrant added during titration and corresponding changes in millivolts where the steepest point in the titration curve defines the equivalent point. Chloride content is determined from the milliliters of silver nitrate used to reach the equivalent point, and the sample weight.

License ID 4017173 Program version tiamo 2.5 - 116 - 1
Computer name Titration-909
User Metrohm Titration 2022-02-06 10:56:15 AM

Results report

Determination of Acid-Soluble (ASTM C 1152) or Water-Soluble (ASTM C 1218) Chloride Contents

Method . . . . . DET U Chloride Auto 808
Method saving date 2020-12-05 13:32:13 UTC-5

Sample data

ID1 . . . . . CMC 0122103
ID2 . . . . . EC-2P
ID3 . . . . . 1 inch.
Sample size . . . . . 10.015 g

End points

DET U **DET U Chloride Auto 808.1**

EP1 . . . . . 152.3 mV . . . . . 3.5171 mL

Results

% Chloride . . . . . **0.0622 %**

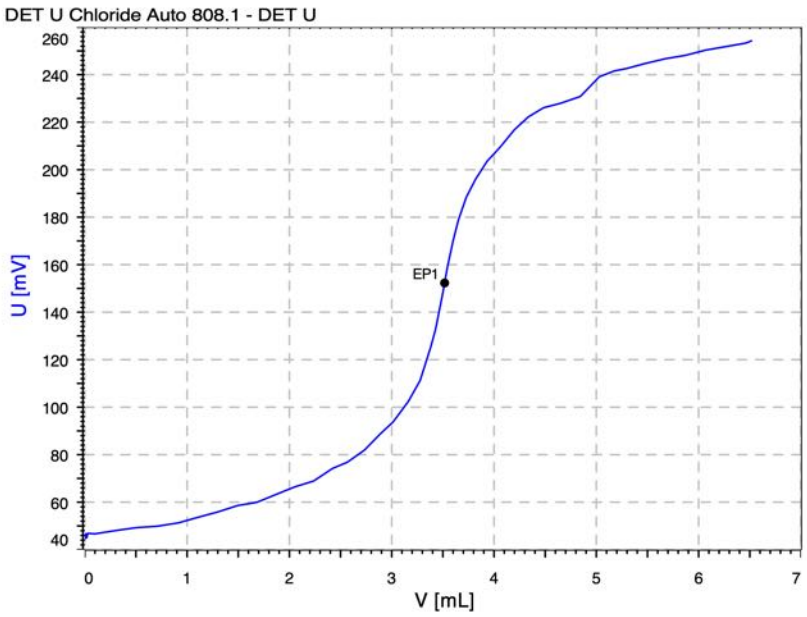

tiamo Page 1 of 1 Metrohm

Figure 45: Water-soluble chloride analysis from potentiometric titration of the filtrate from digestion of concrete powder in deionized water, where chloride content is determined from the equivalent point of titration plotted against milliliters of silver chloride titrant added during titration and corresponding changes in millivolts where the steepest point in the titration curve defines the equivalent point. Chloride content is determined from the milliliters of silver nitrate used to reach the equivalent point, and the sample weight.

License ID 4017173 Program version tiamo 2.5 - 116 - 1
Computer name Titration-909
User Metrohm Titration 2022-02-06 10:56:13 AM

Results report

Determination of Acid-Soluble (ASTM C 1152) or Water-Soluble (ASTM C 1218) Chloride Contents

Method . . . . . DET U Chloride Auto 808
Method saving date 2020-12-05 13:32:13 UTC-5

Sample data

ID1 . . . . . CMC 0122103
ID2 . . . . . EC-2P
ID3 . . . . . 3 inch.
Sample size . . . . . 10.124 g

End points

DET U **DET U Chloride Auto 808.1**
EP1 . . . . . 159.3 mV . . . . . 2.7970 mL

Results

% Chloride . . . . . **0.0489 %**

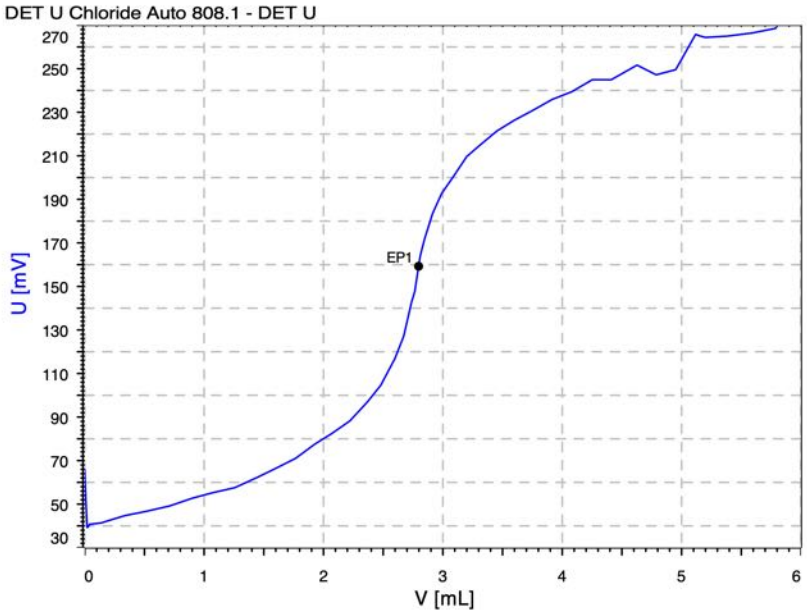

tiamo Page 1 of 1 Metrohm

Figure 46: Water-soluble chloride analysis from potentiometric titration of the filtrate from digestion of concrete powder in deionized water, where chloride content is determined from the equivalent point of titration plotted against milliliters of silver chloride titrant added during titration and corresponding changes in millivolts where the steepest point in the titration curve defines the equivalent point. Chloride content is determined from the milliliters of silver nitrate used to reach the equivalent point, and the sample weight.

License ID 4017173 Program version tiamo 2.5 - 116 - 1
Computer name Titration-909
User Metrohm Titration 2022-02-06 10:56:12 AM

Results report

Determination of Acid-Soluble (ASTM C 1152) or Water-Soluble (ASTM C 1218) Chloride Contents

Method . . . . . DET U Chloride Auto 808
Method saving date 2020-12-05 13:32:13 UTC-5

Sample data

ID1 . . . . . CMC 0122103
ID2 . . . . . EC-2P
ID3 . . . . . 5 inch.
Sample size . . . . . 10.962 g

End points

DET U **DET U Chloride Auto 808.1**

EP1 . . . . . 151.4 mV . . . . . 1.6329 mL

Results

% Chloride . . . . . **0.0264 %**

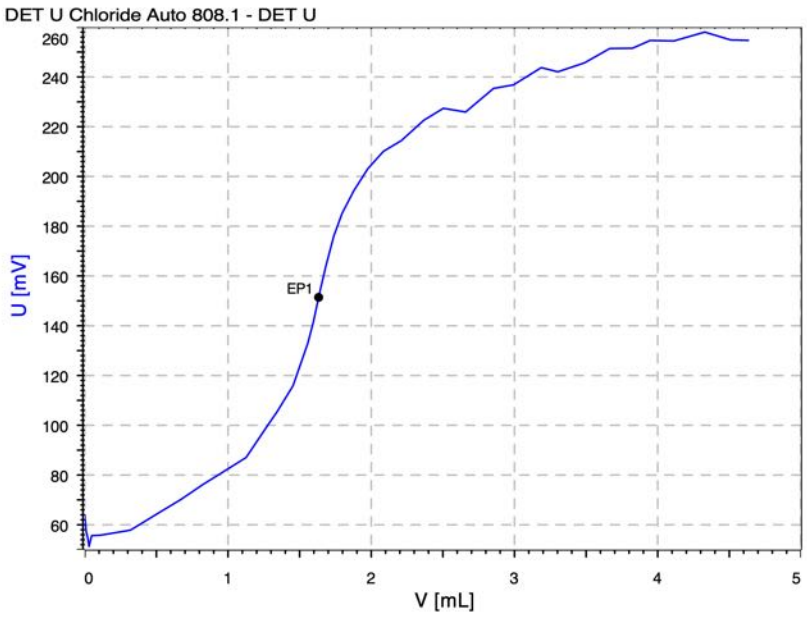

tiamo Page 1 of 1 Metrohm

Figure 47: Water-soluble chloride analysis from potentiometric titration of the filtrate from digestion of concrete powder in deionized water, where chloride content is determined from the equivalent point of titration plotted against milliliters of silver chloride titrant added during titration and corresponding changes in millivolts where the steepest point in the titration curve defines the equivalent point. Chloride content is determined from the milliliters of silver nitrate used to reach the equivalent point, and the sample weight.

License ID 4017173 Program version tiamo 2.5 - 116 - 1
Computer name Titration-909
User Metrohm Titration 2022-02-06 10:56:11 AM

Results report

Determination of Acid-Soluble (ASTM C 1152) or Water-Soluble (ASTM C 1218) Chloride Contents

Method . . . . . DET U Chloride Auto 808
Method saving date 2020-12-05 13:32:13 UTC-5

Sample data

ID1 . . . . . CMC 0122103
ID2 . . . . . EC-2P
ID3 . . . . . 10 inch.
Sample size . . . . . 10.016 g

End points

DET U **DET U Chloride Auto 808.1**
EP1 . . . . . 150.9 mV . . . . . 1.1293 mL

Results

% Chloride . . . . . **0.0200 %**

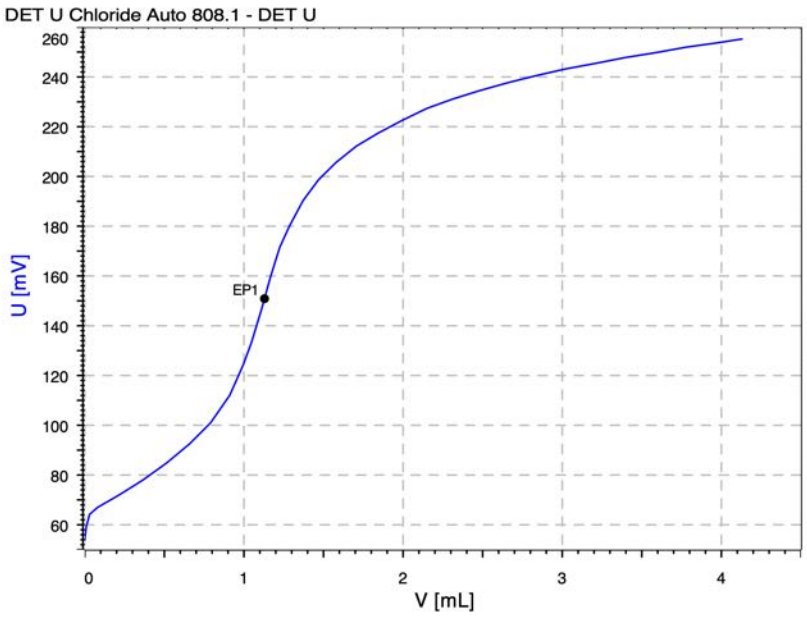

tiamo Page 1 of 1 Metrohm

Figure 48: Water-soluble chloride analysis from potentiometric titration of the filtrate from digestion of concrete powder in deionized water, where chloride content is determined from the equivalent point of titration plotted against milliliters of silver chloride titrant added during titration and corresponding changes in millivolts where the steepest point in the titration curve defines the equivalent point. Chloride content is determined from the milliliters of silver nitrate used to reach the equivalent point, and the sample weight.

License ID 4017173 Program version tiamo 2.5 - 116 - 1
Computer name Titration-909
User Metrohm Titration 2022-02-06 10:56:09 AM

Results report

Determination of Acid-Soluble (ASTM C 1152) or Water-Soluble (ASTM C 1218) Chloride Contents

Method . . . . . DET U Chloride Auto 808
Method saving date 2020-12-05 13:32:13 UTC-5

Sample data

ID1 . . . . . CMC 0122103
ID2 . . . . . EC-2P
ID3 . . . . . 15 inch.
Sample size . . . . . 10.106 g

End points

DET U **DET U Chloride Auto 808.1**

EP1 . . . . . 84.1 mV . . . . . 0.1786 mL
EP2 . . . . . 149.4 mV . . . . . 1.1168 mL

Results

% Chloride . . . . . **0.0031 %**

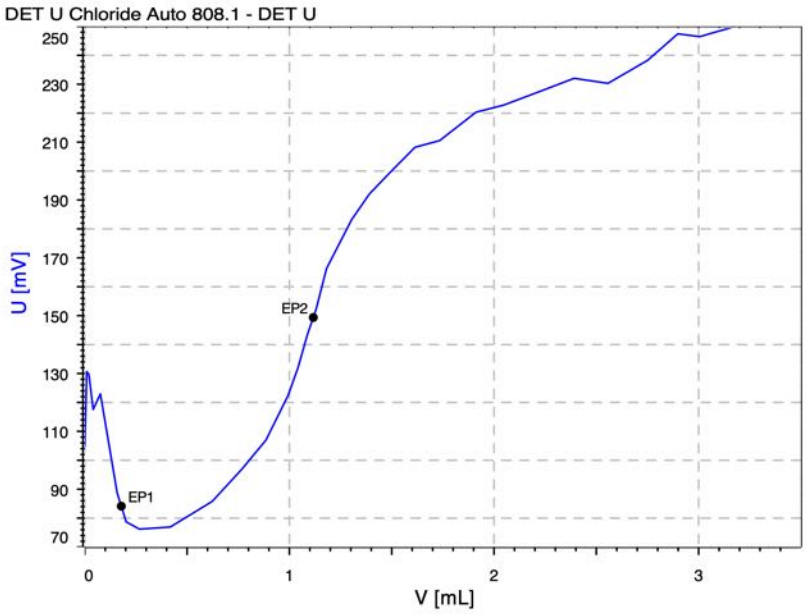

tiamo Page 1 of 1 Metrohm

Figure 49: Water-soluble chloride analysis from potentiometric titration of the filtrate from digestion of concrete powder in deionized water, where chloride content is determined from the equivalent point of titration plotted against milliliters of silver chloride titrant added during titration and corresponding changes in millivolts where the steepest point in the titration curve defines the equivalent point. Chloride content is determined from the milliliters of silver nitrate used to reach the equivalent point, and the sample weight.

License ID 4017173 Program version tiamo 2.5 - 116 - 1
Computer name Titration-909
User Metrohm Titration 2022-02-06 10:57:29 AM

Results report

Determination of Acid-Soluble (ASTM C 1152) or Water-Soluble (ASTM C 1218) Chloride Contents

Method . . . . . DET U Chloride Auto 808
Method saving date 2020-12-05 13:32:13 UTC-5

Sample data

ID1 . . . . . CMC 0122103
ID2 . . . . . EC-3
ID3 . . . . . 1 inch.
Sample size . . . . . 9.241 g

End points

DET U **DET U Chloride Auto 808.1**
EP1 . . . . . 152.1 mV . . . . . 2.2484 mL

Results

% Chloride . . . . . **0.0431 %**

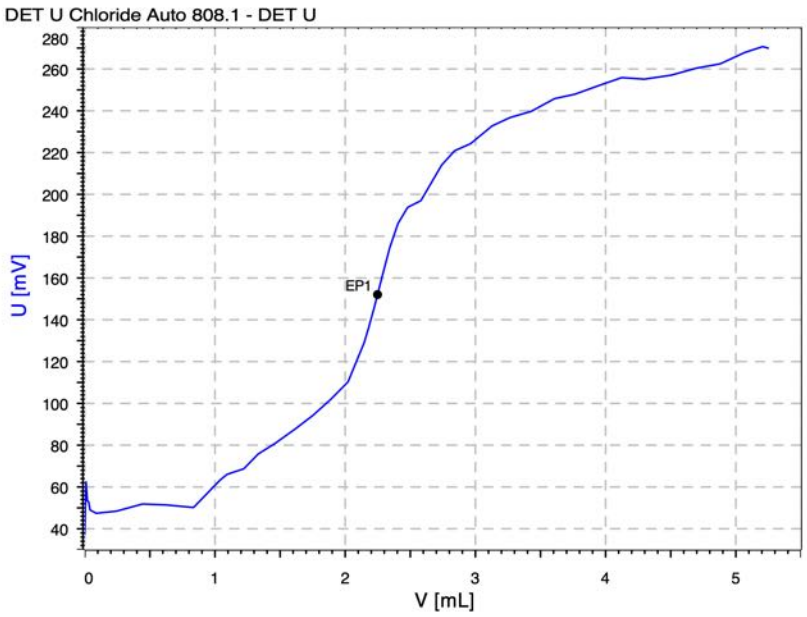

tiamo Page 1 of 1 Metrohm

Figure 50: Water-soluble chloride analysis from potentiometric titration of the filtrate from digestion of concrete powder in deionized water, where chloride content is determined from the equivalent point of titration plotted against milliliters of silver chloride titrant added during titration and corresponding changes in millivolts where the steepest point in the titration curve defines the equivalent point. Chloride content is determined from the milliliters of silver nitrate used to reach the equivalent point, and the sample weight.

License ID 4017173 Program version tiamo 2.5 - 116 - 1
Computer name Titration-909
User Metrohm Titration 2022-02-06 10:57:28 AM

Results report

Determination of Acid-Soluble (ASTM C 1152) or Water-Soluble (ASTM C 1218) Chloride Contents

Method . . . . . DET U Chloride Auto 808
Method saving date 2020-12-05 13:32:13 UTC-5

Sample data

ID1 . . . . . CMC 0122103
ID2 . . . . . EC-3
ID3 . . . . . 3 inch.
Sample size . . . . . 10.224 g

End points

DET U **DET U Chloride Auto 808.1**
EP1 . . . . . 163.0 mV . . . . . 1.2054 mL

Results

% Chloride . . . . . **0.0209 %**

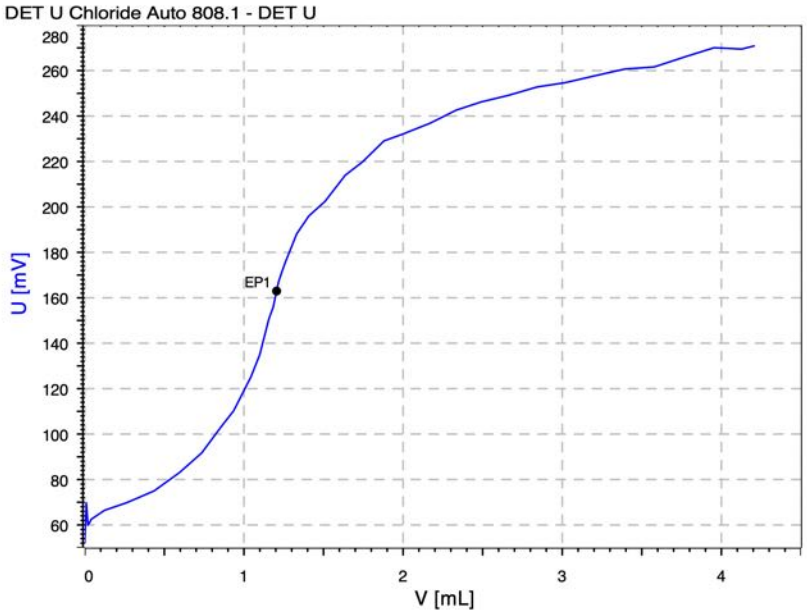

tiamo Page 1 of 1 Metrohm

Figure 51: Water-soluble chloride analysis from potentiometric titration of the filtrate from digestion of concrete powder in deionized water, where chloride content is determined from the equivalent point of titration plotted against milliliters of silver chloride titrant added during titration and corresponding changes in millivolts where the steepest point in the titration curve defines the equivalent point. Chloride content is determined from the milliliters of silver nitrate used to reach the equivalent point, and the sample weight.

License ID 4017173 Program version tiamo 2.5 - 116 - 1
Computer name Titration-909
User Metrohm Titration 2022-02-06 10:57:27 AM

Results report

Determination of Acid-Soluble (ASTM C 1152) or Water-Soluble (ASTM C 1218) Chloride Contents

Method . . . . . DET U Chloride Auto 808
Method saving date 2020-12-05 13:32:13 UTC-5

Sample data

ID1 . . . . . CMC 0122103
ID2 . . . . . EC-3
ID3 . . . . . 5 inch.
Sample size . . . . . 10.044 g

End points

DET U **DET U Chloride Auto 808.1**

EP1 . . . . . 155.4 mV . . . . . 2.8706 mL

Results

% Chloride . . . . . **0.0506 %**

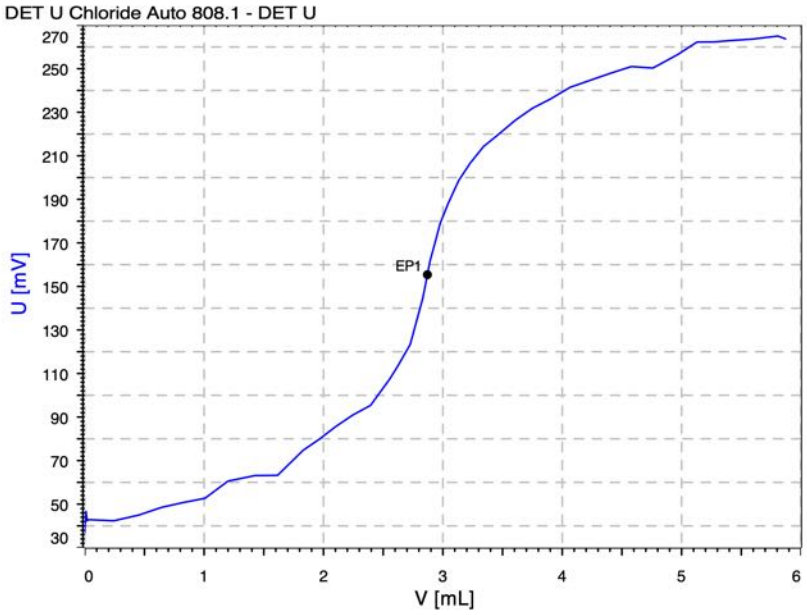

tiamo Page 1 of 1 Metrohm

Figure 52: Water-soluble chloride analysis from potentiometric titration of the filtrate from digestion of concrete powder in deionized water, where chloride content is determined from the equivalent point of titration plotted against milliliters of silver chloride titrant added during titration and corresponding changes in millivolts where the steepest point in the titration curve defines the equivalent point. Chloride content is determined from the milliliters of silver nitrate used to reach the equivalent point, and the sample weight.

License ID 4017173 Program version tiamo 2.5 - 116 - 1
Computer name Titration-909
User Metrohm Titration 2022-02-06 10:57:25 AM

Results report

Determination of Acid-Soluble (ASTM C 1152) or Water-Soluble (ASTM C 1218) Chloride Contents

Method . . . . . DET U Chloride Auto 808
Method saving date 2020-12-05 13:32:13 UTC-5

Sample data

ID1 . . . . . CMC 0122103
ID2 . . . . . EC-3
ID3 . . . . . 10 inch.
Sample size . . . . . 10.708 g

End points

DET U **DET U Chloride Auto 808.1**
EP1 . . . . . 157.4 mV . . . . . 1.9329 mL

Results

% Chloride . . . . . **0.0320 %**

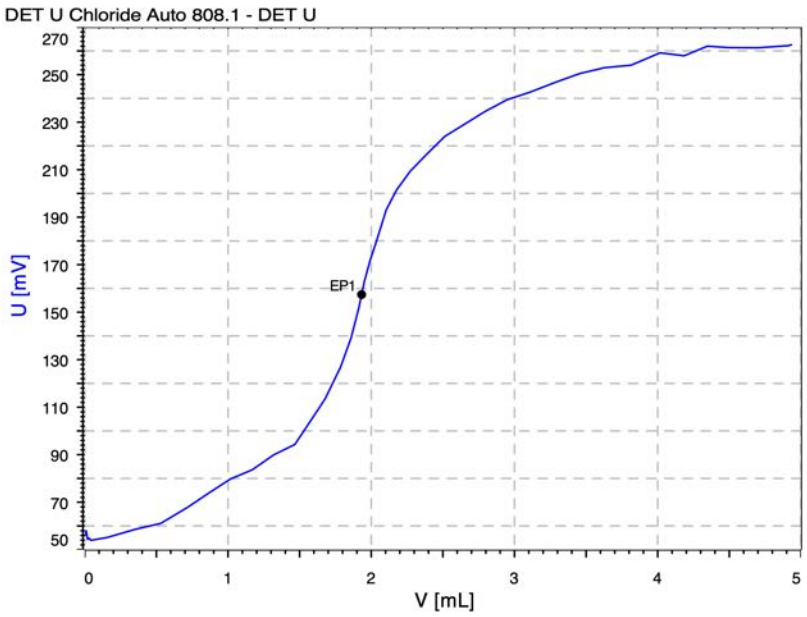

tiamo Page 1 of 1 Metrohm

Figure 53: Water-soluble chloride analysis from potentiometric titration of the filtrate from digestion of concrete powder in deionized water, where chloride content is determined from the equivalent point of titration plotted against milliliters of silver chloride titrant added during titration and corresponding changes in millivolts where the steepest point in the titration curve defines the equivalent point. Chloride content is determined from the milliliters of silver nitrate used to reach the equivalent point, and the sample weight.

License ID 4017173 Program version tiamo 2.5 - 116 - 1
Computer name Titration-909
User Metrohm Titration 2022-02-06 10:59:30 AM

Results report

Determination of Acid-Soluble (ASTM C 1152) or Water-Soluble (ASTM C 1218) Chloride Contents

Method . . . . . DET U Chloride Auto 808
Method saving date 2020-12-05 13:32:13 UTC-5

Sample data

ID1 . . . . . CMC 0122103
ID2 . . . . . EC-3
ID3 . . . . . 15 inch.
Sample size . . . . . 10.552 g

End points

DET U **DET U Chloride Auto 808.1**

EP1 . . . . . 74.6 mV . . . . . 0.0486 mL
EP2 . . . . . 145.7 mV . . . . . 1.0363 mL

Results

% Chloride . . . . . **0.0008 %**

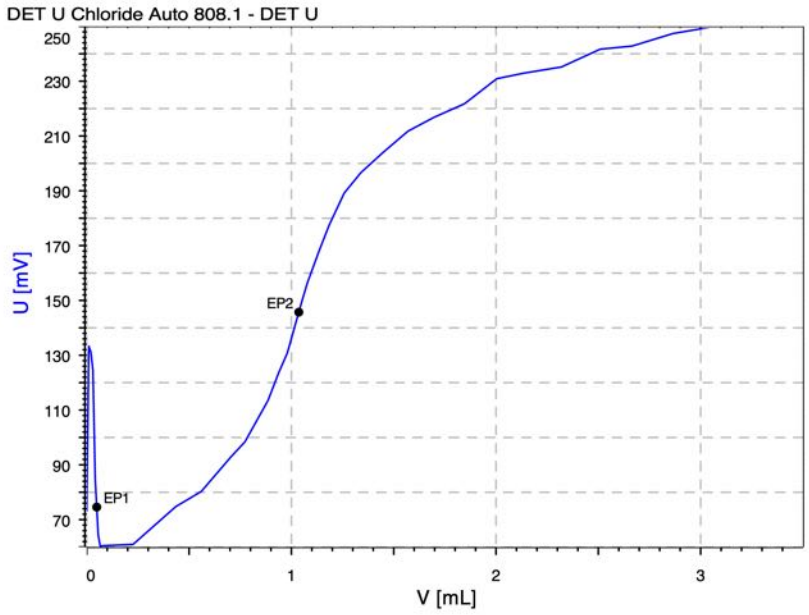

tiamo Page 1 of 1 Metrohm

Figure 54: Water-soluble chloride analysis from potentiometric titration of the filtrate from digestion of concrete powder in deionized water, where chloride content is determined from the equivalent point of titration plotted against milliliters of silver chloride titrant added during titration and corresponding changes in millivolts where the steepest point in the titration curve defines the equivalent point. Chloride content is determined from the milliliters of silver nitrate used to reach the equivalent point, and the sample weight.

License ID 4017173 Program version tiamo 2.5 - 116 - 1
Computer name Titration-909
User Metrohm Titration 2022-02-06 10:59:50 AM

Results report

Determination of Acid-Soluble (ASTM C 1152) or Water-Soluble (ASTM C 1218) Chloride Contents

Method . . . . . DET U Chloride Auto 808
Method saving date 2020-12-05 13:32:13 UTC-5

Sample data

ID1 . . . . . CMC 0122103
ID2 . . . . . EC-4
ID3 . . . . . 1 inch.
Sample size . . . . . 10.022 g

End points

DET U **DET U Chloride Auto 808.1**

EP1 . . . . . 86.3 mV . . . . . 0.5106 mL
EP2 . . . . . 153.5 mV . . . . . 1.9438 mL

Results

% Chloride . . . . . **0.0090 %**

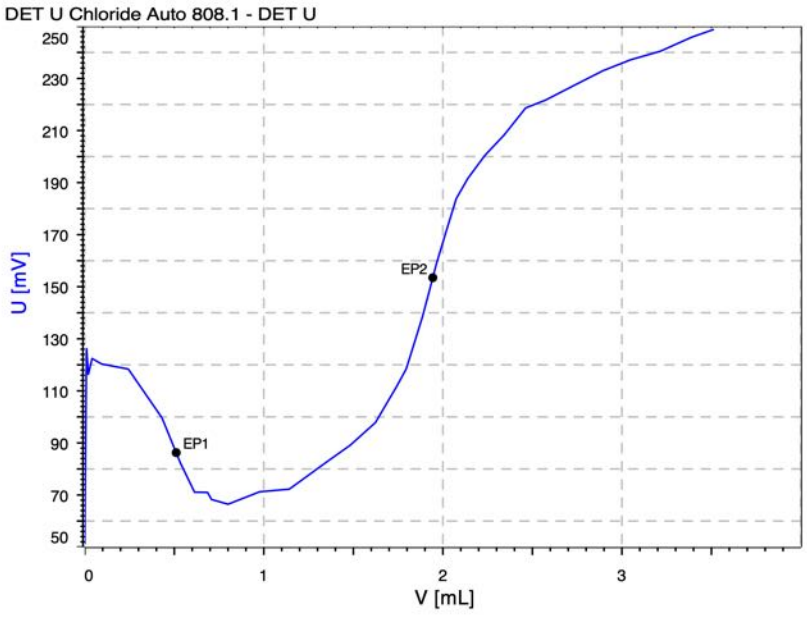

tiamo Page 1 of 1 Metrohm

Figure 55: Water-soluble chloride analysis from potentiometric titration of the filtrate from digestion of concrete powder in deionized water, where chloride content is determined from the equivalent point of titration plotted against milliliters of silver chloride titrant added during titration and corresponding changes in millivolts where the steepest point in the titration curve defines the equivalent point. Chloride content is determined from the milliliters of silver nitrate used to reach the equivalent point, and the sample weight.

License ID 4017173 Program version tiamo 2.5 - 116 - 1
Computer name Titration-909
User Metrohm Titration 2022-02-06 1:02:08 PM UTC-

Results report

Determination of Acid-Soluble (ASTM C 1152) or Water-Soluble (ASTM C 1218) Chloride Contents

Method . . . . . DET U Chloride Auto 808
Method saving date 2020-12-05 13:32:13 UTC-5

Sample data

ID1 . . . . . CMC 0122103
ID2 . . . . . EC-4
ID3 . . . . . 3 inch.
Sample size . . . . . 10.241 g

End points

DET U **DET U Chloride Auto 808.1**
EP1 . . . . . 156.8 mV . . . . . 0.8481 mL

Results

% Chloride . . . . . **0.0147 %**

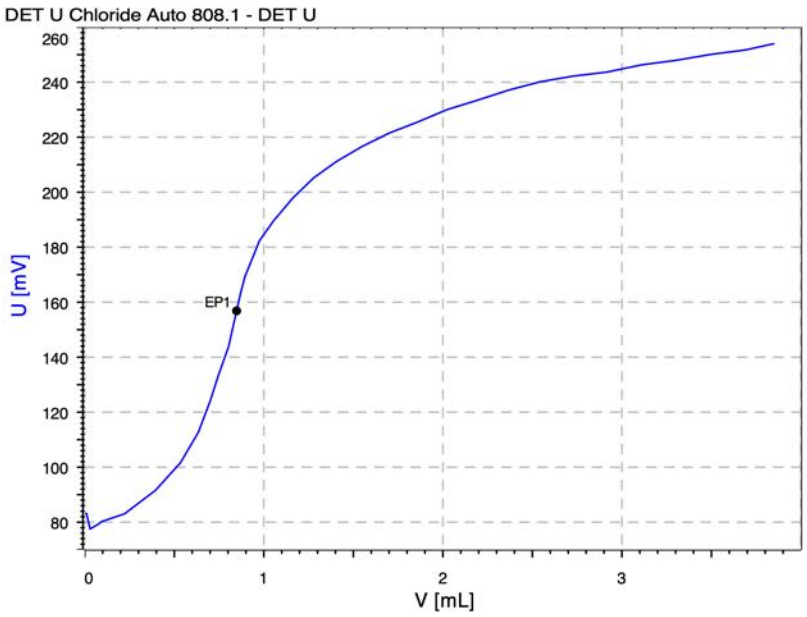

tiamo Page 1 of 1 Metrohm

Figure 56: Water-soluble chloride analysis from potentiometric titration of the filtrate from digestion of concrete powder in deionized water, where chloride content is determined from the equivalent point of titration plotted against milliliters of silver chloride titrant added during titration and corresponding changes in millivolts where the steepest point in the titration curve defines the equivalent point. Chloride content is determined from the milliliters of silver nitrate used to reach the equivalent point, and the sample weight.

License ID 4017173 Program version tiamo 2.5 - 116 - 1
Computer name Titration-909
User Metrohm Titration 2022-02-06 1:02:51 PM UTC-

Results report

Determination of Acid-Soluble (ASTM C 1152) or Water-Soluble (ASTM C 1218) Chloride Contents

Method . . . . . DET U Chloride Auto 808
Method saving date 2020-12-05 13:32:13 UTC-5

Sample data

ID1 . . . . . CMC 0122103
ID2 . . . . . EC-4
ID3 . . . . . 5 inch.
Sample size . . . . . 10.102 g

End points

DET U **DET U Chloride Auto 808.1**

EP1 . . . . . 153.5 mV . . . . . 3.2951 mL

Results

% Chloride . . . . . **0.0577 %**

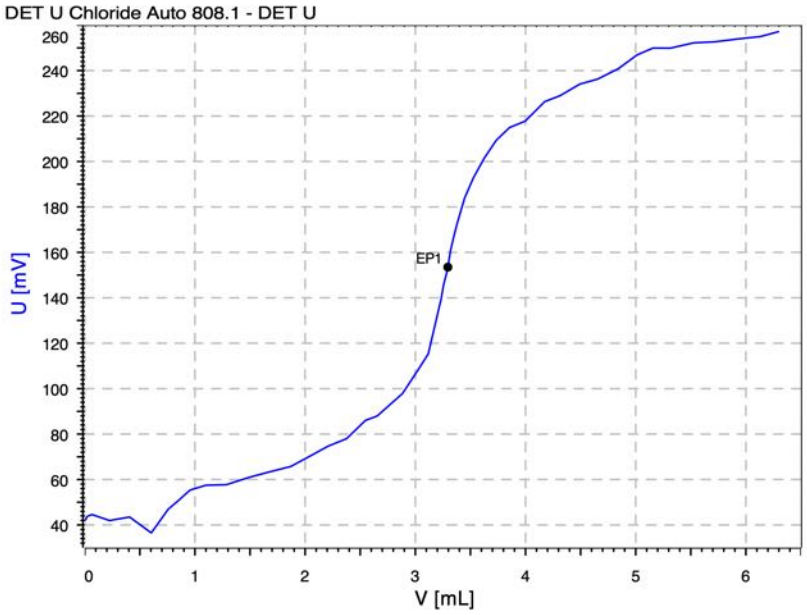

tiamo Page 1 of 1 Metrohm

Figure 57: Water-soluble chloride analysis from potentiometric titration of the filtrate from digestion of concrete powder in deionized water, where chloride content is determined from the equivalent point of titration plotted against milliliters of silver chloride titrant added during titration and corresponding changes in millivolts where the steepest point in the titration curve defines the equivalent point. Chloride content is determined from the milliliters of silver nitrate used to reach the equivalent point, and the sample weight.

License ID 4017173 Program version tiamo 2.5 - 116 - 1
Computer name Titration-909
User Metrohm Titration 2022-02-06 1:03:14 PM UTC-

Results report

Determination of Acid-Soluble (ASTM C 1152) or Water-Soluble (ASTM C 1218) Chloride Contents

Method . . . . . DET U Chloride Auto 808
Method saving date 2020-12-05 13:32:13 UTC-5

Sample data

ID1 . . . . . CMC 0122103
ID2 . . . . . EC-4
ID3 . . . . . 10 inch.
Sample size . . . . . 10.290 g

End points

DET U **DET U Chloride Auto 808.1**
EP1 . . . . . 148.0 mV . . . . . 4.8432 mL

Results

% Chloride . . . . . **0.0833 %**

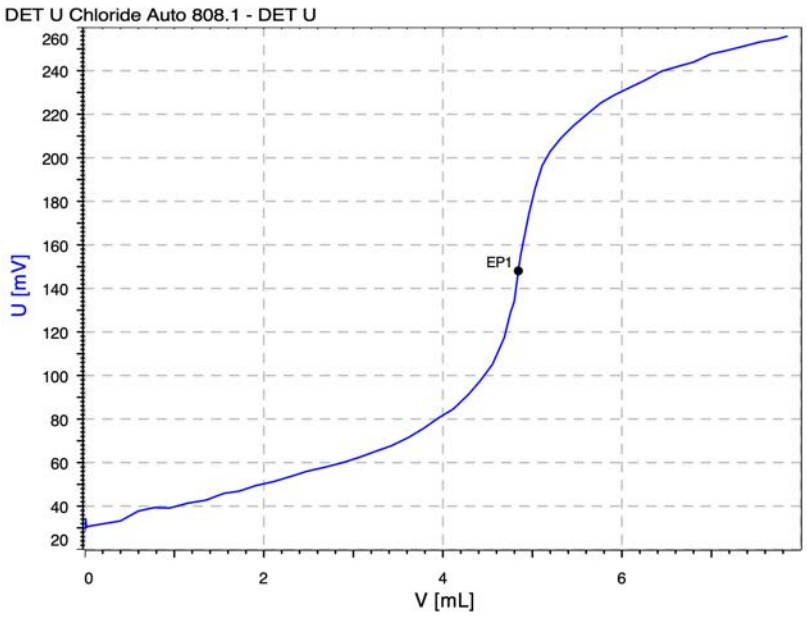

tiamo Page 1 of 1 Metrohm

Figure 58: Water-soluble chloride analysis from potentiometric titration of the filtrate from digestion of concrete powder in deionized water, where chloride content is determined from the equivalent point of titration plotted against milliliters of silver chloride titrant added during titration and corresponding changes in millivolts where the steepest point in the titration curve defines the equivalent point. Chloride content is determined from the milliliters of silver nitrate used to reach the equivalent point, and the sample weight.

License ID 4017173 Program version tiamo 2.5 - 116 - 1
Computer name Titration-909
User Metrohm Titration 2022-02-06 1:03:35 PM UTC-

Results report

Determination of Acid-Soluble (ASTM C 1152) or Water-Soluble (ASTM C 1218) Chloride Contents

Method . . . . . DET U Chloride Auto 808
Method saving date 2020-12-05 13:32:13 UTC-5

Sample data

ID1 . . . . . CMC 0122103
ID2 . . . . . EC-4
ID3 . . . . . 15 inch.
Sample size . . . . . 10.661 g

End points

DET U **DET U Chloride Auto 808.1**

EP1 . . . . . 145.3 mV . . . . . 2.6485 mL

Results

% Chloride . . . . . **0.0440 %**

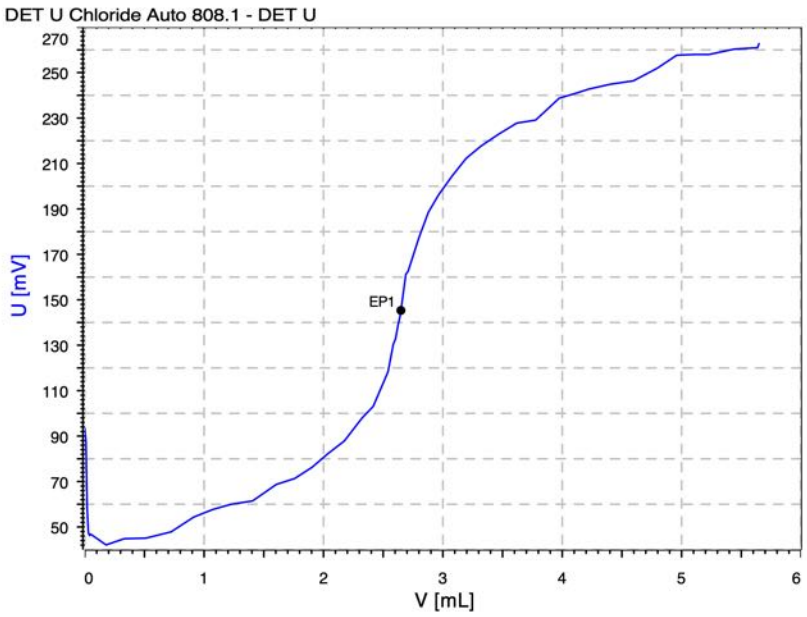

tiamo Page 1 of 1 Metrohm

Figure 59: Water-soluble chloride analysis from potentiometric titration of the filtrate from digestion of concrete powder in deionized water, where chloride content is determined from the equivalent point of titration plotted against milliliters of silver chloride titrant added during titration and corresponding changes in millivolts where the steepest point in the titration curve defines the equivalent point. Chloride content is determined from the milliliters of silver nitrate used to reach the equivalent point, and the sample weight.

License ID 4017173 Program version tiamo 2.5 - 116 - 1
Computer name Titration-909
User Metrohm Titration 2022-02-064:54:06 PM UTC-

Results report

Determination of Acid-Soluble (ASTM C 1152) or Water-Soluble (ASTM C 1218) Chloride Contents

Method . . . . . DET U Chloride Auto 808
Method saving date 2020-12-05 13:32:13 UTC-5

Sample data

ID1 . . . . . CMC 0122103
ID2 . . . . . WC-1P
ID3 . . . . . 1 inch.
Sample size . . . . . 9.740 g

End points

DET U **DET U Chloride Auto 808.1**

EP1 . . . . . 93.3 mV . . . . . 3.4046 mL
EP2 . . . . . 146.4 mV . . . . . 3.8172 mL

Results

% Chloride . . . . . **0.0619 %**

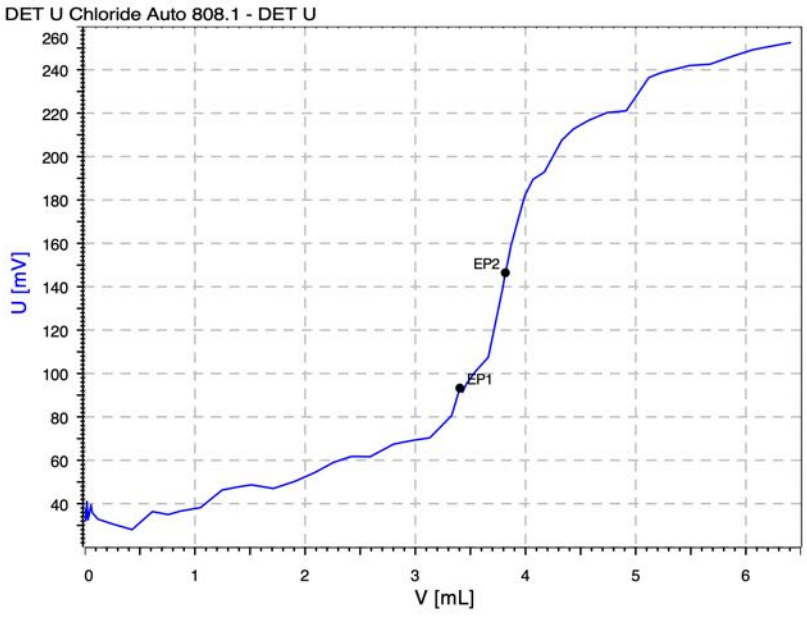

tiamo Page 1 of 1 Metrohm

Figure 60: Water-soluble chloride analysis from potentiometric titration of the filtrate from digestion of concrete powder in deionized water, where chloride content is determined from the equivalent point of titration plotted against milliliters of silver chloride titrant added during titration and corresponding changes in millivolts where the steepest point in the titration curve defines the equivalent point. Chloride content is determined from the milliliters of silver nitrate used to reach the equivalent point, and the sample weight.

License ID 4017173 Program version tiamo 2.5 - 116 - 1
Computer name Titration-909
User Metrohm Titration 2022-02-064:54:05 PM UTC-

Results report

Determination of Acid-Soluble (ASTM C 1152) or Water-Soluble (ASTM C 1218) Chloride Contents

Method . . . . . DET U Chloride Auto 808
Method saving date 2020-12-05 13:32:13 UTC-5

Sample data

ID1 . . . . . CMC 0122103
ID2 . . . . . WC-1P
ID3 . . . . . 3 inch.
Sample size . . . . . 9.933 g

End points

DET U **DET U Chloride Auto 808.1**
EP1 . . . . . 162.2 mV . . . . . 4.4874 mL

Results

% Chloride . . . . . **0.0800 %**

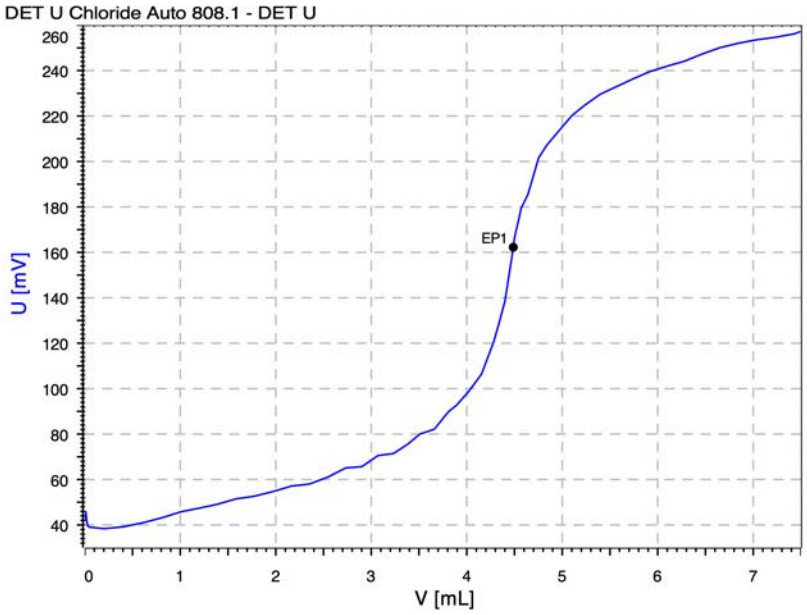

tiamo Page 1 of 1 Metrohm

Figure 61: Water-soluble chloride analysis from potentiometric titration of the filtrate from digestion of concrete powder in deionized water, where chloride content is determined from the equivalent point of titration plotted against milliliters of silver chloride titrant added during titration and corresponding changes in millivolts where the steepest point in the titration curve defines the equivalent point. Chloride content is determined from the milliliters of silver nitrate used to reach the equivalent point, and the sample weight.

License ID 4017173 Program version tiamo 2.5 - 116 - 1
Computer name Titration-909
User Metrohm Titration 2022-02-064:54:03 PM UTC-

Results report

Determination of Acid-Soluble (ASTM C 1152) or Water-Soluble (ASTM C 1218) Chloride Contents

Method . . . . . DET U Chloride Auto 808
Method saving date 2020-12-05 13:32:13 UTC-5

Sample data

ID1 . . . . . CMC 0122103
ID2 . . . . . WC-1P
ID3 . . . . . 5 inch.
Sample size . . . . . 9.714 g

End points

DET U **DET U Chloride Auto 808.1**

EP1 . . . . . 155.7 mV . . . . . 2.0333 mL

Results

% Chloride . . . . . **0.0370 %**

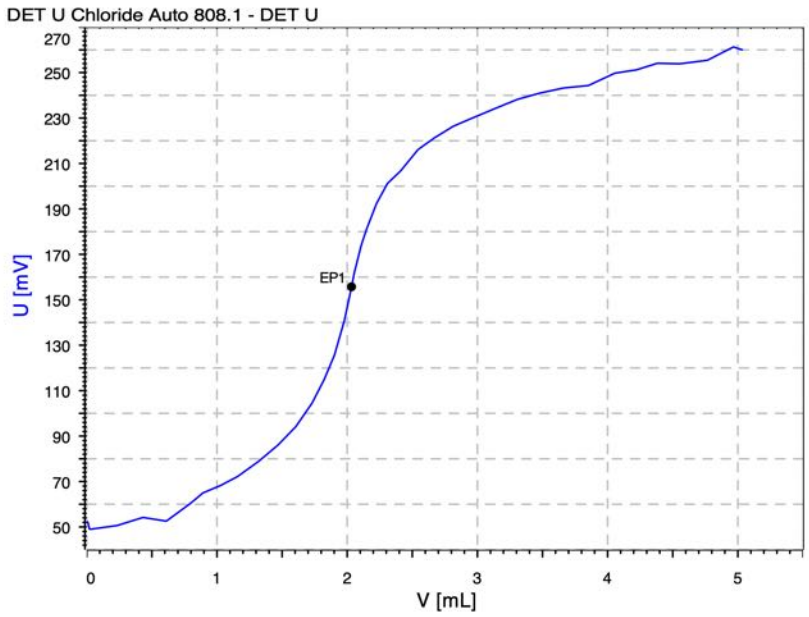

tiamo Page 1 of 1 Metrohm

Figure 62: Water-soluble chloride analysis from potentiometric titration of the filtrate from digestion of concrete powder in deionized water, where chloride content is determined from the equivalent point of titration plotted against milliliters of silver chloride titrant added during titration and corresponding changes in millivolts where the steepest point in the titration curve defines the equivalent point. Chloride content is determined from the milliliters of silver nitrate used to reach the equivalent point, and the sample weight.

License ID 4017173 Program version tiamo 2.5 - 116 - 1
Computer name Titration-909
User Metrohm Titration 2022-02-064:54:02 PM UTC-

Results report

Determination of Acid-Soluble (ASTM C 1152) or Water-Soluble (ASTM C 1218) Chloride Contents

Method . . . . . DET U Chloride Auto 808
Method saving date 2020-12-05 13:32:13 UTC-5

Sample data

ID1 . . . . . CMC 0122103
ID2 . . . . . WC-1P
ID3 . . . . . 10 inch.
Sample size . . . . . 10.536 g

End points

DET U **DET U Chloride Auto 808.1**

EP1 . . . . . 150.6 mV . . . . . 1.9273 mL

Results

% Chloride . . . . . **0.0324 %**

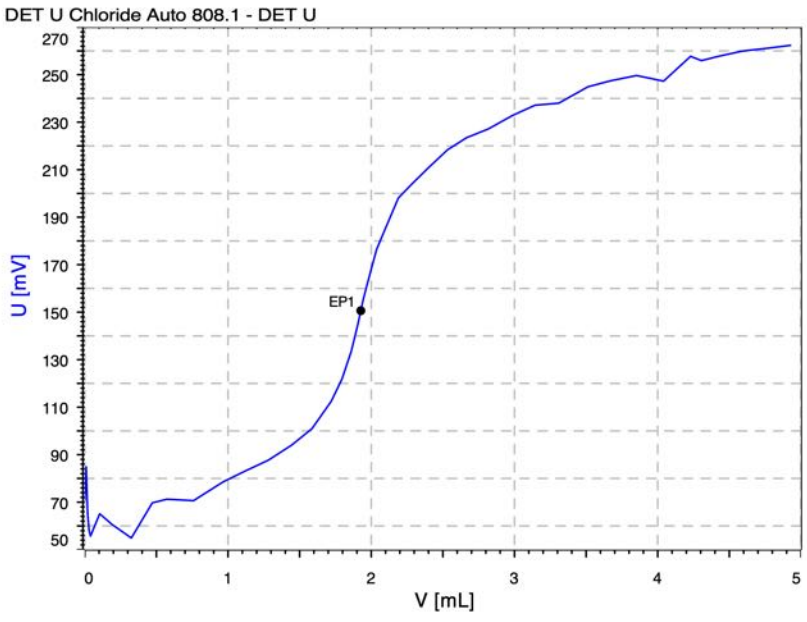

tiamo Page 1 of 1 Metrohm

Figure 63: Water-soluble chloride analysis from potentiometric titration of the filtrate from digestion of concrete powder in deionized water, where chloride content is determined from the equivalent point of titration plotted against milliliters of silver chloride titrant added during titration and corresponding changes in millivolts where the steepest point in the titration curve defines the equivalent point. Chloride content is determined from the milliliters of silver nitrate used to reach the equivalent point, and the sample weight.

License ID 4017173 Program version tiamo 2.5 - 116 - 1
Computer name Titration-909
User Metrohm Titration 2022-02-064:54:00 PM UTC-

Results report

Determination of Acid-Soluble (ASTM C 1152) or Water-Soluble (ASTM C 1218) Chloride Contents

Method . . . . . DET U Chloride Auto 808
Method saving date 2020-12-05 13:32:13 UTC-5

Sample data

ID1 . . . . . CMC 0122103
ID2 . . . . . WC-1P
ID3 . . . . . 15 inch.
Sample size . . . . . 10.044 g

End points

DET U **DET U Chloride Auto 808.1**
EP1 . . . . . 152.5 mV . . . . . 1.0303 mL

Results

% Chloride . . . . . **0.0182 %**

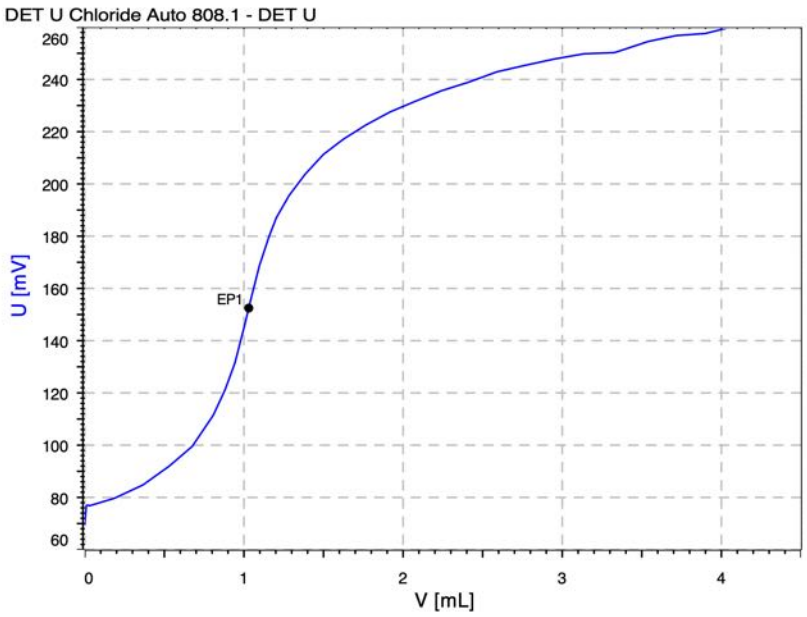

tiamo Page 1 of 1 Metrohm

Figure 64: Water-soluble chloride analysis from potentiometric titration of the filtrate from digestion of concrete powder in deionized water, where chloride content is determined from the equivalent point of titration plotted against milliliters of silver chloride titrant added during titration and corresponding changes in millivolts where the steepest point in the titration curve defines the equivalent point. Chloride content is determined from the milliliters of silver nitrate used to reach the equivalent point, and the sample weight.

License ID 4017173 Program version tiamo 2.5 - 116 - 1
Computer name Titration-909
User Metrohm Titration 2022-02-064:55:25 PM UTC-

Results report

Determination of Acid-Soluble (ASTM C 1152) or Water-Soluble (ASTM C 1218) Chloride Contents

Method . . . . . DET U Chloride Auto 808
Method saving date 2020-12-05 13:32:13 UTC-5

Sample data

ID1 . . . . . CMC 0122103
ID2 . . . . . WC-2P
ID3 . . . . . 1 inch.
Sample size . . . . . 10.414 g

End points

DET U **DET U Chloride Auto 808.1**

EP1 . . . . . 155.8 mV . . . . . 2.3380 mL

Results

% Chloride . . . . . **0.0397 %**

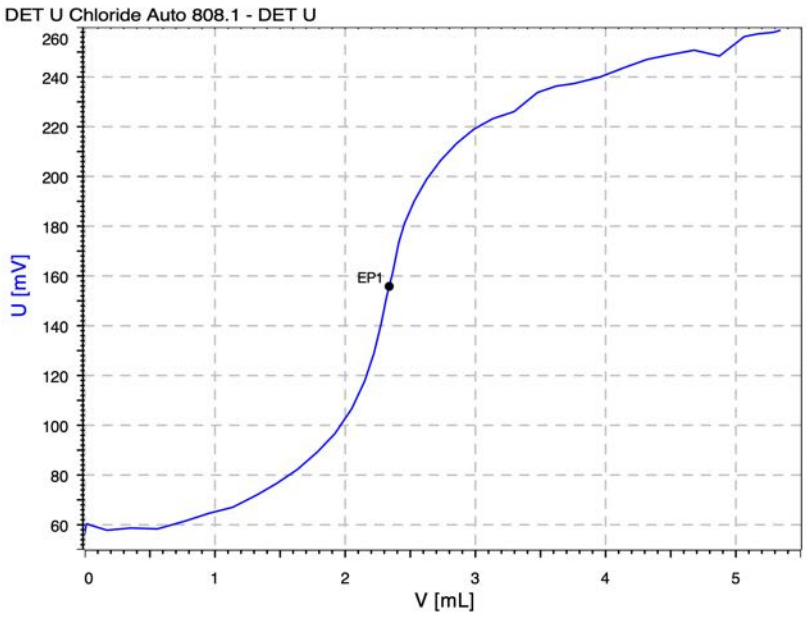

tiamo Page 1 of 1 Metrohm

Figure 65: Water-soluble chloride analysis from potentiometric titration of the filtrate from digestion of concrete powder in deionized water, where chloride content is determined from the equivalent point of titration plotted against milliliters of silver chloride titrant added during titration and corresponding changes in millivolts where the steepest point in the titration curve defines the equivalent point. Chloride content is determined from the milliliters of silver nitrate used to reach the equivalent point, and the sample weight.

License ID 4017173 Program version tiamo 2.5 - 116 - 1
Computer name Titration-909
User Metrohm Titration 2022-02-064:55:23 PM UTC-

Results report

Determination of Acid-Soluble (ASTM C 1152) or Water-Soluble (ASTM C 1218) Chloride Contents

Method . . . . . DET U Chloride Auto 808
Method saving date 2020-12-05 13:32:13 UTC-5

Sample data

ID1 . . . . . CMC 0122103
ID2 . . . . . WC-2P
ID3 . . . . . 3 inch.
Sample size . . . . . 10.681 g

End points

DET U **DET U Chloride Auto 808.1**

EP1 . . . . . 150.8 mV . . . . . 1.5031 mL

Results

% Chloride . . . . . **0.0249 %**

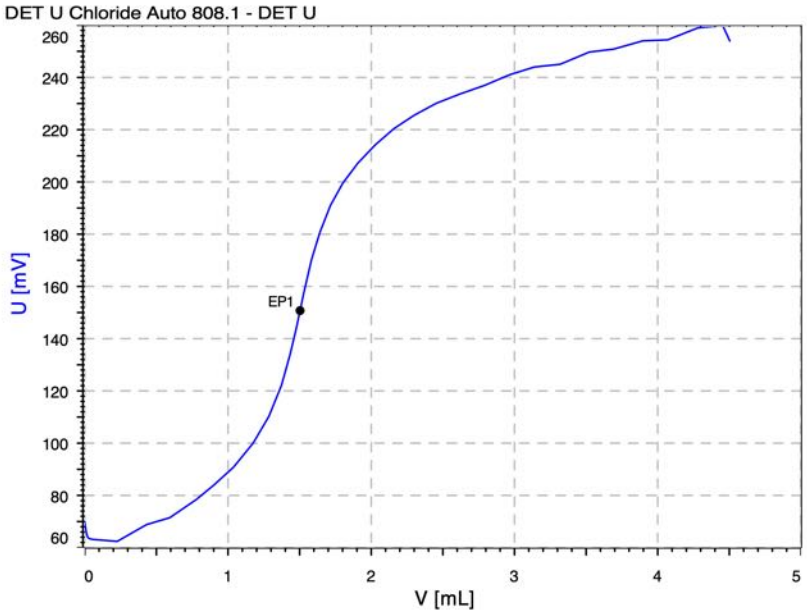

tiamo Page 1 of 1 Metrohm

Figure 66: Water-soluble chloride analysis from potentiometric titration of the filtrate from digestion of concrete powder in deionized water, where chloride content is determined from the equivalent point of titration plotted against milliliters of silver chloride titrant added during titration and corresponding changes in millivolts where the steepest point in the titration curve defines the equivalent point. Chloride content is determined from the milliliters of silver nitrate used to reach the equivalent point, and the sample weight.

License ID 4017173 Program version tiamo 2.5 - 116 - 1
Computer name Titration-909
User Metrohm Titration 2022-02-064:55:22 PM UTC-

Results report

Determination of Acid-Soluble (ASTM C 1152) or Water-Soluble (ASTM C 1218) Chloride Contents

Method . . . . . DET U Chloride Auto 808
Method saving date 2020-12-05 13:32:13 UTC-5

Sample data

ID1 . . . . . CMC 0122103
ID2 . . . . . WC-2P
ID3 . . . . . 5 inch.
Sample size . . . . . 9.363 g

End points

DET U **DET U Chloride Auto 808.1**

EP1 . . . . . 149.6 mV . . . . . 0.7099 mL

Results

% Chloride . . . . . **0.0134 %**

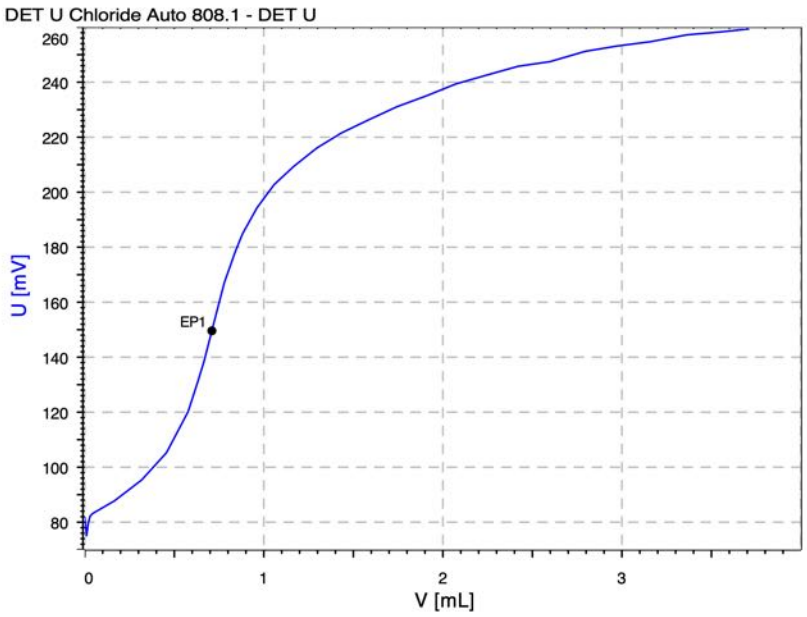

tiamo Page 1 of 1 Metrohm

Figure 67: Water-soluble chloride analysis from potentiometric titration of the filtrate from digestion of concrete powder in deionized water, where chloride content is determined from the equivalent point of titration plotted against milliliters of silver chloride titrant added during titration and corresponding changes in millivolts where the steepest point in the titration curve defines the equivalent point. Chloride content is determined from the milliliters of silver nitrate used to reach the equivalent point, and the sample weight.

License ID 4017173 Program version tiamo 2.5 - 116 - 1
Computer name Titration-909
User Metrohm Titration 2022-02-067:55:58 PM UTC-

Results report

Determination of Acid-Soluble (ASTM C 1152) or Water-Soluble (ASTM C 1218) Chloride Contents

Method . . . . . DET U Chloride Auto 808
Method saving date 2020-12-05 13:32:13 UTC-5

Sample data

ID1 . . . . . CMC 0122103
ID2 . . . . . WC-2P
ID3 . . . . . 10 inch.
Sample size . . . . . 10.347 g

End points

DET U **DET U Chloride Auto 808.1**
EP1 . . . . . 163.9 mV . . . . . 0.3229 mL

Results

% Chloride . . . . . **0.0055 %**

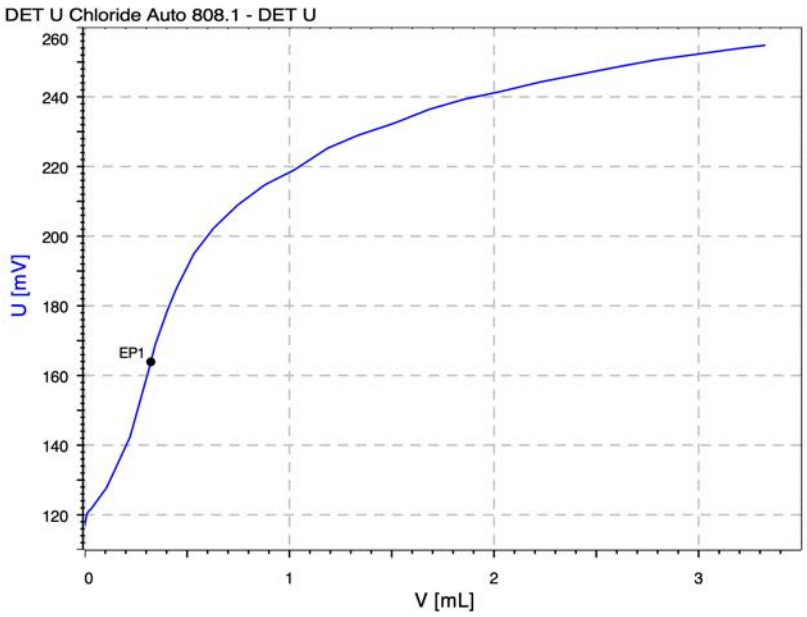

tiamo Page 1 of 1 Metrohm

Figure 68: Water-soluble chloride analysis from potentiometric titration of the filtrate from digestion of concrete powder in deionized water, where chloride content is determined from the equivalent point of titration plotted against milliliters of silver chloride titrant added during titration and corresponding changes in millivolts where the steepest point in the titration curve defines the equivalent point. Chloride content is determined from the milliliters of silver nitrate used to reach the equivalent point, and the sample weight.

License ID 4017173 Program version tiamo 2.5 - 116 - 1
Computer name Titration-909
User Metrohm Titration 2022-02-067:56:49 PM UTC-

Results report

Determination of Acid-Soluble (ASTM C 1152) or Water-Soluble (ASTM C 1218) Chloride Contents

Method . . . . . DET U Chloride Auto 808
Method saving date 2020-12-05 13:32:13 UTC-5

Sample data

ID1 . . . . . CMC 0122103
ID2 . . . . . WC-2P
ID3 . . . . . 15 inch.
Sample size . . . . . 10.372 g

End points

DET U **DET U Chloride Auto 808.1**
EP1 . . . . . 158.3 mV . . . . . 0.3241 mL

Results

% Chloride . . . . . **0.0055 %**

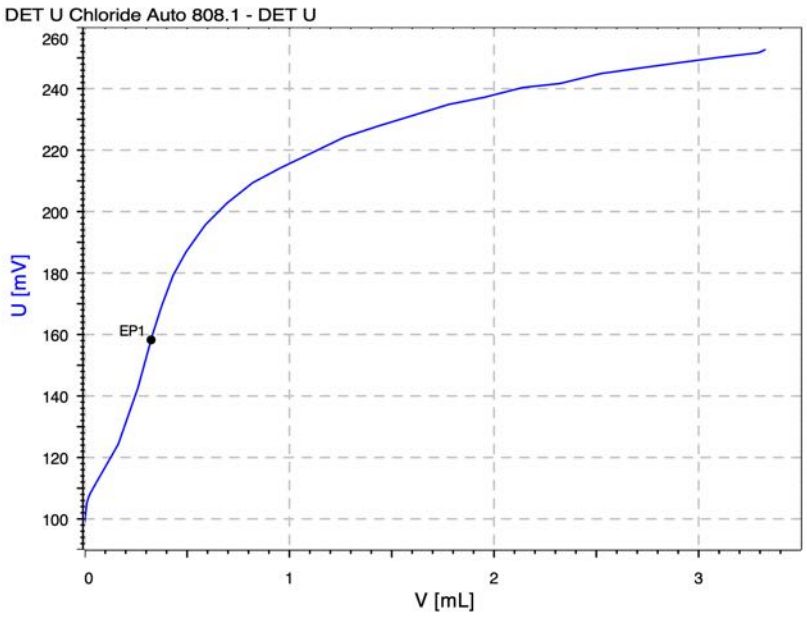

tiamo Page 1 of 1 Metrohm

Figure 69: Water-soluble chloride analysis from potentiometric titration of the filtrate from digestion of concrete powder in deionized water, where chloride content is determined from the equivalent point of titration plotted against milliliters of silver chloride titrant added during titration and corresponding changes in millivolts where the steepest point in the titration curve defines the equivalent point. Chloride content is determined from the milliliters of silver nitrate used to reach the equivalent point, and the sample weight.

License ID 4017173 Program version tiamo 2.5 - 116 - 1
Computer name Titration-909
User Metrohm Titration 2022-02-067:57:23 PM UTC-

Results report

Determination of Acid-Soluble (ASTM C 1152) or Water-Soluble (ASTM C 1218) Chloride Contents

Method . . . . . DET U Chloride Auto 808
Method saving date 2020-12-05 13:32:13 UTC-5

Sample data

ID1 . . . . . CMC 0122103
ID2 . . . . . WC-3
ID3 . . . . . 1 inch.
Sample size . . . . . 9.910 g

End points

DET U **DET U Chloride Auto 808.1**
EP1 . . . . . 155.8 mV . . . . . 1.3753 mL

Results

% Chloride . . . . . **0.0246 %**

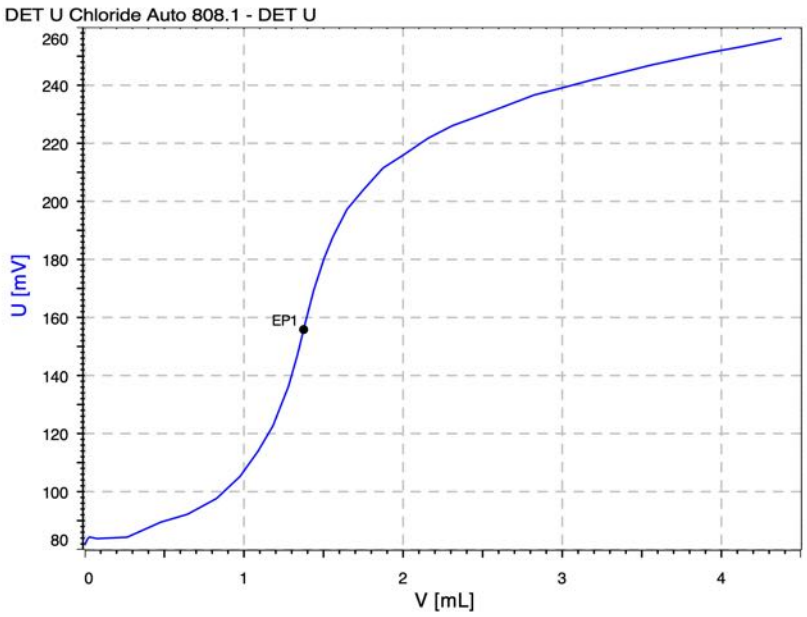

tiamo Page 1 of 1 Metrohm

Figure 70: Water-soluble chloride analysis from potentiometric titration of the filtrate from digestion of concrete powder in deionized water, where chloride content is determined from the equivalent point of titration plotted against milliliters of silver chloride titrant added during titration and corresponding changes in millivolts where the steepest point in the titration curve defines the equivalent point. Chloride content is determined from the milliliters of silver nitrate used to reach the equivalent point, and the sample weight.

License ID 4017173 Program version tiamo 2.5 - 116 - 1
Computer name Titration-909
User Metrohm Titration 2022-02-067:57:21 PM UTC-

Results report

Determination of Acid-Soluble (ASTM C 1152) or Water-Soluble (ASTM C 1218) Chloride Contents

Method . . . . . DET U Chloride Auto 808
Method saving date 2020-12-05 13:32:13 UTC-5

Sample data

ID1 . . . . . CMC 0122103
ID2 . . . . . WC-3
ID3 . . . . . 3 inch.
Sample size . . . . . 10.309 g

End points

DET U **DET U Chloride Auto 808.1**

EP1 . . . . . 152.1 mV . . . . . 3.0379 mL

Results

% Chloride . . . . . **0.0522 %**

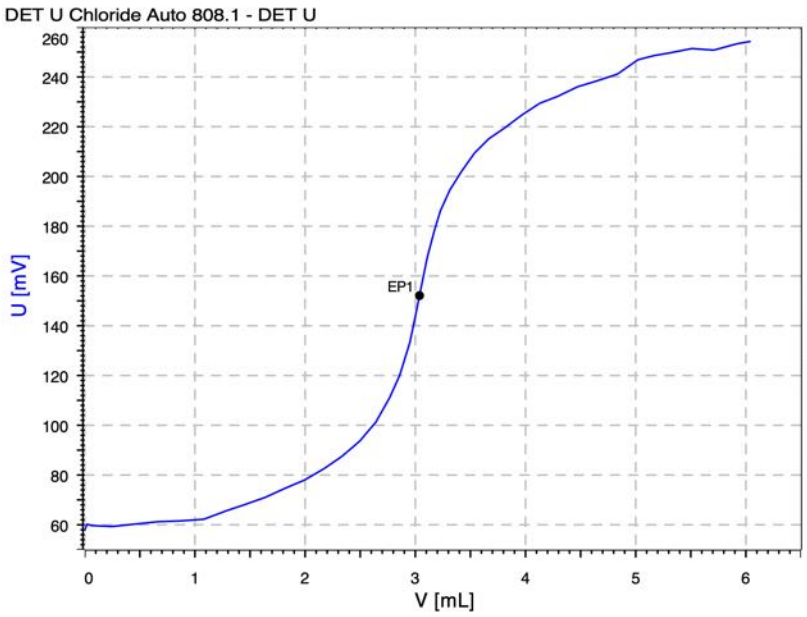

tiamo Page 1 of 1 Metrohm

Figure 71: Water-soluble chloride analysis from potentiometric titration of the filtrate from digestion of concrete powder in deionized water, where chloride content is determined from the equivalent point of titration plotted against milliliters of silver chloride titrant added during titration and corresponding changes in millivolts where the steepest point in the titration curve defines the equivalent point. Chloride content is determined from the milliliters of silver nitrate used to reach the equivalent point, and the sample weight.

License ID 4017173 Program version tiamo 2.5 - 116 - 1
Computer name Titration-909
User Metrohm Titration 2022-02-067:57:20 PM UTC-

Results report

Determination of Acid-Soluble (ASTM C 1152) or Water-Soluble (ASTM C 1218) Chloride Contents

Method . . . . . DET U Chloride Auto 808
Method saving date 2020-12-05 13:32:13 UTC-5

Sample data

ID1 . . . . . CMC 0122103
ID2 . . . . . WC-3
ID3 . . . . . 5 inch.
Sample size . . . . . 9.890 g

End points

DET U **DET U Chloride Auto 808.1**

EP1 . . . . . 152.0 mV . . . . . 2.6892 mL

Results

% Chloride . . . . . **0.0481 %**

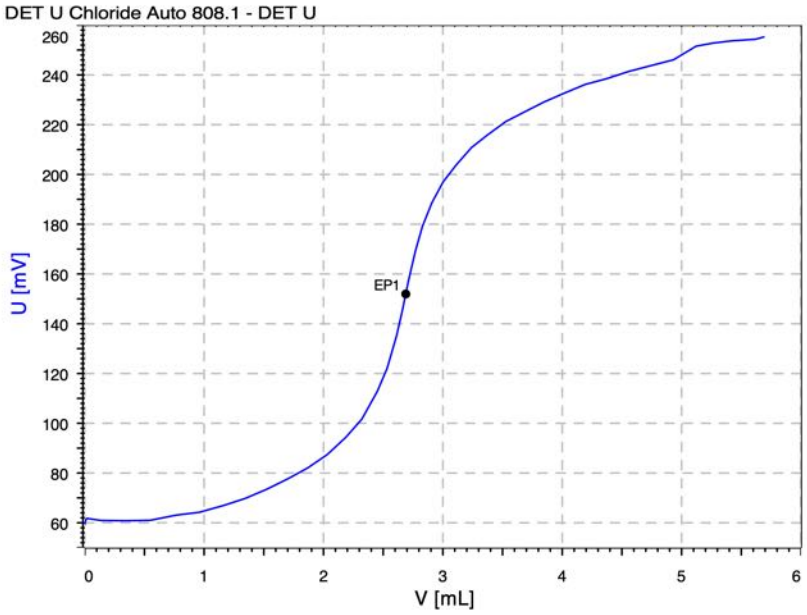

tiamo Page 1 of 1 Metrohm

Figure 72: Water-soluble chloride analysis from potentiometric titration of the filtrate from digestion of concrete powder in deionized water, where chloride content is determined from the equivalent point of titration plotted against milliliters of silver chloride titrant added during titration and corresponding changes in millivolts where the steepest point in the titration curve defines the equivalent point. Chloride content is determined from the milliliters of silver nitrate used to reach the equivalent point, and the sample weight.

License ID 4017173 Program version tiamo 2.5 - 116 - 1
Computer name Titration-909
User Metrohm Titration 2022-02-067:57:18 PM UTC-

Results report

Determination of Acid-Soluble (ASTM C 1152) or Water-Soluble (ASTM C 1218) Chloride Contents

Method . . . . . DET U Chloride Auto 808
Method saving date 2020-12-05 13:32:13 UTC-5

Sample data

ID1 . . . . . CMC 0122103
ID2 . . . . . WC-3
ID3 . . . . . 10 inch.
Sample size . . . . . 10.026 g

End points

DET U **DET U Chloride Auto 808.1**

EP1 . . . . . 148.6 mV . . . . . 1.7145 mL

Results

% Chloride . . . . . **0.0303 %**

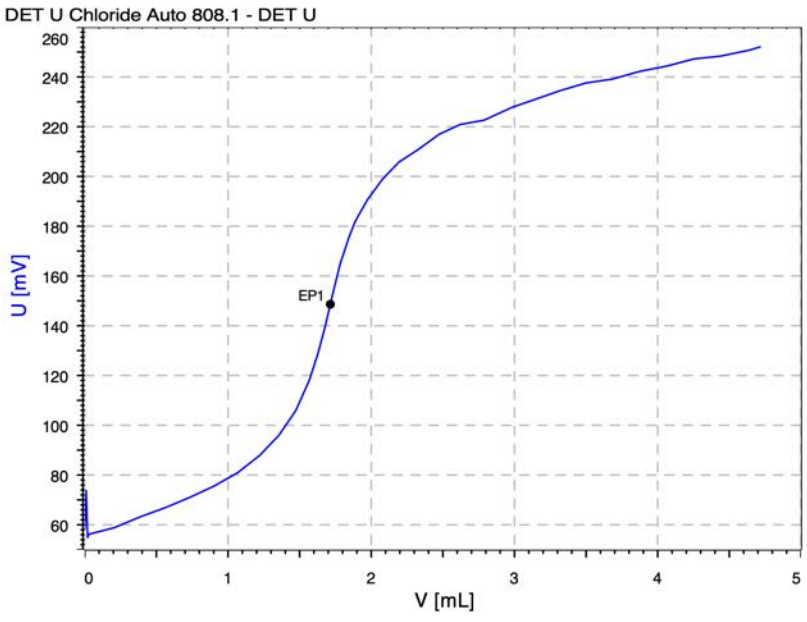

tiamo Page 1 of 1 Metrohm

Figure 73: Water-soluble chloride analysis from potentiometric titration of the filtrate from digestion of concrete powder in deionized water, where chloride content is determined from the equivalent point of titration plotted against milliliters of silver chloride titrant added during titration and corresponding changes in millivolts where the steepest point in the titration curve defines the equivalent point. Chloride content is determined from the milliliters of silver nitrate used to reach the equivalent point, and the sample weight.

License ID 4017173 Program version tiamo 2.5 - 116 - 1
Computer name Titration-909
User Metrohm Titration 2022-02-067:57:17 PM UTC-

Results report

Determination of Acid-Soluble (ASTM C 1152) or Water-Soluble (ASTM C 1218) Chloride Contents

Method . . . . . DET U Chloride Auto 808
Method saving date 2020-12-05 13:32:13 UTC-5

Sample data

ID1 . . . . . CMC 0122103
ID2 . . . . . WC-3
ID3 . . . . . 15 inch.
Sample size . . . . . 9.931 g

End points

DET U **DET U Chloride Auto 808.1**
EP1 . . . . . 142.2 mV . . . . . 0.7503 mL

Results

% Chloride . . . . . **0.0134 %**

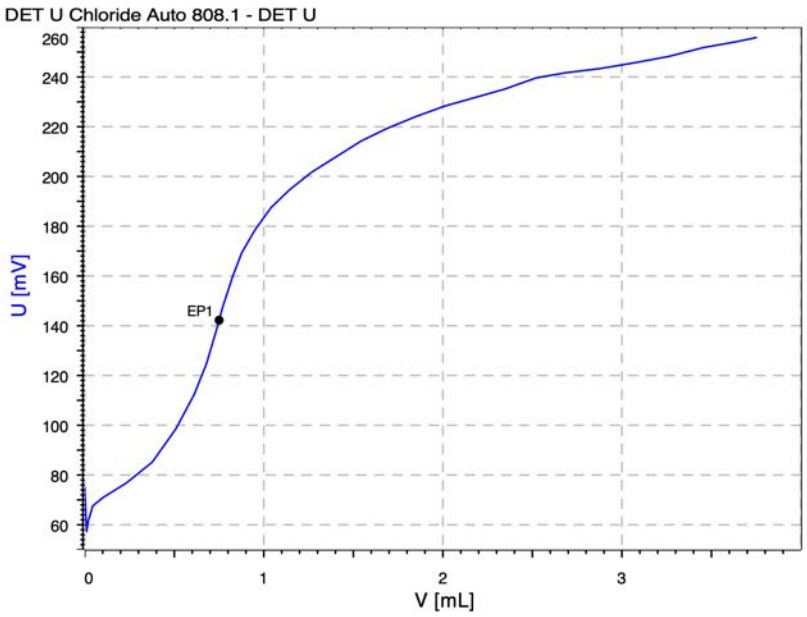

tiamo Page 1 of 1 Metrohm

Figure 74: Water-soluble chloride analysis from potentiometric titration of the filtrate from digestion of concrete powder in deionized water, where chloride content is determined from the equivalent point of titration plotted against milliliters of silver chloride titrant added during titration and corresponding changes in millivolts where the steepest point in the titration curve defines the equivalent point. Chloride content is determined from the milliliters of silver nitrate used to reach the equivalent point, and the sample weight.

License ID 4017173 Program version tiamo 2.5 - 116 - 1
Computer name Titration-909
User Metrohm Titration 2022-02-067:58:50 PM UTC-

Results report

Determination of Acid-Soluble (ASTM C 1152) or Water-Soluble (ASTM C 1218) Chloride Contents

Method . . . . . DET U Chloride Auto 808
Method saving date 2020-12-05 13:32:13 UTC-5

Sample data

ID1 . . . . . CMC 0122103
ID2 . . . . . WC-4
ID3 . . . . . 1 inch.
Sample size . . . . . 9.747 g

End points

DET U **DET U Chloride Auto 808.1**

EP1 . . . . . 132.1 mV . . . . . 4.9133 mL
EP2 . . . . . 169.4 mV . . . . . 5.0552 mL

Results

% Chloride . . . . . **0.0892 %**

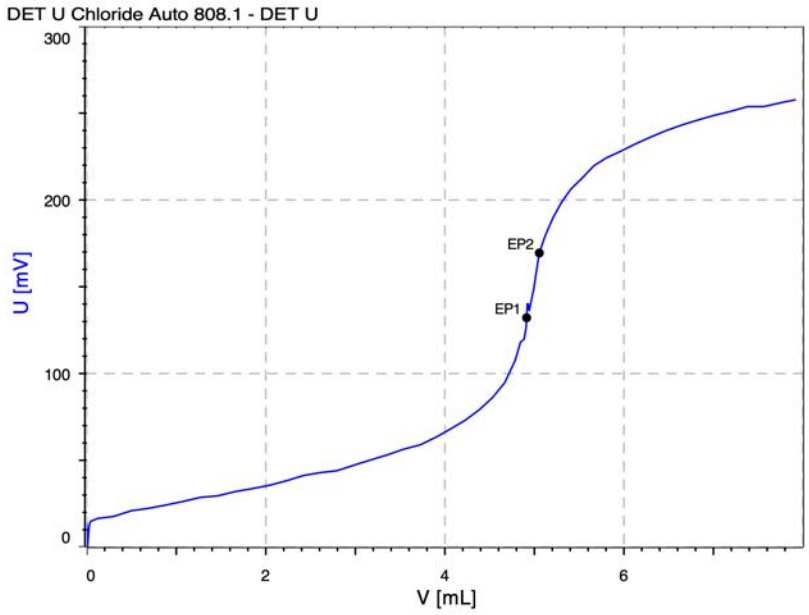

tiamo Page 1 of 1 Metrohm

Figure 75: Water-soluble chloride analysis from potentiometric titration of the filtrate from digestion of concrete powder in deionized water, where chloride content is determined from the equivalent point of titration plotted against milliliters of silver chloride titrant added during titration and corresponding changes in millivolts where the steepest point in the titration curve defines the equivalent point. Chloride content is determined from the milliliters of silver nitrate used to reach the equivalent point, and the sample weight.

License ID 4017173 Program version tiamo 2.5 - 116 - 1
Computer name Titration-909
User Metrohm Titration 2022-02-068:52:54 PM UTC-

Results report

Determination of Acid-Soluble (ASTM C 1152) or Water-Soluble (ASTM C 1218) Chloride Contents

Method . . . . . DET U Chloride Auto 808
Method saving date 2020-12-05 13:32:13 UTC-5

Sample data

ID1 . . . . . CMC 0122103
ID2 . . . . . WC-4
ID3 . . . . . 3 inch.
Sample size . . . . . 9.733 g

End points

DET U **DET U Chloride Auto 808.1**

EP1 . . . . . 152.9 mV . . . . . 7.6688 mL

Results

% Chloride . . . . . **0.1395 %**

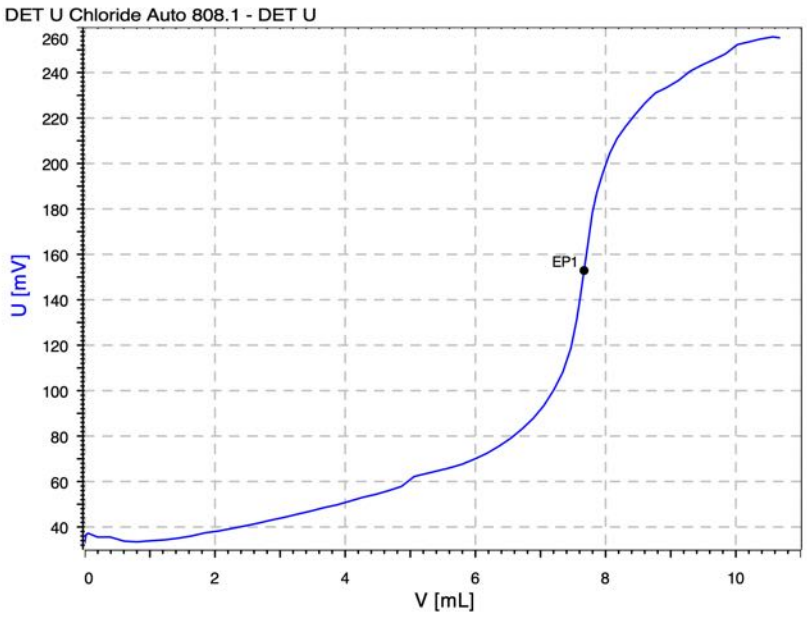

tiamo Page 1 of 1 Metrohm

Figure 76: Water-soluble chloride analysis from potentiometric titration of the filtrate from digestion of concrete powder in deionized water, where chloride content is determined from the equivalent point of titration plotted against milliliters of silver chloride titrant added during titration and corresponding changes in millivolts where the steepest point in the titration curve defines the equivalent point. Chloride content is determined from the milliliters of silver nitrate used to reach the equivalent point, and the sample weight.

License ID 4017173 Program version tiamo 2.5 - 116 - 1
Computer name Titration-909
User Metrohm Titration 2022-02-068:53:16 PM UTC-

Results report

Determination of Acid-Soluble (ASTM C 1152) or Water-Soluble (ASTM C 1218) Chloride Contents

Method . . . . . DET U Chloride Auto 808
Method saving date 2020-12-05 13:32:13 UTC-5

Sample data

ID1 . . . . . CMC 0122103
ID2 . . . . . WC-4
ID3 . . . . . 5 inch.
Sample size . . . . . 10.138 g

End points

DET U **DET U Chloride Auto 808.1**

EP1 . . . . . 148.7 mV . . . . . 3.1907 mL

Results

% Chloride . . . . . **0.0557 %**

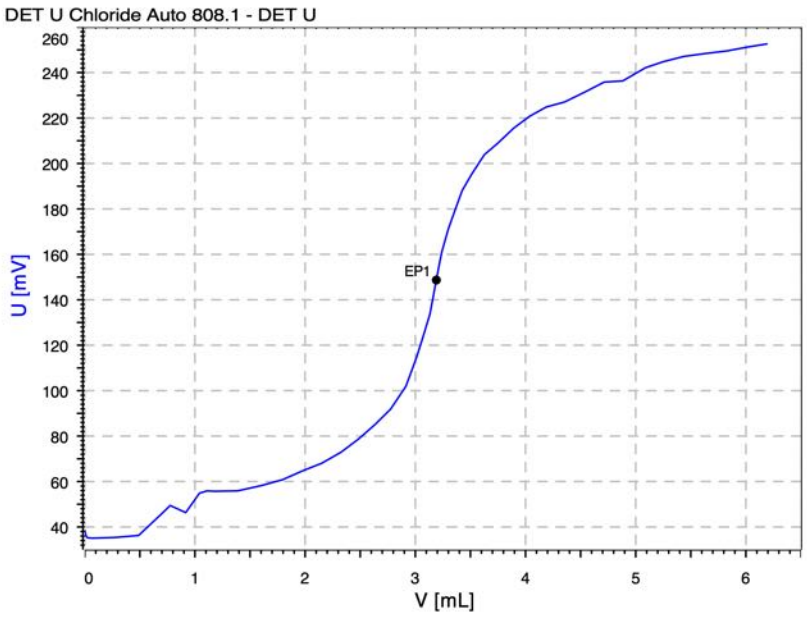

tiamo Page 1 of 1 Metrohm

Figure 77: Water-soluble chloride analysis from potentiometric titration of the filtrate from digestion of concrete powder in deionized water, where chloride content is determined from the equivalent point of titration plotted against milliliters of silver chloride titrant added during titration and corresponding changes in millivolts where the steepest point in the titration curve defines the equivalent point. Chloride content is determined from the milliliters of silver nitrate used to reach the equivalent point, and the sample weight.

License ID 4017173 Program version tiamo 2.5 - 116 - 1
Computer name Titration-909
User Metrohm Titration 2022-02-068:53:40 PM UTC-

Results report

Determination of Acid-Soluble (ASTM C 1152) or Water-Soluble (ASTM C 1218) Chloride Contents

Method . . . . . DET U Chloride Auto 808
Method saving date 2020-12-05 13:32:13 UTC-5

Sample data

ID1 . . . . . CMC 0122103
ID2 . . . . . WC-4
ID3 . . . . . 10 inch.
Sample size . . . . . 10.701 g

End points

DET U **DET U Chloride Auto 808.1**
EP1 . . . . . 146.8 mV . . . . . 2.6318 mL

Results

% Chloride . . . . . **0.0435 %**

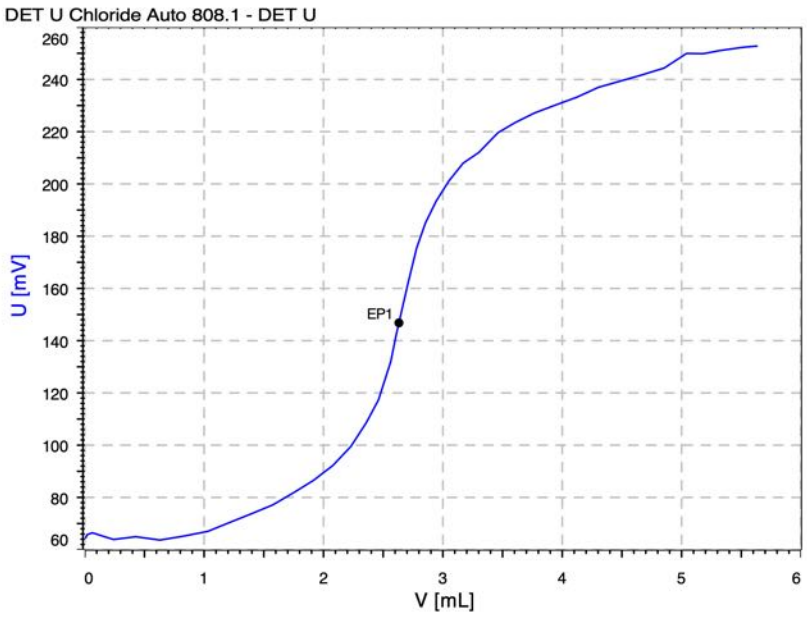

tiamo Page 1 of 1 Metrohm

Figure 78: Water-soluble chloride analysis from potentiometric titration of the filtrate from digestion of concrete powder in deionized water, where chloride content is determined from the equivalent point of titration plotted against milliliters of silver chloride titrant added during titration and corresponding changes in millivolts where the steepest point in the titration curve defines the equivalent point. Chloride content is determined from the milliliters of silver nitrate used to reach the equivalent point, and the sample weight.

License ID 4017173 Program version tiamo 2.5 - 116 - 1
Computer name Titration-909
User Metrohm Titration 2022-02-069:09:07 PM UTC-

Results report

Determination of Acid-Soluble (ASTM C 1152) or Water-Soluble (ASTM C 1218) Chloride Contents

Method . . . . . DET U Chloride Auto 808
Method saving date 2020-12-05 13:32:13 UTC-5

Sample data

ID1 . . . . . CMC 0122103
ID2 . . . . . WC-4
ID3 . . . . . 15 inch.
Sample size . . . . . 10.535 g

End points

DET U **DET U Chloride Auto 808.1**

EP1 . . . . . 148.7 mV . . . . . 1.2403 mL

Results

% Chloride . . . . . **0.0208 %**

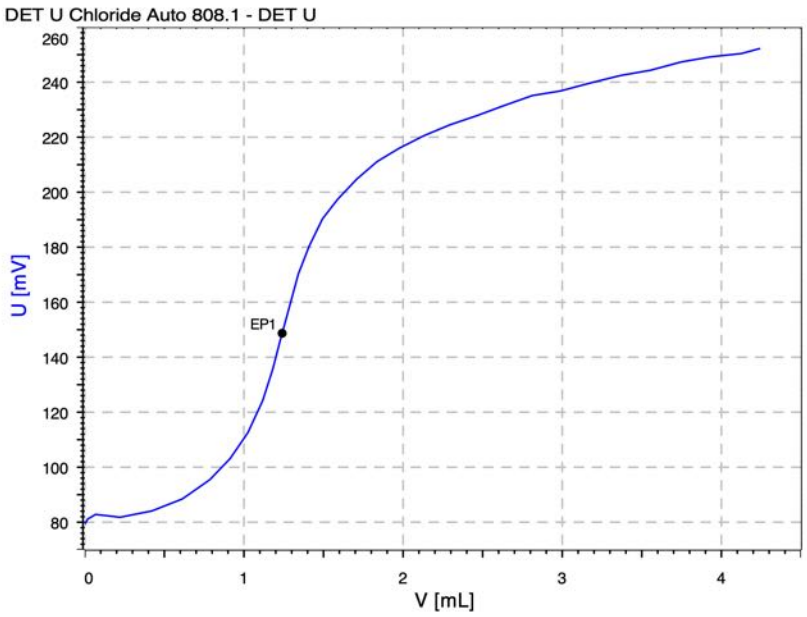

tiamo Page 1 of 1 Metrohm

Figure 79: Water-soluble chloride analysis from potentiometric titration of the filtrate from digestion of concrete powder in deionized water, where chloride content is determined from the equivalent point of titration plotted against milliliters of silver chloride titrant added during titration and corresponding changes in millivolts where the steepest point in the titration curve defines the equivalent point. Chloride content is determined from the milliliters of silver nitrate used to reach the equivalent point, and the sample weight.

DISCUSSIONS

ALKALI-SILICA REACTIONS OF REACTIVE STRAINED QUARTZITE GRAVEL COARSE AGGREGATES

The quartzite gravel coarse aggregate particles contain highly strained quartz grains with characteristic undulose extinction, which are known to be potentially alkali-silica reactive in the presence of moisture and high alkalis in the pore solution. As a result, evidence of alkali-silica reaction is found in the cores as (a) microcracking within the particles, (b) microcracking extending from the reactive particles to neighboring paste, and (c) alkali-silica reaction gels in microcracks and air voids in the vicinity of reactive quartzite gravels. Profuse development of secondary ettringite deposits lining the walls of coarser air voids, filling the smaller air voids, and filling some microcracks are testaments of prolonged presence of moisture in the concrete during service, which is the main pre-requisite for alkali-silica reaction, besides having the reactive quartz and a high level of alkali in the pore solution.

AIR ENTRAINMENT AND FREEZE-THAW DURABILITY

Despite the presence of air entrainment, the total estimated air contents of cores are from 3.5 to 5.5 percent where entrained air contents in most cases are lower than that needed for protection of concrete against distress due to cyclic freezing and thawing at critically saturated conditions. Therefore, due to the low estimated air contents, potential for freezing-related distress, such as cracking and spalling are present, especially at locations where air contents are less than 4½ percent.

HIGH CHLORIDE CONTENTS AND POTENTIAL FOR CHLORIDE-INDUCED CORROSION OF STEEL IN CONCRETE

Figure 39 shows results of water-soluble chloride analyses from 1 in. to 15 in. distances from the exposed ends in all four cores where chloride contents at various depths in all cores show higher than the industry-recommended threshold maximum chloride content of 0.2 percent by mass of cement above which chloride-induced corrosion of reinforcing steel in concrete is possible in the presence of oxygen and moisture. Therefore, the observed reddish-brown corrosion stains seen in the field photos are judged to be due to chloride-induced corrosion of steel in concrete.

COMPRESSIVE STRENGTHS

Compressive strengths of cores are from 3450 psi to 4330 psi, which are less than the common industry--recommended minimum strength of 4500 psi for a moist outdoor concrete exposed to cyclic freezing and thawing. Microcracking developed from alkali-silica reaction of many reactive strained quartzite gravel coarse aggregate particles have deleteriously affected the compressive strength.

BENEFICIAL ASPECT OF PROTECTIVE MEMBRANES

Due to the presence of high levels of chloride and lack of adequate air entrainment a protective membrane is beneficial for protection of concrete from penetration of moisture and potentially deleterious chemicals into the concrete. A protective membrane is found at the exposed ends of Cores EC-2P and WC-2P, which are beneficial for preventing penetration of deleterious external agents during service.

LONG-TERM DURABILITY AND SERVICEABILITY

Due to the evidence of (a) alkali-silica rection of many reactive quartzite gravel coarse aggregate particles, (b) lack of adequate air entrainment to generate around 6 percent air, and (c) high levels of chlorides in all four cores at various depths long-term serviceability of the bridge substructure is questionable unless the existing concrete can be adequately protected with protective membrane to prevent penetration of moisture and potentially deleterious chemicals into the concrete.

REFERENCES

ASTM C 856 "Standard Practice for Petrographic Examination of Hardened Concrete," Vol. 4.02, ASTM International, West Conshohocken, PA, 2017.

ASTM C 1218 "Standard Test Method for Water-Soluble Chloride in Mortar and Concrete," Vol. 4.02, ASTM International, West Conshohocken, PA, 2017.

Jana, D., "Sample Preparation Techniques in Petrographic Examinations of Construction Materials: A State-of-the-Art Review," *Proceedings of the 28th Conference on Cement Microscopy (ICMA)*, 2006, pp. 23-70.

✪ ✪ ✪ END OF TEXT ✪ ✪ ✪

END OF REPORT[1]

[1] The CMC logo is made using a lapped polished section of a 1930's concrete from an underground tunnel in the U.S. Capitol.